CRITICAL PHENOMENA WITH RENORMALIZATION GROUP ANALYSIS OF A HIERARCHICAL MODEL OF FINANCIAL CRASHES

by

Tian Kuang (Tim) Wu

B.Sc. (Statistics), Simon Fraser University, 2008

B.A. (Finance), Ji Nan University, 2003

A Thesis submitted in partial fulfillment
of the requirements for the degree of
Master of Science

in the
Department of Mathematics
Faculty of Science

SIMON FRASER UNIVERSITY
Summer 2012

APPROVAL

Name: Tian Kuang (Tim) Wu

Degree: Master of Science

Title of Thesis: Critical phenomena with renormalization group analysis of a hierarchical model of financial crashes

Examining Committee: Dr. Zhaosong Lu,
Associate Professor, Department of Mathematics
Chair

Dr. Peter Borwein, Senior Supervisor,
Professor, Department of Mathematics

Dr. Alexander (Sandy) Rutherford, Supervisor,
Adjunct Professor, Department of Mathematics

Dr. Ramazan Gençay, Committee Member,
Professor, Department of Economics

Dr. Paul Tupper, Internal External Examiner,
Associate Professor, Department of Mathematics

Date Approved: July 30, 2012

Partial Copyright Licence

Abstract

Financial market models are able to help the investors foresee the risk of a financial market crash and reduce the probability of its occurrence. Modelling in financial markets is categorized into microscopic models and macroscopic models. The microscopic models study the mechanisms behind the market and their behaviour. These models assist in an understanding of the causes of financial market crashes. Macroscopic models find the disciplines and rules from the historical macroscopic data for the prediction of market trends, directions and crashes. They aim to provide forecasts of when the crashes should occur. Except for large fluctuations, the stock market price or index movements can be characterized by a random walk. The stock price trajectory possesses the properties of self-similarity and scale invariance, and hence mimics fractals. Furthermore, the stock price movement is a manifestation of the actions and interactions of stock traders. The hierarchical model with fractal structures, representing the interaction structure of the stock traders, is applicable to the study of the microscopic mechanisms of stock price movements. In the language of statistical mechanics, stock market crashes are viewed as critical phenomena where a crash occurs only at the critical point with a phase transition. The renormalization group is a mathematical apparatus that allows the decomposition of a macroscopic problem viewed at different scales. The renormalization group analysis of the hierarchical model finds that the time to reach the critical point of a system is a function of the interaction degree of stock traders in a power law. Moreover, the hierarchical model with the renormalization group formalism shows that the behavior of the fraction of all stock traders putting buy orders over time follows a power law coupled with log-periodic oscillations. Based on the renormalization group analysis results of the hierarchical model, a log-periodic power law model is derived by constructing an renormalization group formalism from the risk-driven model. In the log-periodic power law model, the expected time to crash is always finite. Therefore, market crashes are inevitable, but the existence of bubbles and crash risks is foreseen by the model.

Keywords: Financial Market Crashes; Hierarchical Model; Renormalization Group; Log-Periodic Power Law; Critical Phenomena; Phase Transition

Acknowledgments

My thesis would never have been possible without the guidance, the help and the support of the kind people around me who have had a tremendous impact on my work and the journey to my defence.

I wish to thank my committee members. My Senior Supervisor Professor Peter Borwein provided valuable advice on my work, financial support for the research and encouragements throughout the process. It is with immense gratitude that I acknowledge my Supervisor Professor Sandy Rutherford for his excellent guidance, caring, patience, and providing me with an excellent atmosphere for doing research. He made the whole process to the defence running through smoothly and provided full support at all times. He provided me and helped me achieve necessary financial support for this work. He encouraged me throughout the process and never lost confidence in me. Professor Ramazan Gençay generously offered me the stock market data in this thesis and provided guidance in the area of finance. My Internal External Examiner Dr. Paul Tupper provided his thoughtful comments on my work. I would also like to thank Dr. Zhaosong Lu for agreeing to chair my defence.

I would like to express my utmost gratitude to my friend Dr. Christopher Giles who spent a lot of time in editing my thesis thoroughly and patiently. He provided a tremendous amount of insightful feedback on various versions and on various levels, including contents, structure, format and language, of this thesis.

I would also like to express my gratitude to the Complex Systems Modelling Group (CSMG) members for their support and help with various stages of the process. Dr. Alexa van der Waall gave me valuable suggestions in academic writing. Dr. Yanchao Wang was always willing to help and shared her successful experience of the process. Andrew Adams proofread my work and provided useful feedback.

I am grateful to Professor Vahid Dabbaghian for the offer of the award of MoCSSy Graduate Scholarship in Spring and Summer 2012. I would also like to thank my friend Jon Wen for his help. Last, but by no means least, I would like to express my gratitude to my families. My wife Cherry Mo was always there cheering me up and stood by me with the good and bad time. My parents were always unselfishly supporting and encouraging me with their best wishes not only during the thesis process, but also throughout my journey in life.

Contents

Approval ii

Abstract iii

Acknowledgments iv

Contents v

List of Tables viii

List of Figures ix

1 Introduction 1

2 Financial Market Models 6

2.1 Microscopic Mechanism Models 6

2.1.1 Reaction-Diffusion Model 6

2.1.2 Stochastic Multi-Agent Model 8

2.1.3 Cont-Bouchaud Percolation Model 12

2.2 Market Prediction Models 14

2.2.1 Dow Theory 15

2.2.2 Elliott Wave Theory 17

3 Fundamental Principles in Financial Markets 20

3.1 Random Walk 20

3.2 Fractals 24

3.2.1 Introduction 24

3.2.2 Fractal Dimension 25

3.2.3 Application in Financial Markets 26

3.2.4 Hierarchical Model 31

3.3 Phase Transition: Critical Phenomena . . . 32

4 Renormalization Group 35

4.1 Background . . . 35
4.2 Two Main Transformation . . . 35
4.2.1 Decimation . . . 36
4.2.2 Rescaling . . . 41
4.3 General Formalism . . . 43
4.3.1 Elements of RG theory . . . 43
4.3.2 Calculation . . . 45
4.3.3 Real and Complex Exponent Solutions . . . 49

5 Hierarchical Model 51

5.1 Model Definition and Structure . . . 52
5.2 Modelling Formulation and Solutions . . . 54
5.2.1 Special Solution for the Case of $\beta = 1$ . . . 54
5.2.2 Special Solution for the Case of $\beta \to 0$ and $\beta \to \infty$ . . . 56
5.2.3 General Solution . . . 63
5.2.4 Simulation of General Solutions . . . 72
5.3 Construction of the Power-Law Regression Model . . . 78
5.4 General Form . . . 84

6 Data Analysis 91

6.1 Fitting Procedure . . . 91
6.1.1 Least Square Estimations. . . . 92
6.1.2 Taboo Search . . . 93
6.1.3 Quasi-Newton Method with Line Search . . . 97
6.2 Bubble vs. Anti-Bubble . . . 100
6.3 Results Discussion . . . 103
6.3.1 Analysis of Crash Prediction in 1987 . . . 104
6.3.2 Prediction Comparison of Bubble Regimes . . . 106
6.3.3 Fitted Data Selection . . . 109

7 Conclusion 113

Appendix A Convergent Time Vs. Interaction Parameter 117

Appendix B Simulation of the Hierarchical Model 120

Bibliography **126**

Index **135**

List of Tables

5.1 Relationship of interaction strength β vs. crash time t_c. 72

6.1 Estimated parameters of the LPPL fitted by unsmoothed and smoothed data. 106
6.2 Comparison of estimations by the LPPL model of the three bubble regimes. 106
6.3 Fitting results of fitted data with different start dates. The end date is on September 15^{th}, 1987. 110
6.4 Fitting results of fitted data with different end dates. The start date is on December 4^{th}, 1984. 111

List of Figures

2.1 Stochastic multi-agents model. 9
2.2 An example of a single wave structure. Reprinted from Copsey [19]. 17
2.3 An example of complex wave structure. Reprinted from Copsey [19]. 18

3.1 An example of a single 1-dimension random walk of 1000 steps with a step length '1' and same probability (50%) for either step direction at each time interval '1'. . 21
3.2 One thousand of 1-dimension random walks of 1000 steps with a step length '1' and same probability (50%) for either step direction at each time interval '1'. 21
3.3 Normal probability plot for the displacement of the 1000 random walks at time $t = 1000$. 22
3.4 The top five iterations of the construction of the triadic Cantor set. 24
3.5 An example of self-similarity of random walk. The left diagram is an arbitrary random walk with 10000 steps. The right one is part of the whole of the left. They are similar at different time scales. 27
3.6 An example of fractal characteristics in stock index movements. The data is from FTSE 100 index at different time scales. The top figure is the plot of weekly end index values. The bottom one is the plot daily end index values. Both are observed to have similar movement patterns with different scales in both time and amplitude directions. 29
3.7 Example of Hierarchical Model structure with $n + 1$ levels and group members of 2. 31
3.8 Phase diagram of H_2O with critical point. Ice is in solid phase, water is in liquid phase, and vapor is in gas phase. (Source: [118]) 33

4.1 The construction of the first three magnification of a diamond lattice. 46

5.1 Example of Hierarchical Model structure with $n + 1$ levels and group members of 2. 51
5.2 Starting from $t = 0$, the trader i makes the first purchase of a stock at time t_{i1}. The time from t_{i1} to the trader's second purchase is t_{i2}. 53
5.3 Cobweb diagram for the function $f(x) = x^2$ starting from $x_0 = 0.8$. 57

5.4 The *cdf* curve of each level is beneath the *cdf* curve of the adjacent lower level with a later time approaching 1. 58
5.5 Cobweb diagram for the function $f(x) = 2x - x^2$ starting from $x_0 = 0.2$. 61
5.6 The *cdf* curve of each level is over the *cdf* curve of the adjacent lower level with a later time approaching 0. 62
5.7 Plot for the relationship between the crash time and the interaction strength between traders. The initial distribution $p_0(t)$ is exponential with $\lambda = 1$. The fit to the power law of expression 5.70 gives the estimated values $\bar{t} = 0.9602$ and $\mu = 0.6685$ with the coefficient of determination of $R^2 = 0.9349$. 73
5.8 Examples of the evolution of traders buying stock in the hierarchical model. . . . 74
5.9 Total number of traders who have bought the stock as a function of time with an interaction parameter of 5 and an exponential initial distribution. 78
5.10 Log-Log plot of five simulation runs of total number of traders who have bought the stock over time with an interaction parameter of 5 and an exponential initial distribution. 79

6.1 Taboo Search Process. 95
6.2 The Argentinian stock market bubble and anti-bubble of 1992. Reprinted from [52]. 101
6.3 The Polish stock market bullish anti-bubble of 1998-2000. Reprinted from [39]. . . 102
6.4 FTSE 100 index daily closing from Apr. 4, 1984 to Jan. 20, 2012. 104
6.5 FTSE 100 index daily closing from Apr. 4, 1984 to Jun. 28, 1988. 105
6.6 Fitting LPPL to the data of FTSE 100 index daily closing for the 1987 crash. . . . 105
6.7 Comparison of the unsmoothed and smoothed data plots. 107

Chapter 1

Introduction

Financial market crashes have major impacts on the society. For example, the crash of the US housing market in 2007 and 2008 not only directly affects housing related industries, such as real estate, home builders, home valuations, but also has significant impacts on home supply retailers, credit markets, stock markets, manufacturers. It nearly sank the US mortgage market and resulted in an increasing risk of economic recession. Financial market crashes tend to be associated with steep increases in many social issues, such as unemployment, family breakdown, crime, and suicide. There are many components of financial markets: the capital market, the money market, the commodity market, the foreign exchange market, and the insurance market. These can be divided into numerous sub-categories. For example, the capital market contains the stock market and the bond market. It can also be categorized into the primary market and the secondary market.[1]

Other than banks, the stock market is the most common place for "small" investors. However, as a result of its prevalence, a stock market crash has wider and deeper effects on the economy than other financial markets. There were four notable stock market crashes in the history of finance that occurred in 1929, 1987, 2000 (1997 in Asia) and 2008. The loss of wealth from a crash affects people through direct stock ownership, mutual funds investments, and investments in education funds and pension funds. A stock market crash usually results in an economic recession,[2] such as the crash in 1929, or leads to a financial

[1]The primary market deals with the issuance of new securities. The secondary market is the market where securities are traded after initially issued in the primary market.

[2]GDP growth is negative for two consecutive years.

aspect of crisis, such as the Black Monday in 1987. The crash in 1929 was followed by a worldwide economic depression, known as the Great Depression, lasting ten years in most countries. Black Monday on October 19, 1987 led to the Savings and Loan Crisis in the United States.

The most common questions that investors have about these crashes are why they occur, whether they are predicable or avoidable, and when they would happen in the future. The most simple answer to the question of 'why' is that there are more sellers than buyers in the market. The sellers are trying to sell their stocks immediately with little consideration of the price. since they would rather take a small loss than be exposed to the crash. The problem is the cause of those seller behaviors, which leads to crash concerns and the decision of selling theirs stocks at the same moment.

The financial market is a complex system[3] characterized by many natural and social systems. Price change is the result of the buying and selling actions of all interacting traders in the market. Similar to behaviors in physics, price change is a 'macroscopic' behavior and the trading of market participants is a 'microscopic' behavior.

At the 'microscopic' level, as discussed by Sornette (2003) [94], there are a number of explanations for a crash, such as computer trading, derivative securities, and over valuation. At the 'macroscopic' level, the crashes are inevitable when the price reaches a critical point – traders reinforce imitation by other investors. This is the fundamental idea of the analysis in this thesis. The basic assumption in the thesis is that there are herding behaviors among traders. Herding behavior means that interactions among traders exist which reinforces trading in the same direction (buy or sell). At the critical point, the millions of small minor events trigger the occurrence of an extreme event.

A suitable model of the financial market assists in the prediction of financial market crashes. Market traders are able to foresee the high risks in the stock market when the market bubbles emerge and increase through the model.

Financial market crash modelling is a simulation of the behaviors of the market participants that applies the analytical theories and techniques of critical phenomena in physics, statistics and mathematics. The price changes in financial markets are simulated by the

[3]A complex system is any system comprised of a number of interacting entities, processes, or agents, whose aggregate activity is nonlinear and typically exhibits hierarchical self-organized, but unpredictable behaviors.

movements of a random walk in physics. Each price change is considered as an event, and a large price change, such as a crash, is an extreme event. The extreme value theory in the study of extreme events is used to evaluate the probability of the occurrence of extreme events [95].

The Renormalization Group (RG) is a technique of finding the macroscopic behavior of a complex system by decomposing it into a succession of problems with a decreasing number of microscopic interacting parts at different scales [94, 95]. Analogous to critical phenomena in physics, a financial market crash can be considered as a transit from one phase to another. The susceptibility of a system diverges and anomalies arise in specific quantities, like a bomb explosion or a big earthquake. The theory of critical phenomena, developed in 1937 by Landau [60], naturally explains universality and is devoted to describing such critical behavior. The problem becomes finding the critical point of a critical phenomenon.

Technical analysts have attempted to model the behavior of financial market prices for forecasting purposes. The moving average is a widely used measure of market trend direction. Early research focuses on finding patterns in the financial market price movements. The classic Dow theory, which was derived from 255 journals in 1890s and 1900s, is the oldest technical analysis principles of stock market theory and it is still used in market trend analysis [45, 25]. It assists to confirm the primary trend of the market by analyzing several market parameters, such as average high and low, volume, and sector rotation. Ralf Nelson Elliott discovered, after the crash of 1929, that the trend in financial market prices is explained as pattern recognition with self-similar fractal geometry, called Elliott Wave Principle [31]. Elliott asserted that financial market price changes are the result of the collective behaviors of the traders in the market. Following Elliott, Collins, Frost, and Prechter published Elliott's Wave Principles during the 1980s. Advances in computing science allow for increased data and volume computation for modelling financial markets. Similar to critical phenomena in physics, the behavior of market traders was studied and analysts found that the increasing trend of homogeneous characteristics of market traders explains financial market crashes in over long time periods.

Starting from the mid-1990s, many academic and financial institutions, and physicists examined and researched financial market modelling. They discovered many characteristics in financial markets have analogous behaviors in physics, such that certain theories and

models in physics are applicable in financial market analysis, such as chaos in dynamical systems [17], entropy [35], and thermodynamics [80]. Didier Sornette [94] recognized that models of financial market crashes follows the non-linear regression of the power laws associated with log-periodic oscillatory corrections to critical phenomena. He posits the existence of self-reinforcement imitation and herding behaviors among investors. Most research confirms the log-periodic power law characteristic. The study of financial market crashes is interdisciplinary and includes finance, mathematics, statistics, physics, geometry, computer science, psychology, and social science.

The questions of predictability and crash time lead to a paradox in modelling financial market crashes. The financial market is not a completely objective and independent system, and crash events are not experimentally repeatable. The reliability and accuracy of the model analysis results have mutual effects on the 'microscopic' units (traders) in the system. The occurrence of an extreme event is not solely based on the intrinsic characteristics, but also on the outside information, outside events, and modelling results. For example, the tsunami in Japan resulted in a nearly 20% index drop of Nikkei225. There are several possible outcomes of the influence of modelling results on a financial market. First, if everyone believes a crash prediction of the model, people are motivated to sell their stocks which triggers an earlier crash time than predicted, and makes the model less reliable. Second, if a sufficiently large amount of people believe the crash prediction, the stock price drops without a crash, and makes the model unreliable. Third, everyone continues their original trading strategies without confidence in the the model outcomes, and the market collapses as predicted. This makes the model predictions more reliable. Even if the last case occurs, some may consider it as 'lucky' if there is a prediction without the validation of statistical repetition [87]. Therefore, it is more reasonable to consider the financial market modelling as a tool for explaining the behavior of the system rather than as a prediction tool.

This thesis introduces the reader to major financial market theories and models of current research. Two main aspects in the research of financial markets are investment analysis and market modelling. Investment analysis focuses on forecasting the direction and trend of prices based on the study of past market data and financial information. Market modelling examines the pricing mechanism of financial products through the simulation of

the market operations. This thesis concentrates on the modelling analysis for the stock market crashes. Notwithstanding, no financial market can be isolated from others. One financial market crash can trigger crashes in other markets (i.e., the stock market crash in 2008). This thesis comprises both aspects of the financial market study. The purpose of this thesis is to illustrate how stock markets are modeled in a hierarchical structure with the Renormalization Group (RG) techniques. It shows how to mathematically derive a model, so called Log-Periodic Power Law model, for the prediction of the stock market crashes, and shows how to fit the model to financial data.

Following Sornette's LPPL model [87], this thesis introduces the modelling of financial market crashes through the hazard rate with the techniques of renormalization group analysis of critical phenomena in physics. It focuses on the mathematical theories deriving the model and proves the relationship between the crash time and the interaction degree. In addition, it deduces and validates the model with real data fitted to the model. Moreover, as a mathematical thesis in a interdisciplinary field, it introduces the reader to knowledge in other fields relevant to the modelling financial systems.

This thesis is organized as follows. Chapter 2 presents a selection of classic financial market models. Chapter 3 explains the mathematical and physical theories and methods relevant to the analysis of the financial markets. Chapter 4 describes the techniques of Renormalization Group analysis used in the hierarchical modelling. Chapter 5 presents the structure and design of the hierarchical model as applied to financial market behavior. This chapter also shows the methodology of applying RG analysis. Chapter 6 introduces the tools and techniques for fitting the non-linear regression, and the validation of the model through data analysis. The last section of Chapter 6 provides an example of fitting the model to the data and proposes a profile. Chapter 7 provides conclusions of the research and recommendations for future research on modelling financial markets.

Chapter 2

Financial Market Models

The financial market is a complex system. The modeling of the microscopic mechanisms behind the market and the market behavior, such as price trajectory and market crashes, has been widely studied, but the results are ambiguous.

2.1 Microscopic Mechanism Models

The microscopic mechanism model is constructed by the analysis of the microscopic mechanisms. It explains market phenomena, such as oscillations and distributions, and simulates market behaviors, like the Hierarchical model and Ising model in chapter 5. A microscopic mechanism model can be used to construct a prediction model, such as the Log-Periodic Power Law model.

2.1.1 Reaction-Diffusion Model

In 1997, Bak, Paczuski and Shubik proposed a reaction-diffusion model [4, 107] for the stock market. The traders are split into two groups: rational traders and noise traders. Rational traders, which are termed "fundamentalists", are those whose behaviors are derived from fundamental analysis of the stock price. Noise traders, which are termed "chartists", are those whose behaviors are governed solely by studying the market dynamics. This categorization is widely used in many subsequent microscopic model studies.

Suppose that the model market comprises only N traders and one stock with $N/2$ shares. Each trader has at most 1 share, so half of the traders have the stock and become potential

sellers. The other half traders then become potential buyers. There are several assumptions in this model:

- The ratio of fundamentalists to chartists is fixed.
- The traders in either of the two groups do not transfer to the other.
- Each trader has its own pricing strategy, which is fixed.
- The amounts of the dividend are set at two possible values only, distributed by a Bernoulli process, which is A with probability ρ or B with probability $1-\rho$.
- The annual interest rate is fixed at i.

Initially, the shares are randomly assigned to $N/2$ traders, including fundamentalists and chartists. Each trader determines his/her own willing-to-buy price p_b for potential buyers, or willing-to-sell price p_s for potential sellers in the range of $[0, p_{max}]$. The utility function for the fundamentalists determines the buying/selling price:

$$U = \nu \min[A, B] + (1-\nu)[\rho A + (1-\rho)B], \tag{2.1}$$

where ν represents the risk aversion posture of the trader ranged in $[0, 1]$ with $\nu = 1$ for total risk aversion and $\nu = 0$ for risk neutral. The values of ν are in any fixed distribution. Also, the buy/sell decision of fundamentalists is influenced by the interest rate i. They only buy the stock when its return rate is greater than $i + \Delta_1$, or sell when less than $i + \Delta_2$, where Δ_1 and Δ_2 are determined characteristic behavior parameters. For the chartists, the prices p_b and p_s at time t are uniformly distributed in $[0, p(t)]$ and $[p(t), p_{max}]$, respectively, or randomly picked from a previous transaction price. In the actual simulation, Bak et al. [4] neglected the effects of the distributions of p_b and p_s, and assumed that they are not important if the mean of p_b is less than the mean of p_s.

For each simulation step at time t, p_b and p_s are updated, and one of the N traders is randomly picked. If the trader is a buyer with p_b, then the trader with the least p_s is found and the values of p_b and p_s are compared. If $p_b \geq p_s$, the transaction is made and the p_s becomes the current market price $p(t)$. Otherwise, if the trader is a seller, the transaction is made at the greatest p_b under the condition $p_b \geq p_s$, and p_b becomes $p(t)$.

The model simulation results found that:

1. If the market has fundamentalists only, it converges to an equilibrium without transactions.

2. If the market is comprised by independent chartists, the price variation has a Hurst exponent $H = 1/4$.[1]

3. If the market is composed by chartists with self-simulation behavior, the price variation has a Hurst exponent $H = 1/2$, which is consistent with the random walk.

This model can explain the "fat tails" in the probability distribution for price variations from the microscopic mechanisms of the financial market.

2.1.2 Stochastic Multi-Agent Model

Lux proposed a new microscopic model, called stochastic multi-agent model, in 1999 [71, 72, 75]. This model separated the traders/agents in the market into three groups: fundamentalists, optimistic chartists, and pessimistic chartists. As shown in Figure 2.1 traders can transit from one group to another together with endogenous price changes resulting from the traders operations.

The transition probability of agents from one group to another in a unit time step is denoted by π. The probability of switches during a small time increment Δt is then $\pi\Delta t$. The first subscript of π denotes the group of inflow, and the second subscript denotes the group of outflow. The transition of agents between groups is the substantial difference from the reaction-diffusion model. The key of this model is to decide the function for the π's in Figure 2.1.

Suppose the total number of agents is N, containing n_f fundamentalists and n_c chartists, such that $N = n_f + n_c$. The n_c chartists are split up into n_+ optimistic chartists and n_- pessimistic chartists, such that $n_c = n_+ + n_-$. In the model, two factors affect the transition between the two groups of chartists: the majority opinion of their fellow agents $x = (n_+ - n_-)/n_c$ and the price trend $dp(t)/dt$. A transition function U_1 is defined as

[1]The Hurst exponent (H) is a statistical measure used to classify time series. $H = 0.5$ indicates a random series while $H > 0.5$ indicates a persistent series, and $H < 0.5$ indicates an anti-persistent series [78].

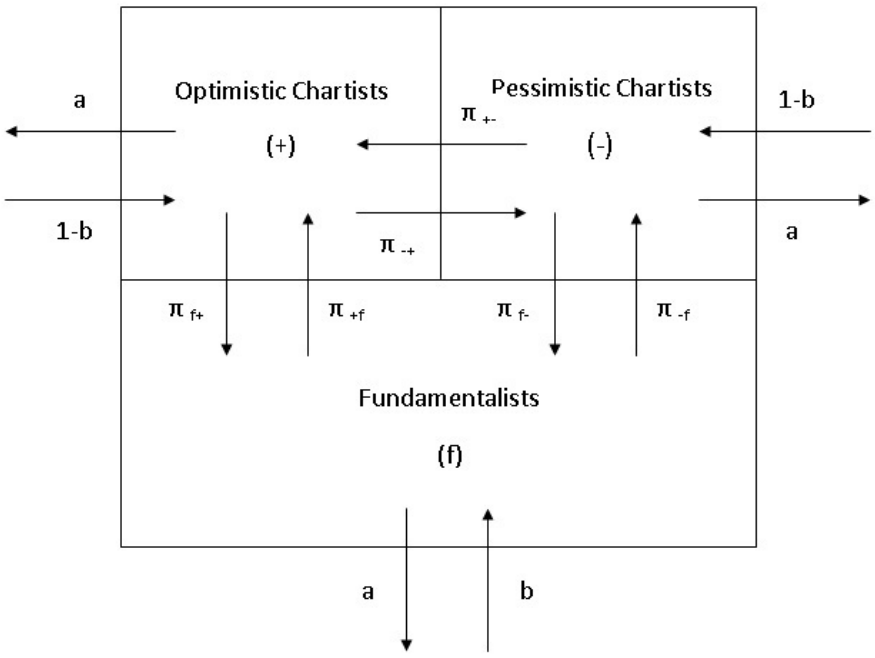

Figure 2.1: Stochastic multi-agents model.

the sum of those two factors weighted by the measure of their importances α_1 and α_2 respectively:

$$U_1 = \alpha_1 \frac{n_+ - n_-}{n_c} + \alpha_2 \frac{dp(t)}{dt} = \alpha_1 x + \alpha_2 \dot{p}. \tag{2.2}$$

The larger proportion of optimists in the chartists or the larger increase in price produces a higher probability that pessimistic chartists transit to optimistic chartists, and vice versa. Then

$$\pi_{+-} = \nu_1 \exp(U_1), \tag{2.3}$$

$$\pi_{-+} = \nu_1 \exp(-U_1), \tag{2.4}$$

where ν_1 is the frequency of revaluation of opinions. The transition function $U_{2,1}$ from the fundamentalists to the optimistic chartists is determined by the comparison between the relative profit of the chartists and the expected profit of the fundamentalists, which is defined as:

$$U_{2,1} = \alpha_3 \left[\frac{r + \frac{\dot{p}}{\nu_2}}{p} - R - s\frac{|p_f - p|}{p} \right], \tag{2.5}$$

where R is the average real risk-adjusted return available from other investments, p_f is the fundamental price, $r = R \cdot p_f$ is the nominal dividends, ν_2 is the frequency of reconsideration of trading strategies, and s is the discount factor due to the uncertain time horizon of return to the fundamental value. Similar to equations 2.3 and 2.4, the transition probabilities between fundamentalists and optimistic chartists are:

$$\pi_{+f} = \nu_2 \exp(U_{2,1}), \tag{2.6}$$

$$\pi_{f+} = \nu_2 \exp(-U_{2,1}). \tag{2.7}$$

Likewise, the transition function and transition probabilities between fundamentalists and

pessimistic chartists are defined as:

$$U_{2,2} = \alpha_3 \left[R - \frac{r + \frac{\dot{p}}{\nu_2}}{p} - s\frac{|p_f - p|}{p} \right], \tag{2.8}$$

$$\pi_{-f} = \nu_2 \exp(U_{2,2}), \tag{2.9}$$

$$\pi_{f-} = \nu_2 \exp(-U_{2,2}), \tag{2.10}$$

The price fluctuation is driven by the difference in total demand and total supply at the time. A variable named excess demand $D = D_c + D_f$, which is the sum of the excess demand of chartists and fundamentalists is defined. The excess demand of chartists is:

$$D_c = (n_+ - n_-)V_c, \tag{2.11}$$

where V_c is the average trading volume per transaction among chartists. The excess demand of fundamentalists is:

$$D_f = n_f \gamma \frac{p_f - p}{p}, \tag{2.12}$$

where γ is the strength of reaction of fundamentalists on price deviation. The price change is then:

$$dp/dt = \beta(D_c + D_f) = \beta \left[(n_+ - n_-)V_c + n_f \gamma \frac{p_f - p}{p} \right]. \tag{2.13}$$

The change of the number of agents in each group is determined by the transitions between each of two groups, which are controlled by the transition probabilities π, and the exit and entry probabilities at each time step, which are the probabilities a and b, respectively.

Using the model described above, Lux derived a dynamical system with three variables: the market confidence index $x = (n_+ - n_-)/n_c$, the market rationality index $y = n_f/N$,

and the price p. The three dimensional differential equations of the system are defined as:

$$\begin{cases} \dot{x} = 2\nu_1(1-a)(1-y)[\tanh(U_1) - x]\cosh(U_1) + \nu_2(1-a)(1-x^2)[\sinh(U_{2,1}) - \sinh(U_{2,2})] \\ \dot{y} = -\nu_2(1-a)y(1-y)[(1+x)\sinh(U_{2,1}) + (1-x)\sinh(U_{2,2})] - a(1-b)y + ab(1-y) \\ \dot{p} = \beta[x(1-y)V_c + y(p_f - p)V_f] \end{cases} \tag{2.14}$$

where $V_f \equiv \gamma N$, and U_1, $U_{2,1}$ and $U_{2,2}$ are as defined in equations 2.2, 2.5, and 2.8, respectively.

Through the simulation of this model, Lux and Marchesi found that the price variation has a "fat tail" distribution and is in accordance with absence of long memory in empirical financial returns. However, the absolute returns have strong volatility. Also, they asserted theoretically that the model has equilibrium and stability regimes. Yu, who followed Lux and Marchesi's model in later works [121, 120], successfully simulated four kinds of dynamic regimes in the model: fundamental equilibrium, non-fundamental equilibrium, periodicity, and chaos. The simulation shows the power law scaling and temporal dependence in volatility. One disadvantage of this model is that the fraction of chartists relaxes fast to about zero as $N \to 0$, which indicates that it has strong finite-size effects [26]. Another disadvantage of this model is that there are too many parameters. To simulate a realistic market, a lot of adjustments to the parameters are necessary to find the equilibrium.

2.1.3 Cont-Bouchaud Percolation Model

Cont and Bouchaud [18] proposed another microscopic model to explain the power law distribution with exponential tail in the price fluctuation of financial markets. This model simulates the herding behavior through the imitation among market traders. It observes that the return rates have a "fat tail" distribution. Therefore, the herding behavior is considered the microscopic mechanism of the "fat tail" distribution. This model does not include the effects of outside factors on the market and traders. The market traders form clusters through mutual communications and influences. All traders in the same cluster apply the same trading strategy. The simulation generates the macroscopic market behaviors and rules. The clusters are analogous to various funds, such as mutual fund and hedge fund.

The Cont-Bouchaud percolation model applies percolation theory to the stock market [98]. Consider N traders in the market trading one single asset. Any pair of traders are linked with the probability π. The connection probability π is constant and independent of the traders. All the connected traders form a trading cluster. With n_s clusters, a cluster i has s_i traders. Within every cluster, all traders have the same trading behavior. Three trading behaviors are denoted by $a_i = +1$ for buying, by $a_i = -1$ for selling, and by $a_i = 0$ for no trading action [99]. At a time t, the price change Δx during the time step Δt is determined by the excess demand $D(t)$:

$$\Delta x = x(t + \Delta t) - x(t) = D(t)/\lambda, \tag{2.15}$$

where λ is the market depth [10].[2] The excess demand is equal to the difference between the sum of buying orders and the sum of selling orders placed at time t. Thus,

$$\Delta x = D(t)/\lambda = \frac{1}{\lambda} \sum_{i=1}^{n_s} s_i a_i. \tag{2.16}$$

After the completion of the trading at time t, all traders are disconnected and form new clusters at time $t + \Delta t$. The behavior of every trader is independent to its behavior in the previous time step.

The model shows that the tails of the price change density asymptotically have an exponentially truncated power law form as $\Delta x \to \infty$:

$$p(\Delta x) \underset{|\Delta x| \to \infty}{\sim} |\Delta x|^{-u} \cdot \exp\left(-\frac{\Delta x}{\Delta x_0}\right), \tag{2.17}$$

where Δx_0 is the value after which the *pdf* is exponentially truncated and u is about $5/2$ for stocks and market indexes [18]. This implies that the return rate approximates the power law with a heavy tail when the microscopic market is approaching the critical point. According to the percolation theory, when a percolation system on a d-dimensional lattice closes to the critical point, the exponent is $5/2$ for $d > 6$. Hence, the Cont-Bouchaud model corresponds to the percolation model with 6 or higher dimensions.

Every agent is assumed to have the same probability of buying and selling, which means

[2] Market depth is the excess demand needed to move the price by one unit [18].

that the individual demand is symmetric:

$$P(a_i = +1) = P(a_i = -1) = \nu, \quad P(a_i = 0) = 1 - 2\nu. \tag{2.18}$$

The parameter ν is called the activity parameter. A larger value of ν indicates more transactions of the market. When ν is in certain ranges, the Cont-Bouchaud model simulation illustrates multi-scaling [13] and time-reversal asymmetry [16] of the return rate. Furthermore, varied expanded forms of the model generate many characteristics observed in financial markets. For instance, the different behavior of the price is barely seen if the fundamental value of the traded object is also taken into account other than the herding behavior of the traders [15]. If the probabilities of buying or selling are proportional to the price changes, the asymmetry between sharp peaks and flat valleys of the price trajectory in the real markets is reproduced [97]. The modified Cont-Bouchaud model is able to generate the power law distribution with a "fat tail" without fixing it around the critical point when the model parameters change during the simulation process [113] or when the average number of connections evolves over time [27, 101].

2.2 Market Prediction Models

Market prediction models are built to forecast the price direction of financial products through the study of historical and current macroscopic market data, such as price and volume. They are categorized by the modelling tools and types of data used, such as fundamental analysis,[3] technical analysis,[4] time series method,[5] and neural networks.[6] Stock traders are able to profit from the results of market prediction models if the prediction is accurate. Therefore, market prediction models are used practically by stock traders. However, the explanation of the prediction rules of these models is usually unclear and subjective.

[3]Fundamental analysis is the techniques for stock fundamental price determination and stock selection by applying the principles of the firm foundation theory [85].

[4]Technical analysis is the method of deducing pictured probable future trend of stock prices from the actual trading historical data for the determination of buy or sell time of a stock [25].

[5]Time series method is an analysis method of analyzing historical data and estimating future values of a time series as a linear combination of the historical data [108].

[6]Neural Networks is one of the machine learning techniques that use a set of samples to generate an approximation of the prediction function to forecast stock price [33].

Moreover, the efficiency of the market prediction model is disputed by the random walk hypothesis of stock prices and the efficient-market hypothesis [94].

2.2.1 Dow Theory

The Dow theory[8] is named after Charles H. Dow. Charles Dow wrote editorials focusing on the rail and industrial averages for The Wall Street Journal. The principles in those articles became the prototype of the Dow theory. From 1902 to 1929 William P. Hamilton extended Dow's work and in editorials to improve Dow's principles. Hamilton systematically explained the principles in his book The Stock Market Barometer' in 1922. In 1932, Robert Robea published The Dow Theory which was resulted from the study of the 252 editorials of Dow and Hamilton.

The core ideas of Dow theory are based in six tenets [25]:

1. **The averages discount everything.** This is the foundation of all technical analysis. It suggests that Dow theory solely focuses on price changes in the analysis.

2. **The three trends.** They are *primary* trends, *secondary* trends and *minor* trends.

3. **Three phases of a primary trend.** A primary uptrend is divisible into an *accumulation* phase, a *participation* phase and an *excess* phase. On the contrary, a primary downtrend is divisible into a *distribution* phase, a *panic* phase and a *discouraged selling* phase.

4. **The two averages must confirm.** In Dow theory, the two averages refer to the Dow Jones Industrial Average (DJIA) and Dow Jones Transportation Average (DJTA). The start or the end of a primary trend is confirmed only if both averages provide the same signal.

5. **Volume goes with the trend.** This means that the volume increases if the price movement has the same direction as the primary trend, and vice versa.

6. **A trend should be assumed to continue in effect until such time as its reversal has been definitely signaled.** This requires investors to distinguish whether a direction change of price movements is a reversal of the primary trend or a secondary trend.

An important part of Dow theory is the ability to recognize the market direction using trend analysis. The price movement trajectory is not a straight line. It has many oscillations between peaks and troughs. In a rising trend, there are a series of higher peaks and troughs. This means that a peak or trough is higher than preceding peaks or troughs. Conversely, there are a series of lower peaks and troughs in a downward trend. The basic tenets of Dow theory are based on the assumption that both primary trends and secondary trends cannot be manipulated. According to the tenets of Dow theory, the trading strategy is buying the stocks when the start of a primary uptrend is confirmed and holding them until the end of the primary uptrend is confirmed. One of difficulties for the users of Dow theory is the accurate and timely recognition of the start or reversal of a trend using the peak and trough analysis.

Dow theory asserts that the primary trend of the stock market could be accurately determined through the analysis of the general economic environment. The stock price is the most important information and it reduces the importance of any other information. As a result, Dow theory only uses daily closing prices for analysis, and pays no attention to the daily highs and lows. Dow theory is a technical analysis tool, which means it predicts price behaviours based on the investigation of price patterns. It requires its users to implement all its tenets carefully and objectively with regard to the price movements. Otherwise, it leads to a subjective analysis result and an erroneousl investment judgement. The accuracy of Dow theory depends on the understanding of the users. Different Dow theory users may produce different analysis results.

A decade after its invention, it is still widely used by investors and speculators, and forms parts of other theories, such as the Elliotte wave theory. There is no doubt that Dow theory is very important in the technical analysis of financial markets. However, its limitations make it difficult as the sole tool for investment strategy. One common criticism of the Dow theory is the possibility of missing a large part of a primary trend. The signal of a trend reversal is not confirmed until a higher or lower peak or trough appears. It results in a lower return rate compared to other analysis tools. Another problem of the Dow theory is its fourth tenet. The industries of the two averages do not dominate in the current economy. More averages should be considered to evaluate the economic environment. However, it is rare to see these averages confirm each other.

2.2.2 Elliott Wave Theory

Elliott wave theory, sometimes called the Elliott wave principle, is a technical analysis tool of price trends invented by Ralph Nelson Elliott in the 1930s [31]. It is a set of rules derived completely from empirical observations. It is used to analyze the stock market price or index trends. It is one of the most widely used analysis tools, but is difficult to understand. Elliott believes that the movements of commodity prices or stock prices are similar to those of tides and waves in the sea. Waves always come one ofter another in cycles following certain patterns. According to these patterns, the investors can predict the future price trends and apply them to trading strategies.

The core theory of the Elliott wave principle is the "eight-wave cycle". The analysis of the eight-wave cycle for prediction is as complicated as it is popular. The basic tenets of the Elliott wave principle are described below [31].

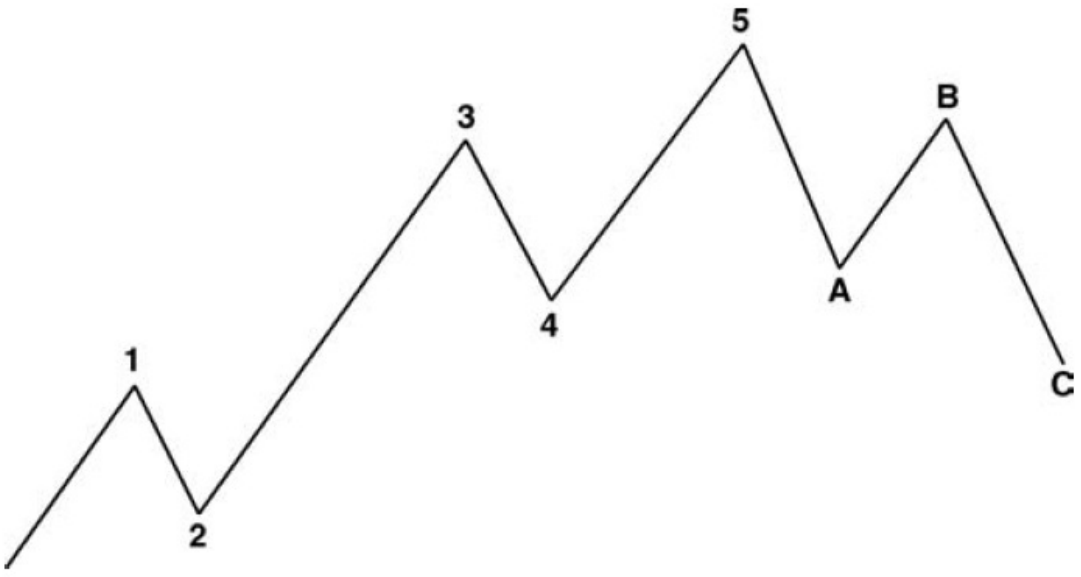

Figure 2.2: An example of a single wave structure. Reprinted from Copsey [19].

1. The stock market unfolds in a basic cycle pattern. Figure 2.2 is an example of a single eight-wave structure. A complete cycle comprises eight waves with five waves (waves 1 to 5) up followed by three waves (waves A to C) down. The five waves in the uptrend constitute the impulsive phase and the three waves in the downtrend constitute the

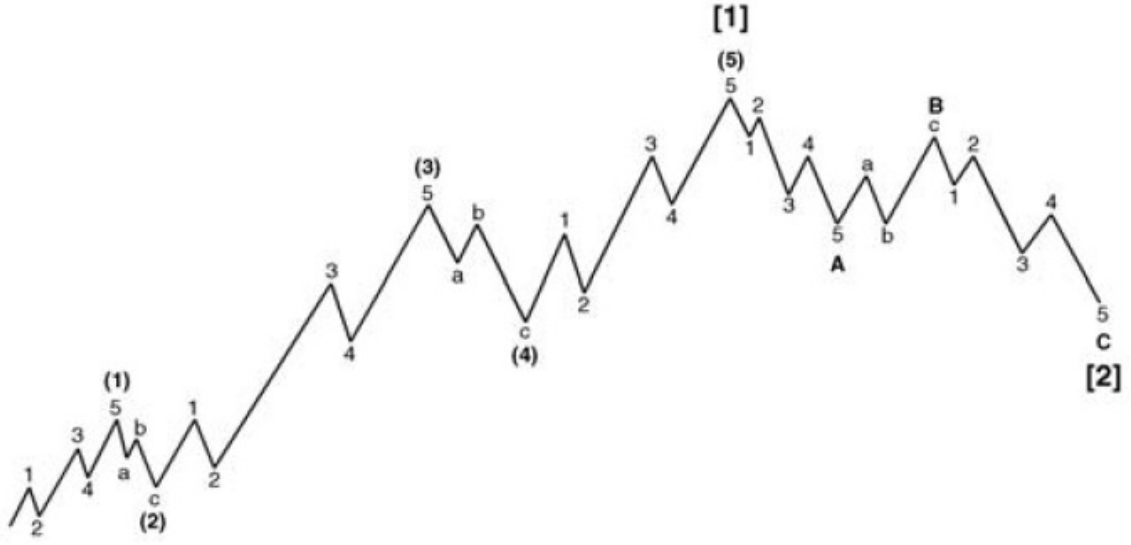

Figure 2.3: An example of complex wave structure. Reprinted from Copsey [19].

corrective phase.

2. A wave is always a component of another wave of higher degree and subdivides into waves of lower degree. Figure 2.3 shows an example of complex wave structure with multi-degrees. This exhibits a fractal structure of the stock price and index movements.

3. Among the three motive waves 1, 3 and 5, wave 3 is not the shortest one.

4. If any one of the three motive waves is extended, the other two have similar length and height.

5. A basic corrective wave is usually in a 3-wave sequence.

6. The Golden ratio is the numerical basis of the wave theory.

7. Classic ratio values of the relations between waves are $0.382, 0.5, 0.618$ and 1.618.

8. The bottom of wave 4 is higher than the top of wave 1.

9. The three most important aspects of the Elliott wave principle in order are: pattern, time and ratio.

10. The Elliott wave principle reflects the predominant psychology of the masses. The more participants the market has, the more accurate the prediction will be.

Both Dow theory and Elliott wave theory are essentially wave theories analogous to the movements of the sea. In comparison to Dow theory, Elliott's concept of wave action has a mathematical base, needs only one market average for interpretation, and unfolds according to a specific structure [31]. In addition, the Elliott wave principle is able to provide timely reversal information and a prediction of wave peaks. However, it is not easy for users of Elliott wave theory to derive predictions because of its disadvantages.

The first advantage is that there is no clear definition of a completed wave, so Elliotticians do not agree on the wave counts. The perfect 'five waves up three waves down' pattern does not happen in the real market most of time. Every Elliottician, including R. N. Elliott, has difficulty determining the end of a wave and the start of another wave. Different answers to this question make the wave counts completely subjective. It is dangerous for users making trading decisions to rely on the results of uncertain wave counts. Second, there are no clear rules for the confirmation of extension waves. Hence, the wave counts become random. Third, the complex rules of the theory forces the users to focus on individual fluctuations of price movements so that it is easy to neglect the big picture of the price foundation.

Many Elliott wave advocates have tried to improve the Elliott wave theory, such as Copsey [19] and Swannell [105, 104]. However, the subjectivity in its analysis means that controversy of Elliott wave theory continues.

There are some other wave theories, such as Kondratieff wave theory and the Gann wave theory. All of them are based on empirical observations and complement each other in practice. However, either their principles do not have mathematical foundation or they cannot be mathematically proved or simulated. When they assert a mathematical base, they possess mathematical rules matching some market values devoid of explanations.

Chapter 3

Fundamental Principles in Financial Markets

This thesis is based on the simulation of physical behaviors in financial studies, so that existing physical theories, analysis methods, and models can be used in the modelling of financial markets under specific assumptions. This chapter introduces the phenomena and principles of mathematics and physics that are used in later modelling analysis of financial markets.

3.1 Random Walk

The simplest random walk problem is the 1-dimension walk on a straight line [82]. Starting at time zero, the walker takes a step in one direction or the other with the same step length l and the same probability (50%) in each time interval τ. Therefore the expected value of all steps is zero. Figure 3.1 is an example of a single 1-dimension random walk with 1000 steps. The X axis denotes time t, and the Y axis denotes the displacement $d(t)$ of the walker after t steps. The walker has one step 'up' or 'down' with a step length '1' in each time interval '1'.

The earliest research on the random walk is from the rigorous results on a physical phenomenon called Brownian motion[110]. Considering n random variables with values of l or $-l$ presenting the random walk 'up' or 'down' with a step length of l in n steps, the displacement of the walker after n steps is the sum of the n random variables. Supposing

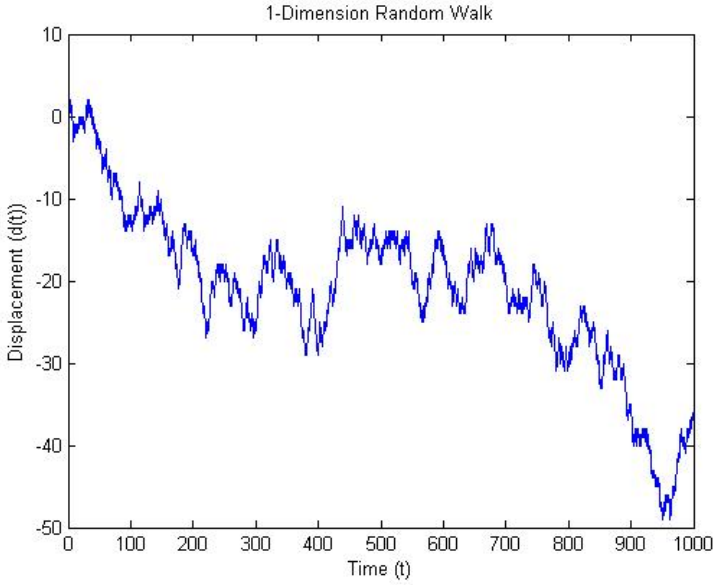

Figure 3.1: An example of a single 1-dimension random walk of 1000 steps with a step length '1' and same probability (50%) for either step direction at each time interval '1'.

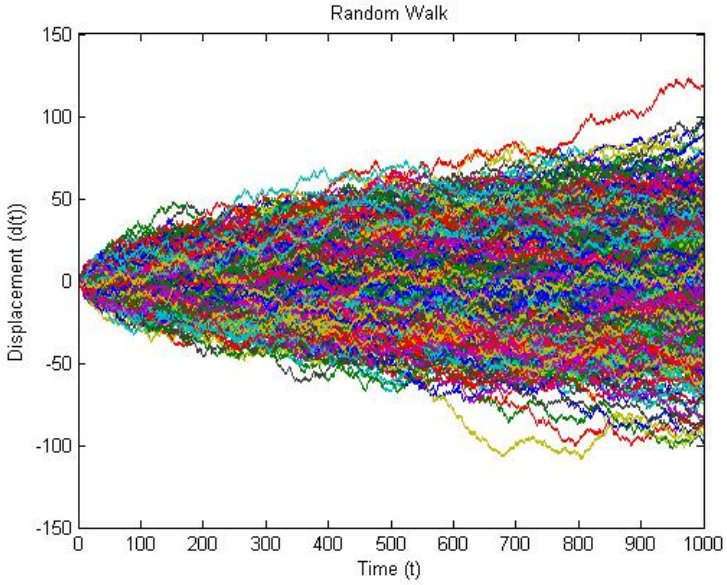

Figure 3.2: One thousand of 1-dimension random walks of 1000 steps with a step length '1' and same probability (50%) for either step direction at each time interval '1'.

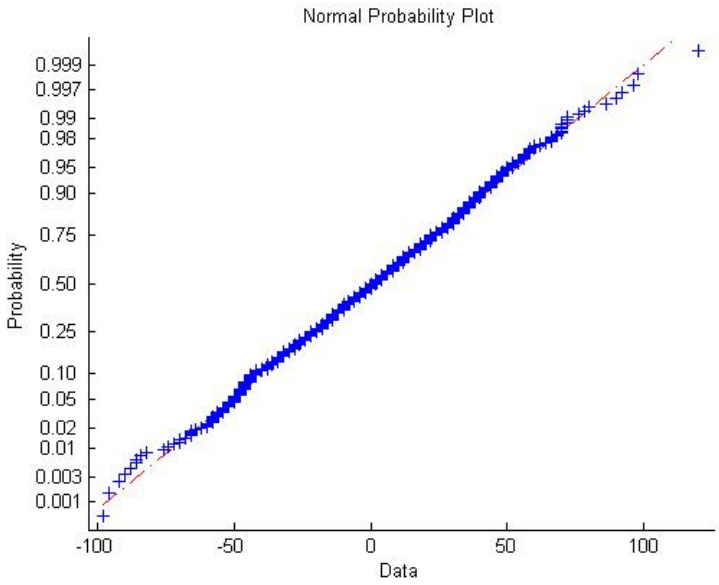

Figure 3.3: Normal probability plot for the displacement of the 1000 random walks at time $t = 1000$.

the probability of step 'up' (50%) or 'down' (50%) is the same, the Central Limit Theorem (CLT) implies that the displacement d of the walker should be normally distributed with mean zero and variance $n\sigma^2$ where σ^2 is the variance of each step, after n steps if n is large enough. Figure 3.2 is a simulation plot of 1000 random walks. Each random walk has 1000 steps with a step length '1' and same probability for either step direction at each time interval '1'. The normal probability plot for the displacement of these 1000 walkers after 1000 steps in Figure 3.3 shows that they are normally distributed with a mean of approximately zero. The calculated mean and variance of this simulation are -0.1380 and 973, respectively.

The expected value and variance of the displacement after n steps can be mathematically calculated [95]. Let $d(t)$ be the displacement of the walker at time t about time zero. The step length $l(t)$ is the random step made between time t and $t + \tau$ where τ is the time interval of one step. All $l(t)$'s are assumed to be independently identically distributed (iid) with a *pdf* $\Pi(l)$. Then the random walk can be described by the equation:

$$d(t + \tau) = d(t) + l(t) \tag{3.1}$$

This equation is a simple example of a stochastic process equivalent to a sum of multiple elementary step lengths:

$$d(t) = l(t-\tau) + l(t-2\tau) + \cdots + l(\tau) + l(0). \tag{3.2}$$

The variable $d(t)$ is defined as a sum of $n = t/\tau$ random variables l_i. It is assumed that all l_i's are distributed with *pdf* $\Pi(l)$ while the expected value of $d(t)$ can be written as:

$$< d(t) > = \sum_{i=1}^{n} < l_i > = n \ < l > = 0. \tag{3.3}$$

Since the l_is are iid, which implies they are uncorrelated with $< l_i l_j >= 0$ where $i \neq j$, the variance of $d(t)$ is:

$$\begin{aligned} < d^2(t) > \ - \ < d(t) > \ ^2 &= \sum_{i=1}^{n}\sum_{j=1}^{n} [\ < l_i l_j > \ - \ < l_i > \ < l_j > \ ] \\ &= \sum_{i=1}^{n}\sum_{\substack{j=1 \\ j\neq i}}^{n} [\ < l_i l_j > \ - \ < l_i > \ < l_j > \ ] + \sum_{i=1}^{n} [\ < l_i^2 > \ - \ < l_i >^2] \\ &= n[\ < l^2 > \ - \ < l >^2] \equiv n\sigma^2, \end{aligned} \tag{3.4}$$

where $\sigma^2 = < l^2 > \ - \ < l >^2$ is the variance of l. If the step length is 1, $l_i = \pm 1$, then the variance σ^2 is 1. The results in equations 3.3 and 3.4 are consistent with the statistics of $d(t)$ given by the CLT. This is an important prediction result of the random walk model. It implies that the variation of the displacement at time zero increases in proportion to the square root of time scale [94]. The recovery of the distribution of $d(t)$ concluded by CLT is shown in the next chapter by renormalization group analysis.

Random walk has been widely applied in several fields: dyadic expansions[1] in number theory, coin tossing and gains in gambling, and price change in stock markets [81]. Except for large fluctuations, the random walk model constitutes a good model of relative changes of stock market prices. Hence, the prediction results and analysis techniques on random walk models are applicable to the analysis of stock market models.

[1] A number expressed in the binary system.

3.2 Fractals

3.2.1 Introduction

Another important concept for financial markets is the '*fractal*'. Coastlines, cauliflower, ferns, mountains, and trees are real world examples of fractals. Although the idea of fractals has been studied since the 17^{th} century, the term "fractals" was not used until 1975 by Benoit Mandelbrot who is known as the "father of fractal geometry". There is no precise definition for fractals, because the idea of fractals is too broad. Although Mandelbrot [74] defines a fractal as a set whose Hausdorff-Besicovitch dimension strictly exceeds its topological dimension, he asserts that fractals "would do better without a definition". Sornette [95] interprets this technical definition of a fractal as "a rough or fragmented geometric shape that can be subdivided into parts, each of which is a reduced-size copy of the whole".

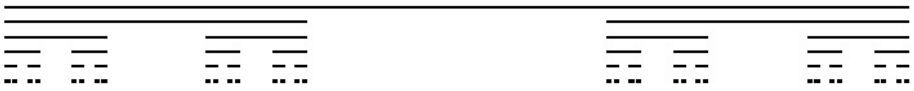

Figure 3.4: The top five iterations of the construction of the triadic Cantor set.

Fractals are based on the fact that the dimension of certain object structures are too narrow to possess a fine structure, or the structure is too irregular to be geometrically described or defined. Instead, several forms of self-similarity and scale invariance called a "fractal dimension" defines those structures [95]. The computation of the Hausdorff-Besicovitch dimension is very complicated, which makes it unsuitable as a computational tool [5]. The fractal dimension is not computationally equivalent to the Hausdorff dimension. Nevertheless, their values coincide for many examples of fractals, and the fractal dimension is much easier to compute. Figure 3.4 is the first five iterations of the triadic Cantor set from top to bottom. It is an example of a fractal set. The construction of the Cantor set starts from the top with a line segment of unit length, labeled the 0^{th} level. At level 1, it cuts out the middle third of level 0. The next iteration cuts out the middle thirds of the two remaining portions of level 1. The continuation of this process cuts out the middle thirds of the remaining portions of the previous level at each iteration, ad infinitum. Notwithstanding, the point becomes a line if the figure is enlarged. Running the iterations

till the n^{th} level as $n \to \infty$, each portion becomes a point with topological dimension 0. However, they are actually a set of discrete points. Obviously, the dimension of a set of discrete points should be different from that of a single point. This leads to the definition of the fractal dimension, which generalizes dimension to non-integer values.

3.2.2 Fractal Dimension

Consider the cases of standard geometry shapes with topological dimension 1, 2 and 3. First, consider a line segment of unit length 1. Equally divide it into three segments, then each of the divided line segments has length of 1/3, and the total number of congruent line segments is 3. This can be expressed by the equation:

$$3 = \left(\frac{1}{1/3}\right)^1.$$

Next, consider a unit square. Equally divide it into nine squares, then each side of the unit square is divided into three of length 1/3, which means the side length of those nine squares is 1/3. Similarly, this can be expressed by the equation:

$$9 = \left(\frac{1}{1/3}\right)^2.$$

Last, consider a unit cube. Equally divide it into 27 cubes, then each side of the unit cube is divided into three of length 1/3, which means the side length of those 27 cubes is 1/3. Thus, the expression is:

$$27 = \left(\frac{1}{1/3}\right)^3.$$

Notice that all these three cases satisfy one equation:

$$N = \left(\frac{1}{l}\right)^d, \tag{3.5}$$

where N is the total number of equal elements divided at the linear scale of l and d is the dimension of the object. Equation 3.5 suggests that the fractal dimension can be defined

as:

$$d_f = \frac{\ln(N)}{\ln(1/l)} \tag{3.6}$$

Returning to the Cantor set example in figure 3.4, the length of a line segment is reduced to 1/3 of the previous, and two segments are produced from one segment of the previous level. Hence, at the n^{th} level, $l = (1/3)^n$ and $N = 2^n$. Inserting into equation 3.6 these values produces the fractal dimension of the Cantor set:

$$d_f = \frac{\ln 2}{\ln 3} \approx 0.63093 \tag{3.7}$$

The definition of the fractal dimension in equation 3.6 produces an equivalent formula for the "mass" M of an object with fractal structure within a sphere of radius R and with a resolution ϵ:

$$M \propto \epsilon^d \left(\frac{R}{\epsilon}\right)^{d_f}, \tag{3.8}$$

where d is the dimension of the space in which the object is embedded and d_f is the fractal dimension given by equation 3.6 [95]. The equivalence of the two expressions is based on the identities $R \sim r/\epsilon$ and $M \sim N\epsilon^d$. For a fixed size object R, the observability of a mass M of the object decreases as ϵ^{d-d_f}, while the resolution of ϵ decreases.

3.2.3 Application in Financial Markets

The random walk is a fractal. It possesses the properties of self-similarity and scale invariance. Self-similarity refers to arbitrary sub-parts of an object that are statistically similar to the whole object provided a suitable magnification is performed in all directions and scale invariance refers to the remaining invariance under a specific scaling transformation. Figure 3.5 is an arbitrary random walk of 10000 steps. It shows that a sub-part (step 400 to 2000) is similar to itself with scaling in both time and displacement. As the random walk has a fractal structure, the notions of formula 3.8 are applicable to a random walk with an appropriate definition of "mass" and "resolution" in the random walk [94, 95].

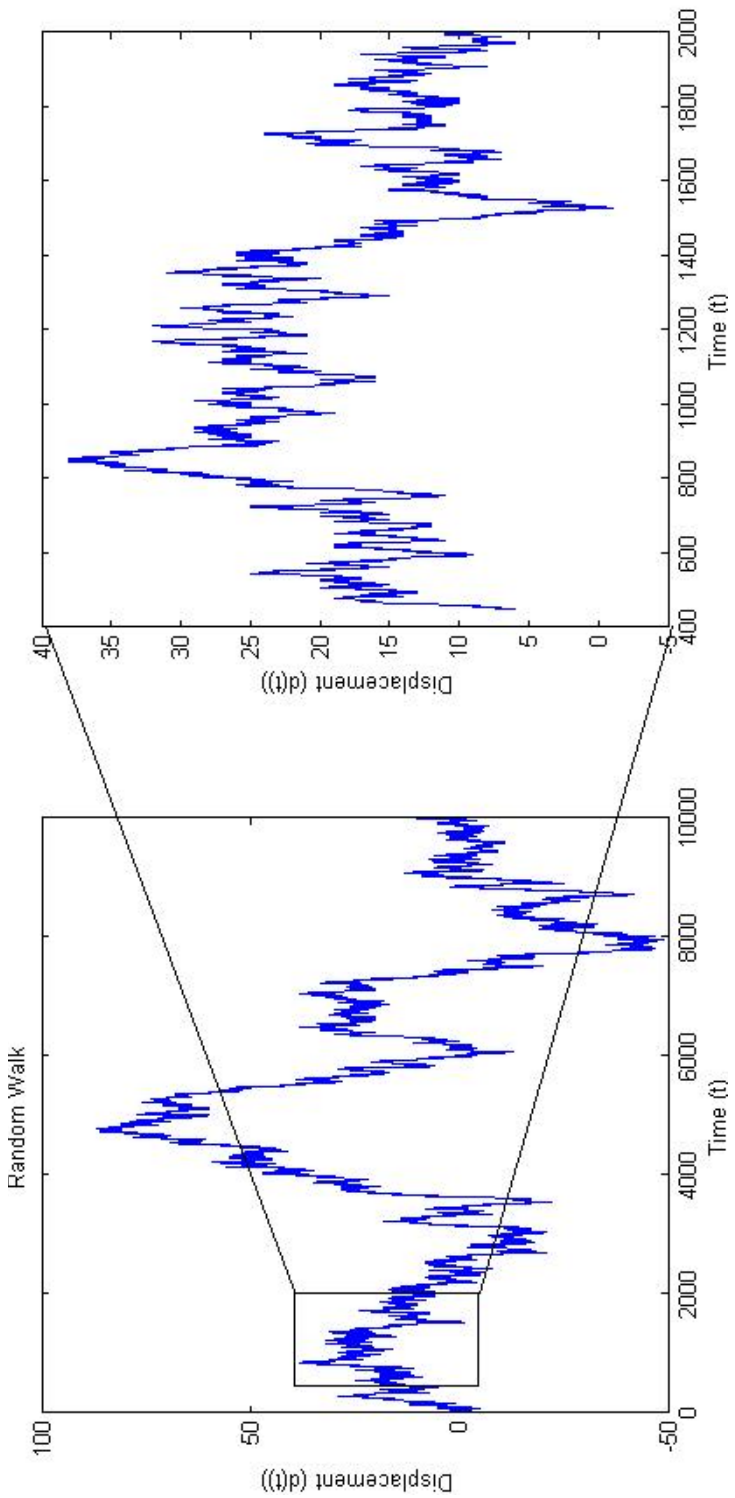

Figure 3.5: An example of self-similarity of random walk. The left diagram is an arbitrary random walk with 10000 steps. The right one is part of the whole of the left. They are similar at different time scales.

With the one-dimensional random walk discussed in the last section, the diffusion coefficient D is defined as:

$$D = \frac{\sigma_0^2}{2\tau}, \tag{3.9}$$

where $\sigma_0^2 =< l^2 > - < l >^2$ is the variance of step length l, and τ is the step time. The diffusion coefficient for the random walk is proportional to the product of l and the walking velocity c between two consecutive changes of direction with the relationship $l \sim c\tau$. Thus, the expression of the diffusion coefficient can be written as:

$$D \sim cl \sim c(c\tau) \sim c^2\tau \sim \frac{l^2}{\tau} \tag{3.10}$$

The variance of the total displacement of the random walk as defined in equation 3.4 is $\sigma^2 = n\sigma_0^2$, then

$$\sigma(t) \sim \sqrt{Dt} \sim l(\frac{t}{\tau})^{1/2} \sim \sigma_0(\frac{t}{\tau})^{1/2}. \tag{3.11}$$

The notation for "mass" of a random walk for the fractal structure can be generally measured by the arc length joining the starting point to the ending point in the space-time diagram with $d = 2$ dimensions

$$L \sim \sqrt{t^2 + \sigma^2(t)} \sim t\sqrt{1 + \left(\frac{\sigma}{t}\right)^2}. \tag{3.12}$$

Interpreting t as the resolution ϵ of the fractal structure notation in formula 3.8, the fractal dimension is equal to $d = 2$ minus the exponent of t. At small scales implying $t < \sigma_0^2/\tau$, then $(\sigma/t)^2 \gg 1$ in 3.12 becomes

$$L \sim t\sqrt{\left(\frac{\sigma}{t}\right)^2} \sim t\sqrt{\frac{\sigma_0^2}{\tau t}} \sim t^{1/2} \tag{3.13}$$

$$\Longrightarrow d_f = 3/2 \tag{3.14}$$

In contrast, at large scales, then $(\sigma/t)^2 \ll 1$ means $L \sim t$, so $d_f = 1$.

Section 3.1 shows that stock market price/index movements can be characterized by a

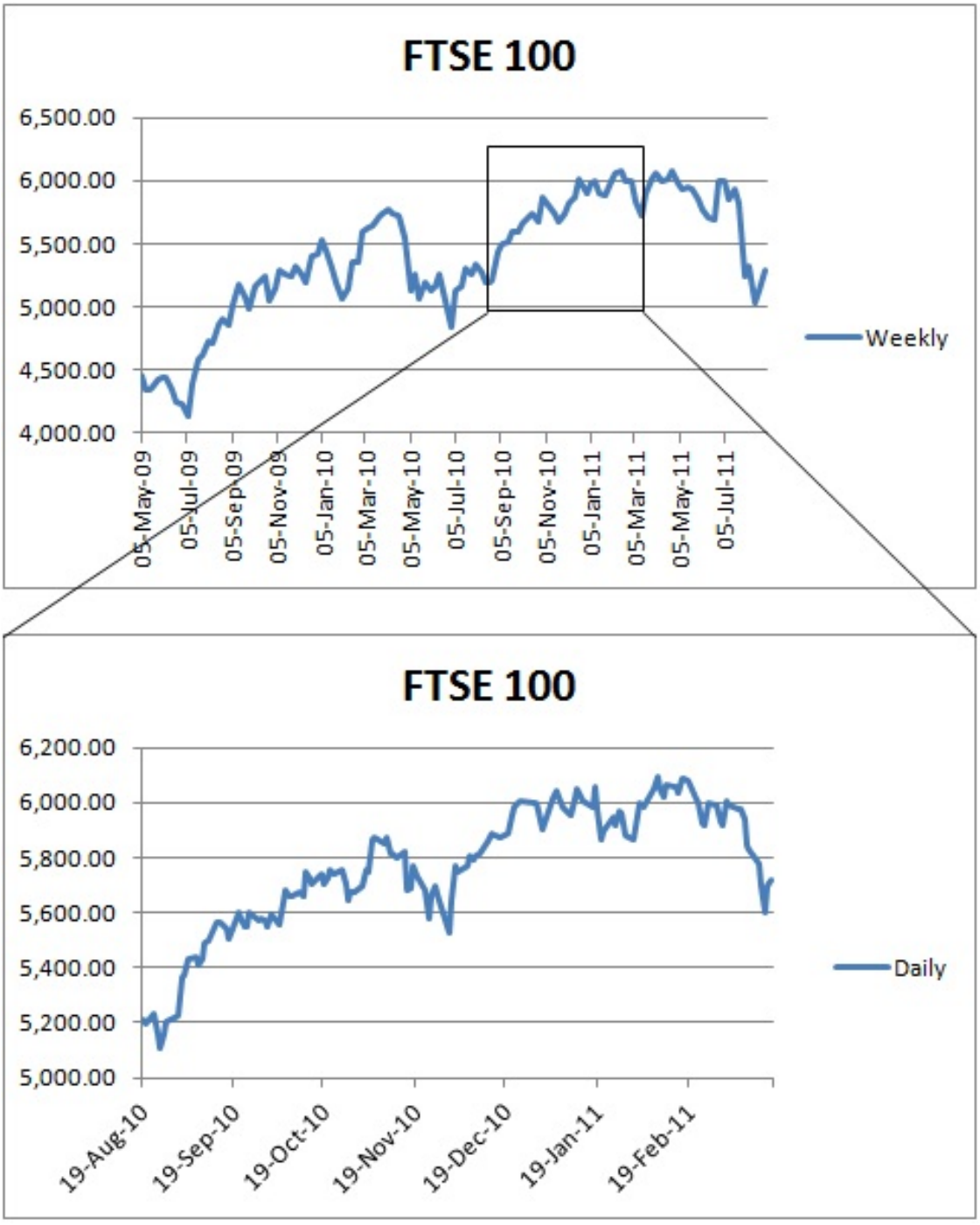

Figure 3.6: An example of fractal characteristics in stock index movements. The data is from FTSE 100 index at different time scales. The top figure is the plot of weekly end index values. The bottom one is the plot daily end index values. Both are observed to have similar movement patterns with different scales in both time and amplitude directions.

random walk. The above discussion shows that a random walk is a fractal. Therefore, stock price/index movements mimic fractals. Fractals are the basis of the Elliott Wave Theory that claims they have similar patterns along all time scales. The stock price or index can be observed per minute, hourly, daily, and weekly. The observation charts are very similar at each different time scale. Figure 3.6 shows an example of fractal properties that appears in Financial Times Stock Exchange (FTSE) 100 stock index[2]. The top figure is the plot of weekly closing index values. The bottom figure is the plot of daily closing index values. Both have similar movement patterns with different scales in both time and index value changes. The finding that these markets have properties of fractals is the principle in stock market technical analysis that history repeats itself.

The Elliot wave principle uses the fractal characteristic of the stock market in its analysis. As the patterns repeat themselves, to get an accurate identification of the Elliot wave pattern for prediction of stock market trends, it is necessary for an analyst to start with a 1-minute chart, to identify all Elliot waves, and then repeat this in half-hourly, hourly, daily and weekly charts. It is important to fit each small fluctuation to a pattern to make sense of the larger move in Elliot wave patterns.

Moreover, this characteristic produces a method to interpret why the price/index oscillations appear as in fractals. This is because each stock price/index movement is a manifestation of the actions (buy/sell) of a number of individual traders. Traders in the market are not isolated from each other. They exchange market information with their neighbours and interact on trading decisions (buy, sell or hold). In addition, the interaction behavior of the traders is observable at different levels, such as the single trader, the broker, the stock agent, the mutual fund, or the bank. Hence, a Hierarchical Model (HM) is feasible for stock price/index modelling. Since the hierarchical structure used to describe trader behavior is a fractal, the behavior of traders in the market also follows fractal. Accordingly, stock market price/index movement unfolds in similar manner.

This result is also useful for chartists who need to understand which time frame chart is more suitable. The market analysis system is made up of various technical tools, such as moving averages, draw-down limits, and trend lines, on the price chart. If the fractal

[2]FTSE 100 index is a stock index of 100 London Stock Exchange listed companies maintained by the FTSE Group, which is jointly owned by Financial Times and London Stock Exchange.

structure of the movement charts are fractals is understood, then the analysis of charts in different time frames is the same. Chart patterns occur in one time frame as frequently as others.

3.2.4 Hierarchical Model

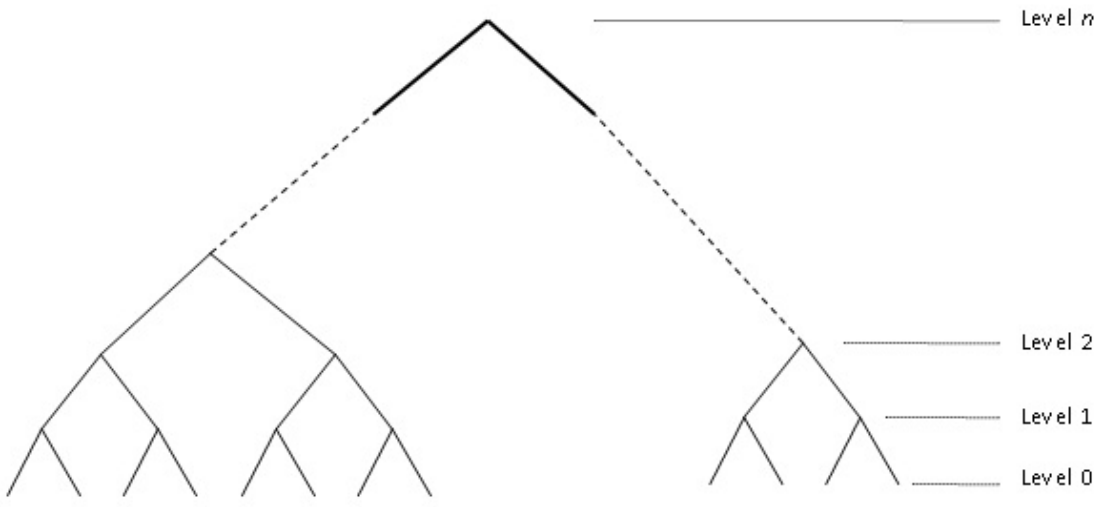

Figure 3.7: Example of Hierarchical Model structure with $n + 1$ levels and group members of 2.

The Hierarchical Model (HM) is suitable for data that come from multilevel or hierarchical social structures in which individuals are nested within larger social units [23]. A HM has the hierarchical structure in the form of a fractal tree [109]. Figure 3.7 is an example of hierarchical model structure with $n + 1$ levels and coordination number 2, which is an example of a perfect binary tree. Any subtree of it has the same structure at different scale, which is a fractal structure.

The assumption is that traders interact and influence the buy/sell behavior of each other. Therefore, individual traders are nested in a larger unit. For example, two traders in the same family can be grouped together, and the traders from two families in the same building may be grouped. In order to study the macroscopic behavior of stock market traders, it is reasonable to construct the trader behavior in the stock market with a hierarchical structure. The Renormalization Group (RG) approach is applicable to the hierarchical

structure for finding macroscopic properties from microscopic behavior. The stock market price can be viewed as the result of the sum of all trader behavior, and the fractal structure in trader behavior leads to the fractal visualization in stock prices. This is consistent with the observation in subsection 3.2.3. Sornette [86] proposed a hierarchical model for stock markets analogous to the hierarchical fiber rupture model with time-dependence. Under the assumption of hierarchical organization of traders, the model considers the individual traders as agents of order 0. Using the renormalization group formalism, the traders are organized in groups of m traders with $m = 2$, where each of these groups becomes a single agent of order 1. Agents of order 1 are organized in groups to form agents of order 2. Continuing this process, a hierarchical organization with order n and 2^n individuals is obtained. This HM is hierarchical because of the time traders spend making a buy order and the position of the agents according to their size. The detailed definition, calculation and application to the financial market is discussed in Chapter 5.

3.3 Phase Transition: Critical Phenomena

The terms "phase" and "critical" have many different meanings in the sciences. In the context of statistical physics, critical phenomena refer to the phenomena observed near a critical point [95]. A critical point is the point at which the system has a phase transition at all existing scales in the system [116]. A phase transition is a transformation of a system or matters from one phase or state to another [116].

There are plenty of examples of phase transition in nature. A common example is the transition from the three phases of H_2O: ice, water and vapor. Figure 3.8 is a phase transition diagram of H_2O [118]. Phase transitions for H_2O occur at certain combinations of temperature and pressure on the phase curves. Temperature and pressure at many scales of length have an equally important effect on the class of phenomena [116]. At each point on the phase curves there exists a phase transition and both phases coexist during the whole process of transition. Transitions between solid and gas occur only below the *Triple Point*. The phase boundary of liquid/gas disappears at the *Critical Point*. It is called the super critical liquid/gas state beyond the *Critical Point* where the distinction between the liquid and gaseous phases is almost non-existent [118].

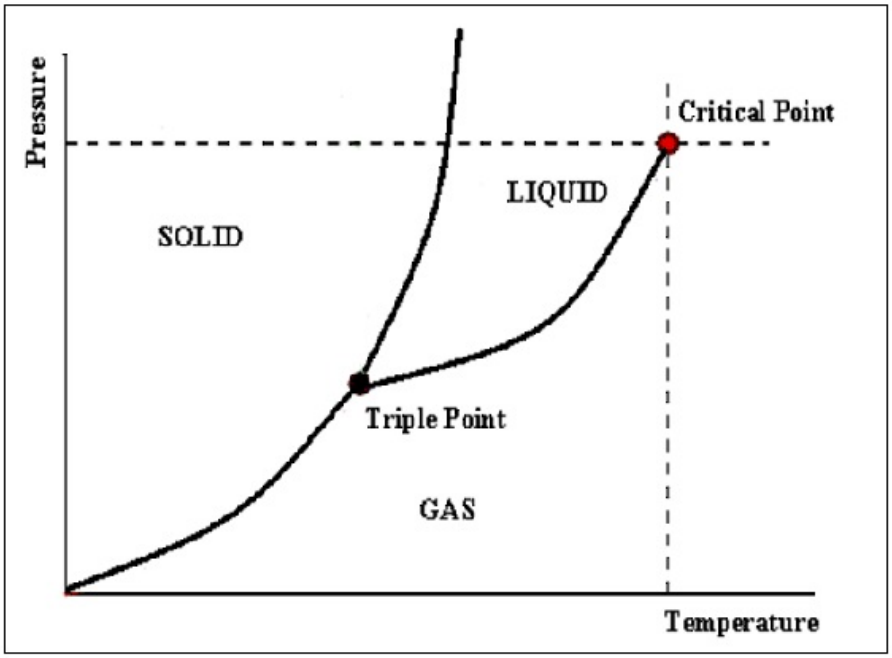

Figure 3.8: Phase diagram of H_2O with critical point. Ice is in solid phase, water is in liquid phase, and vapor is in gas phase. (Source: [118])

Phase transitions are classified into two basic categories: first-order and second-order phase transitions [44]. According to Ehrenfest, a phase transition is of order one if the first derivative of the free energy with respect to some other variables (e.g., temperature and pressure) are discontinuous. Similarly, the phase transition is of the order two if the first derivative is continuous across the phase transition, whereas the second derivative is discontinuous. However, this classification is incorrect for the derivative divergent cases. Landau proposed another classification scheme to deal with discontinuous second derivatives. In the first-order phase transitions the two phases coexist across the phase transition. The solid-liquid-gas phase transitions above are examples of first-order phase transitions. If the two phases do no coexist, it is classified as a second-order or higher-order phase transition. An example of second-order transitions is the ferromagnetic transition at the Curie point.

The word "critical", in the context of statistical physics, implies the occurrence of a second-order phase transition. Criticality at the microscopic level between the order and disorder equilibria transition produces a complex macroscopic behavior characterized by self-similarity of long-range correlations. Fundamentally, the critical behavior results from

the repeated interactions between microscopic elements which progressively phase up and construct a macroscopic self-similar state. Such non-analytic behavior can be dealt with by functions in response to the system at the mathematical level[95].

Many researchers, such as Kaizoji [55], Kiyono et al. [59], Sornette [94, 95], Vandewalle et al. [111], and Yalamova and McKelvey [118], view the financial market crashes as critical phenomena. The trader behavior in the stock market system is categorized into three macroscopic states: the fundamental phase, the bullish phase and the bearish phase. The transitions among these three phases are associated with approach to and retreat from criticality involving a combination of first- and second-order (or spinodal) phase changes [7]. The fundamental phase is a stable equilibrium. The trajectory of the market price performs like a random walk. If this fundamental equilibrium is broken, there is a first-order phase transition from the fundamental phase to the bullish phase. When the system stays in the bullish phase, speculative bubbles occur in the stock market. This accelerates the stock price in a power law. Furthermore, the increasing price stimulates more speculative bubbles. If the investment environment reaches the *critical point*, a second-order phase transition and market crash tends to be observed. This means that at the critical point, the investment attitude of all traders changes from "buy" to "sell". In contrast, if the investment environment reaches the phase transition boundary between bullish and bearish phase without reaching the *critical point*, a first-order phase transition is observed and a crash is avoided. For a certain range across the phase transition, the bullish phase and bearish phase coexist. In this instance, the market is in an anti-bubble regime and returns to the fundamental phase.

Chapter 4

Renormalization Group

4.1 Background

Renormalization Group (RG) theory was invented to address critical phenomena, which are a class of behaviors characterized by structures on many different scales and power law dependences of measurable quantities on the control parameters [95]. It enables a more accurate understanding of ordering phenomena such as magnetism and superconductivity [60]. The Renormalization Group analysis is a mathematical apparatus. It allows the decomposition of the problem of finding the "macroscopic" behavior of a large number of interacting parts into a succession of simpler problems. Every simplified problem has a decreasing number of interacting parts, whose effective properties vary with the scale of observation. The RG approach to modelling consists of breaking down an intractable problem with multiple scales of length into a sequence of smaller problems, each of which is confined to a single scale of length[116]. The RG approach works best when the system possesses the properties of scale invariance and self-similarity of the observables at the critical point.

4.2 Two Main Transformation

A classic example illustrating the RG process is to derive the central limit theorem in two RG steps: Decimation and Rescaling [95]. Decimation means "decimating" the degrees of freedom to transform the problem into a simpler one. The step of decimation finds out

whether or not the distribution type of the X sum is the same as the original distribution type. Rescaling means rescaling the sum of the variables. When a variable is rescaled, the cumulants, which characterizes the *pdf*, are also rescaled. After these two steps, the same *pdf* as the initial *pdf* is found if the distribution is stable.[1]

4.2.1 Decimation

The very first step in RG analysis is to eliminate the degrees of freedom representing short-distance fluctuations involving a certain interval of small wave lengths [62]. There are several types of RG transformations for this step. Conceptually, the RG decimation or thinning of degrees of freedom is the simplest [63]. Originally, the decimation technique is only for exact one-dimensional models with nearest-neighbor tight-binding [115]. Kushnir and Rosenstein [63] illustrated how to perform the decimation transformation in more than one dimension in free theory.

Consider the displacement of a 1-dimensional random walk problem after N steps, to which the decimation technique can be applied. As discussed in Section 3.1, the random walk can be viewed as a stochastic process equivalent to a sum of multiple elementary step lengths. Each step length is identical and independent. In a more general case it is substantially a problem of sum (X) of N random *iid* variables (X_1, X_2, ..., X_N):

$$X = X_1 + X_2 + \ldots + X_N, \tag{4.1}$$

where $N = 2^m$. It is possible to sum each two of these variables to a new variable X'_i as $X'_1 = X_1 + X_2$, $X'_2 = X_3 + X4$, ..., $X'_{N/2} = X_{N-1} + X_N$. Then the original sum variable X is rewritten as:

$$X = X'_1 + X'_2 + \ldots + X'_{N/2}, \tag{4.2}$$

where X'_js are *iid* as their summands are *iid*. This operation decimates half of the degrees of freedom.

[1] A stable distribution function is defined as one such that if X_1 and X_2 are independent random variables with the given distribution, then for every $a_1 > 0$, $a_2 > 0$, there exists $a_3 > 0$ satisfying $a_1X_1 + a_2X_2 = a_3X_3$, where X_3 again has the given distribution. Examples of stable distributions are Gaussian distribution and Lévy distribution. [67].

The probability of the new $N/2$ variables X'_j is the joint probability of X_{2j-1} and X_{2j}. Suppose all the N random variables X_i are *iid* distributed with *pdf* $p(x_i)$, then the *pdf* of X'_j is the integral of the product of $p(x_{2j-1})$ and $p(x_{2j})$ for all values of x_{2j-1} and x_{2j} that satisfy the condition of $x_{2j-1} + x_{2j} = x'_j$. All X'_js have the same *pdf* $p'(x'_j)$. If this *pdf* p' is expressed in terms of p, the decimation process can be repeated m times to reach the *pdf* of the sum $p(x)$. To simplify the notation, let $X = X'_j$, $X_1 = X_{2j-1}$, and $X_2 = X_{2j}$ in the equation:

$$\begin{aligned} p'(x) &= \int_{-\infty}^{\infty} dx_1 p(x_1) \int_{-\infty}^{\infty} dx_2 p(x_2) \delta(x - (x_1 + x_2)) \\ &= \int_{-\infty}^{\infty} dx_1 p(x_1) p(x - x_1), \end{aligned} \tag{4.3}$$

where δ is the Dirac delta fuction defined as:

$$\delta(x) = \begin{cases} \infty, & x = 0 \\ 0, & x \neq 0 \end{cases}$$

constrained with the identity

$$\int_{-\infty}^{+\infty} \delta(x) dx = 1.$$

Equation 4.3 shows that p' is defined as the *convolution* of two identical *pdf*s p.

Convolution

The *convolution* of two functions f and g is defined as:

$$(f * g)(t) = \int_{-\infty}^{+\infty} f(\tau) g(t - \tau) d\tau \tag{4.4}$$

$$= \int_{-\infty}^{+\infty} f(t - \tau) g(\tau) d\tau, \tag{4.5}$$

which is the integral of the product of f and g for all values of τ [21].

The convolution of two *pdf*s, $p_1(x)$ and $p_2(x)$, noted as $p = p_1 * p_2$, is defined as:

$$p(x) = \int_{-\infty}^{+\infty} p_1(x_1) p_2(x - x_1) dx_1, \tag{4.6}$$

which is the *pdf* of the random variable $X = X_1 + X_2$ [95].

The *Fourier Transform* of $f(x)$ [21] is defined as:

$$F(k) = \int_{-\infty}^{+\infty} f(x)e^{-ikx}dx \tag{4.7}$$

$$\text{with inverse } f(x) = \int_{-\infty}^{+\infty} F(k)e^{ikx}\frac{dk}{2\pi}. \tag{4.8}$$

If each *pdf* p above has Fourier transform $\hat{p}$, for the convolution $p = p_1 * p_2$, then

$$\hat{p}(k) = \hat{p}_1(k)\hat{p}_2(k), \tag{4.9}$$

which is called the *Fourier Convolution*. The Fourier transform of $p(x)$ is also called the *characteristic function* $\hat{p}(k)$, which is the expected value of e^{ikX}, in probability theory [114]. Extending the *pdf* convolution of two random variables, for a sum of N independent random variables, its *pdf* is the convolution of the N *pdf*s. A general form for equation 4.9 is then:

$$\hat{p}(k) = \hat{p}_1(k)\hat{p}_2(k)\ldots\hat{p}_N(k). \tag{4.10}$$

Moments, Cumulants and Characteristic Function

The n^{th}-order moment of a random variable X about the origin is defined by the expected value of the n^{th} power of x, denoted by:

$$m_n = <x^n> = \int_{-\infty}^{+\infty} x^n p(x)dx, \tag{4.11}$$

where $p(x)$ is the *pdf* of X [65]. From the right hand side (right hand side) of the definition equation 4.11, it is obvious that the existence of m_n depends on the convergence of $x^n p(x)$, which means that the decay of $p(x)$ has to be faster than the increase of x^n for large values of $|x|$. Although it is not always correct that random variables with the same moments have the same distribution, the knowledge of all moments has the same level of importance as the functional behavior form of the *pdf* [70].

The characteristic function of a *pdf* [22] is defined by the Fourier transform of the *pdf*:

$$\hat{p}(k) = \int_{-\infty}^{+\infty} \exp(ikx)p(x)dx. \tag{4.12}$$

The n^{th}-order moment of the *pdf* is obtained from the n^{th} successive derivatives of the characteristic function at $k = 0$:

$$m_n = (-i)^n \left.\frac{d^n\hat{p}(k)}{dk^n}\right|_{k=0}. \tag{4.13}$$

The n^{th}-order cumulant of the *pdf* is defined by the n^{th} successive derivatives of the logarithm of its characteristic function at $k = 0$:[22]

$$c_n = (-i)^n \left.\frac{d^n \ln\hat{p}(k)}{dk^n}\right|_{k=0}. \tag{4.14}$$

The Taylor series expansion of the characteristic function and the logarithm of the characteristic function shows that the characteristic function can be rewritten in terms of the moments or the cumulants provided that all moments and cumulants exist:

$$\begin{aligned}\hat{p}(k) &= \sum_n^{\infty} \left[\frac{m_n}{n!}(ik)^n\right] \\ &= \exp\sum_n^{\infty} \left[\frac{c_n}{n!}(ik)^n\right].\end{aligned} \tag{4.15}$$

In the expansion of equation 4.15, a moment m_n is a combination of the first n cumulants, and the n^{th} cumulants can be expressed as an n^{th}-degree polynomial of the first n moments [57]. The first moment and cumulant are the same and equal to the mean of the variable. The second cumulant is the variance of X written as $c_2 = m_2 - m_1^2 = \sigma^2$. In contrast, the second moment is the expected value of X^2 expressed as $m_2 = c_2 + c_1^2 = < x^2 >$. With such relationships between the moments and cumulants, under additional analyticity conditions of the characteristic function in the neighborhood of the origin, the knowledge of all cumulants determines the functional behavior of the *pdf*. Specifically, a distribution with identical zero cumulants of order larger than two follows the Gaussian law.

In equation 4.9, the Fourier transform of the *pdf* for the convolution of two *pdf*s is equal to the product of the Fourier transform of the two *pdf*s respectively. As the Fourier

transform of a *pdf* is its characteristic function, given in equation 4.15, suppose the two convolution *pdf*s have the cumulants $c_n^{(1)}$ and $c_n^{(2)}$, then:

$$\begin{aligned}\exp\sum_n^\infty \left[\frac{c_n}{n!}(ik)^n\right] &= \exp\sum_n^\infty \left[\frac{c_n^{(1)}}{n!}(ik)^n\right] \exp\sum_n^\infty \left[\frac{c_n^{(2)}}{n!}(ik)^n\right] \\ &= \exp\left\{\sum_n^\infty \left[\frac{c_n^{(1)}}{n!}(ik)^n\right] + \sum_n^\infty \left[\frac{c_n^{(2)}}{n!}(ik)^n\right]\right\} \\ &= \exp\left\{\sum_n^\infty \left[\frac{c_n^{(1)} + c_n^{(2)}}{n!}(ik)^n\right]\right\}. \end{aligned} \tag{4.16}$$

Thus, another useful property of cumulants is shown that

$$c_n = c_n^{(1)} + c_n^{(2)}. \tag{4.17}$$

With the above attributes of convolution and cumulants, it is simple to obtain the following results of the first step of decimation from equation 4.3:

$$\hat{p}'(k) = \hat{p}(k)\hat{p}(k) = \hat{p}^2(k) \tag{4.18}$$

$$\text{and } c'_n = 2c_n. \tag{4.19}$$

Equation 4.19 provides the *pdf* of X', the sum of two *iid* variables X in terms of the cumulants of X:

$$p'(x', c'_1, c'_2, \ldots, c_l, \ldots) = p'(x', 2c_1, 2c_2, \ldots, 2c_l, \ldots). \tag{4.20}$$

Repeating such a decimation process m times (total number of variables is assumed to be $N = 2^m$), the distribution of $X^{(m)}$ is obtained as:

$$p^{(m)}(x^{(m)}, c_1^{(m)}, c_2^{(m)}, \ldots, c_l^{(m)}, \ldots) = p^{(m)}(x^{(m)}, 2^m c_1, 2^m c_2, \ldots, 2^m c_l, \ldots), \tag{4.21}$$

where $X^{(m)}$ is actually the X in equation 4.1, which is the sum of X_1, X_2, …, X_N.

As the cumulants play the crucial role of the distribution, the *pdf*

$$p^{(m)}(x^{(m)}, 2^m c_1, 2^m c_2, \ldots, 2^m c_l, \ldots)$$

is equivalent to the *pdf* $p(x^{(m)}, 2^m c_1, 2^m c_2, \ldots, 2^m c_l, \ldots)$ at different scales. To find the exact *pdf* of the sum, a rescaling step is necessary.

4.2.2 Rescaling

The second step of the iterative RG procedure is rescaling, which expresses the function in terms of rescaled quantities such that it has the same form as that before the decimation transformation [62]. An inherent property of a *pdf* is the normalization constraint that $\int_{-\infty}^{+\infty} p(x) = 1$. In the right hand side of equation 4.20, the *pdf* p' for X_i', which is the sum of two *iid* variables, has a different form from the original *pdf* p of those two *iid* variables X_i, because the scales of X_i' and X_i are different. To derive the same form of p, it needs to renormalize the *pdf* to conserve probabilities, which is the process of the rescaling step, such that X_i' is changed to the same scale of X_i.

Now we need to find the scale for X_i'. Recall that the random walk problem is the sum of n random variables with values of $\pm l$. Section 3.2.3 shows that the diffusion behavior of a random walk follows $L(t) \sim t^{1/2}$. This is equivalent to $X(N) \sim N^{1/2}$ in the case of the sum of N random variables. For two *iid* random variables X, whose N is 1, the sum of them X' with $N = 2$, we have $X' \sim 2^{1/2}$. If defining a scalar s, such that the X_i' is changed to X_i'/s, then $s = 2^{1/2}$. As the variable is scaled by s, the cumulants c_l, representing the distribution behavior of the random variable, are scaled by s^l, where l is the order of the cumulants. In terms of the conservation of probabilities $p(y)dy = p(x)dx$, a factor of $1/s = 2^{-1/2}$ needs to be multiplied by the probability. Accordingly, equation 4.20 is rewritten as:

$$\begin{aligned} p'(x', c_1', c_2', \ldots, c_l, \ldots) &= p'(x', 2c_1, 2c_2, \ldots, 2c_l, \ldots) \\ &= \frac{1}{2^{1/2}} p(\frac{x'}{2^{1/2}}, 2^{1-1/2}c_1, 2^{1-2\cdot 1/2}c_2, \ldots, 2^{1-l\cdot 1/2}c_l, \ldots). \end{aligned} \tag{4.22}$$

Similarly, repeating this rescaling process after each of decimation step, equation 4.21 becomes:

$$\begin{aligned} & p^{(m)}(x^{(m)}, c_1^{(m)}, c_2^{(m)}, \ldots, c_l^{(m)}, \ldots) \\ =& \frac{1}{2^{1/2m}}\, p\left(\frac{x^{(m)}}{2^{1/2m}}, 2^{m(1-1/2)}c_1, 2^{m(1-2\cdot 1/2)}c_2, \ldots, 2^{m(1-l\cdot 1/2)}c_l, \ldots\right). \end{aligned} \tag{4.23}$$

When $m \to +\infty$, all cumulants with an order greater than two in equation 4.23 approach zero:

$$p^{(m)}(x^{(m)}, c_1^{(m)}, c_2^{(m)}, \ldots, c_l^{(m)}, \ldots) \to \frac{1}{\sqrt{N}}\, p\left(\frac{x^{(m)}}{\sqrt{N}}, \sqrt{N}c_1, c_2, c_3 = 0, \ldots, c_l = 0, \ldots\right). \tag{4.24}$$

The *pdf* on the right hand side of equation 4.24 shows that the distribution is Gaussian as discussed in Section 4.2.1. Therefore, the *pdf* $f(x)$ for the sum of N *iid* random variables is:

$$\begin{aligned} f(x) &= \frac{1}{\sqrt{N}} \frac{1}{\sqrt{2\pi\sigma^2}} \exp - \frac{(x/\sqrt{N} - \sqrt{N}\mu)^2}{2\sigma^2} \\ &= \frac{1}{\sqrt{2\pi N\sigma^2}} \exp - \frac{(x - N\mu)^2}{2N\sigma^2}. \end{aligned} \tag{4.25}$$

This shows that the distribution of the sum of N *iid* random variables with same mean μ and variance σ converges to the Gaussian Law when $N \to \infty$ with mean $N\mu$ and variance $N\sigma^2$, which proves the central limit theorem. In addition, this result shows that the Gaussian law is a fixed point for the transformation from p_{m-1} to p_m in the form of:

$$p_m(x) = \int_{-\infty}^{+\infty} dx_1 p_{m-1}(x_1) p_{m-1}(x - x_1), \tag{4.26}$$

where $p_m(x)$ is the *pdf* of the sum of $N = 2^m$ *iid* random variables.

In the RG process, the combined effect of decimation and rescaling is taken into account through a modification of the coupling constants. There are many RG applications. Decimation is not the only way to reduce the degrees of freedom in the RG transformation. Rescaling is a key step to find the accurate function describing the macroscopic behavior. There is no single universal method for rescaling. Kopietz [62] lists several rescaling methods for important cases.

4.3 General Formalism

4.3.1 Elements of RG theory

The specific problem of the distribution of the sum of N *iid* random variables in the last section shows how the RG analysis follows the "divide and conquer" proverb by organizing the description of a system scale-by-scale [95]. In studies of critical phenomena, the overall behavior of the system is the foremost concern. Such a behavior is viewed as the aggregation of an ensemble of arbitrarily defined sub-systems, as is the behavior of each of these sub-systems. There are a lot of different formalisms in explaining RG approach. They have different analysis techniques, but the same ideas [112]. The Discrete Scale Invariance(DSI) formulation is one of those developed for critical phenomena, such as earthquake faults [84] and financial market crashes. This RG framework leads to a simple power law, or a power law associated with complex exponents, which manifests itself in data by log-periodic corrections to scaling[93]. The presentation in this section follows Sornette [95].

The RG analysis is based on the characteristic of scale invariance and self-similarity. DSI is a weaker kind of scale invariance where the observable system obeys scale invariance only for specific countable, but infinite scales[93]. For illustration purposes, consider the example of free energy F behavior in a spin system. Scale invariance means that the observation F depends on a control parameter x, for an arbitrary change of $x \to \lambda x$. There exists a number μ such that

$$F(x) = \mu F(\lambda x).$$

In the RG formalism, the scale on x defines a RG flow map. To study observable behavior close to the critical point using the RG formalism, we define the control parameter $x = |T_c - T|$ as the distance of temperature T to the critical point T_c, and the transformation of the free energy F under the RG flow map $x' = \phi(x)$ representing the relationship of the values of the free energy F at the temperatures T and T', such that:

$$F(x) = g(x) + \frac{1}{\mu} F[\phi(x)], \tag{4.27}$$

where μ is a constant describing the rescaling of free energy upon the rescaling of temperature distance to the critical point and $g(x)$ defines the non-singular part of $F(x)$. Without

loss of generality, we can assume that $F(0) = 0$.

To find the solution for F in equation 4.27, first, we must define a recurrence relation:

$$f_n(x) = g(x) + \frac{1}{\mu} f_{n-1}[\phi(x)], \qquad n = 1, 2, \ldots \tag{4.28}$$

with $f_0(x) = g(x)$. Then we can list the equation of f_n as following:

$$\begin{aligned}
f_1(x) &= g(x) + \tfrac{1}{\mu} f_0(\phi(x)) &&= g(x) + \tfrac{1}{\mu} g(\phi(x)) \\
f_2(x) &= g(x) + \tfrac{1}{\mu} f_1(\phi(x)) &&= g(x) + \tfrac{1}{\mu}\left[g(\phi(x)) + \tfrac{1}{\mu} g(\phi(\phi(x)))\right] \\
&&&= g(x) + \tfrac{1}{\mu} g(\phi(x)) + \tfrac{1}{\mu^2} g(\phi^{(2)}(x)) \\
f_3(x) &= g(x) + \tfrac{1}{\mu} f_2(\phi(x)) &&= g(x) + \tfrac{1}{\mu}\left[g(\phi(x)) + \tfrac{1}{\mu} g(\phi(\phi(x))) + \tfrac{1}{\mu^2} g(\phi(\phi(\phi(x))))\right] \\
&&&= g(x) + \tfrac{1}{\mu} g(\phi(x)) + \tfrac{1}{\mu^2} g(\phi^{(2)}(x)) + \tfrac{1}{\mu^3} g(\phi^{(3)}(x)) \\
\ldots\ldots & \qquad \ldots\ldots\ldots\ldots\ldots \\
f_n(x) &= g(x) + \tfrac{1}{\mu} f_{n-1}(\phi(x)) &&= \textstyle\sum_{i=0}^{n} \frac{1}{\mu^i} g[\phi^{(i)}(x)], \qquad n > 0.
\end{aligned}$$

The superscripts (i) of $\phi^{(i)}(x)$ represent the number of compositions of the function. The free energy is then equal to f_n as $n \to \infty$:

$$F(x) = \lim_{n\to\infty} f_n(x) = \sum_{i=0}^{\infty} \frac{1}{\mu^i} g[\phi^{(i)}(x)] \tag{4.29}$$

The usefulness of the RG analysis formulation is to mathematically reconstruct the nature of the critical singularities from the embedding of scales, so that the problem is translated into a mathematical problem of critical singularity. In this formalism example, the critical point is described by the singular point of $F(x)$, and the singularity of $F(x)$ corresponds to the unstable fixed point on the RG flow map $\phi(x)$ that describes the change of scale. The unstable fixed point of $\phi(x)$ exists when the absolute value of its derivative at the corresponding fixed point is greater than 1, and is written as $|\lambda| > 1$ where $\lambda = d\phi/dx|_{x=\phi(x)}$. A singular point x of the function $F(x)$ exists when a finite k^{th} derivative of F is infinite at x. Since $F(x)$ is expressed as a sum, its k^{th} derivative is also a sum of the k^{th} derivative of each term. As in equation 4.29 the superscripts (i) below consistently represent the i^{th} term. The first and the second derivative of the i^{th} term of $F(x)$ at the critical point

$x = \phi(x)$ are:

$$\begin{aligned}
\frac{d}{dx}F^{(i)}(x)\bigg|_{x=\phi(x)} &= \frac{1}{\mu^i}\cdot\frac{dg(\phi^{(i)}(x))}{d\phi^{(i)}(x)}\cdot\frac{d\phi^{(i)}(x)}{d\phi^{(i-1)}(x)}\cdot\frac{d\phi^{(i-1)}(x)}{d\phi^{(i-2)}(x)}\cdots\frac{d\phi(x)}{dx}\bigg|_{x=\phi(x)} \\
&= \left(\frac{\lambda}{\mu}\right)^i g'(\phi^{(i)}(x)) \\
\frac{d^2}{dx^2}F^{(i)}(x)\bigg|_{x=\phi(x)} &= \left(\frac{\lambda}{\mu}\right)^i \frac{dg'(\phi^{(i)}(x))}{d\phi^{(i)}(x)}\lambda^i \\
&= \left(\frac{\lambda^2}{\mu}\right)^i g^{(2)}(\phi^{(i)}(x))
\end{aligned}$$

Similarly, the k^{th} derivative is deduced as:

$$\frac{d^k}{dx^k}F^{(i)}(x)\bigg|_{x=\phi(x)} = \left(\frac{\lambda^k}{\mu}\right)^i g^{(k)}(\phi^{(i)}(x)) \sim \left(\frac{\lambda^k}{\mu}\right)^i \tag{4.30}$$

The right hand side term of equation 4.30 shows that no matter what the value of μ is, with the appropriate choice of scale $|\lambda| > 1$, there always exists sufficiently large k, such that $\lambda^k/\mu > 1$, which implies the existence of the infinite value of the k^{th} derivative of $F(x)$. Hence, it implies the existence of a singularity of $F(x)$.

The defined unstable fixed point at $x = 0$ and the linearized RG flow map $\phi(x) = \lambda x + C$ close to the critical point and the solution close to $x = 0$ follows the power law $F(x) \sim x^m$ with $m = \ln\mu/\ln\lambda$ deduced from the solution of $\lambda^m/\mu = 1$. The critical behavior of F solely depends on the exponent m of x, and m is controlled by the two scaling parameters μ and λ.

4.3.2 Calculation

The previous section introduces the general framework and elements in the RG analysis of the free energy. This section presents the RG method applied to a spin system as an example for the calculation of the RG formalism parameters. The illustration of the calculation follows the diamond lattice example in Saleur, Sammis and Sornette[83].

Consider a spin network system in which the spins are put at the vertex of a diamond lattice with 2^p magnification, 4^p bonds, and $\frac{2}{3}(2 + 4^p)$ sites. The first three iterative constructions are shown in figure 4.1. The location of the spins σ_i is at the vertex of the

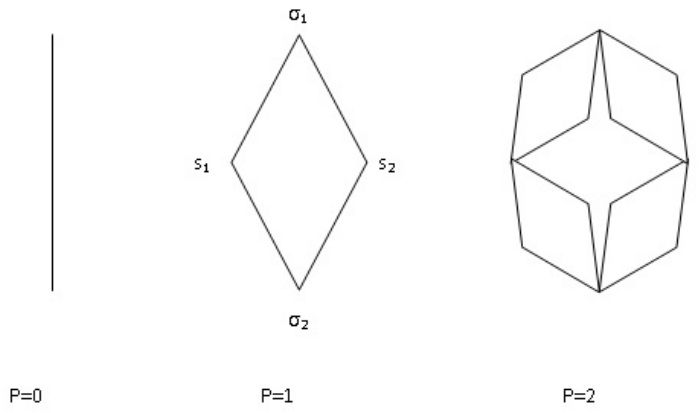

Figure 4.1: The construction of the first three magnification of a diamond lattice.

diamond fractal. Suppose the spins are coupled with interaction energy

$$E = -J \sum_{<ij>} \delta(\sigma_i \sigma_j), \tag{4.31}$$

where J is a coupling parameter. The sum is taken over the nearest neighbors. The δ function value is one if σ_i and σ_j are equal, and zero otherwise. Defining the partition function at p as

$$Z_p = \sum_E e^{-\beta E}, \tag{4.32}$$

such that the normalization of the Boltzmann function, which is the probability to find a system in any given state of energy E,

$$P(E) = Ce^{-\beta E} \tag{4.33}$$

is written as

$$P(E) = \frac{e^{-\beta E}}{Z_p}. \tag{4.34}$$

The parameters β, in equation 4.33 and 4.34, is defined as a function of temperature T:

$$\beta = \frac{1}{k_B T}, \tag{4.35}$$

where k_B is called Boltzmann constant. Thus, the expected value of E is

$$< E >= \sum_E EP(E) = \sum_E E\frac{e^{-\beta E}}{Z_p} = \frac{\partial \ln Z_p}{\partial \beta} \tag{4.36}$$

The definition of free energy in thermodynamics is

$$F = < E > -TS, \tag{4.37}$$

where S is the entropy which is defined by

$$S = -k_B \sum_E P(E) \ln P(E). \tag{4.38}$$

Then the free energy can be expressed using equations 4.32, 4.34, 4.36 and 4.38 as

$$\begin{aligned} F &= < E > -TS \qquad \text{(Definition)} \qquad (4.39)\\ &= \sum_E \left[EP(E) + \frac{1}{\beta} P(E) \ln P(E) \right] \\ &= \sum_E \frac{P(E)}{\beta} \left[\beta E + \ln P(E) \right] \\ &= \frac{1}{\beta} \sum_E P(E) \left[\beta E - \beta E - \ln Z_p \right] \\ &= -\frac{\ln Z_p}{\beta} \sum_E P(E) \\ &= -k_B T \ln Z_p \qquad (4.40) \end{aligned}$$

Consider only one isolated diamond in the lattice, and call the spins σ_1, σ_2 at the extremities and s_1, s_2 of the other two, as shown in figure 4.1. Defining $K = e^{\beta J}$, the contribution of this diamond to $e^{-\beta E}$ is $K^{\delta(\sigma_1,s_1)+\delta(\sigma_2,s_1)+\delta(\sigma_1,s_2)+\delta(\sigma_2,s_2)}$. The contribution

of a single lattice to the total partition function Z_p is

$$\begin{aligned}
&\sum_{s_1,s_2} K^{\delta(\sigma_1,s_1)+\delta(\sigma_2,s_1)+\delta(\sigma_1,s_2)+\delta(\sigma_2,s_2)} \\
=&\begin{cases} (2K+Q-2)^2, & \sigma_1 \neq \sigma_2 \\ (K^2+Q-1)^2, & \sigma_1 = \sigma_2 \end{cases} \\
=&(2K+Q-2)^2\left[1+\left(\frac{(K^2+Q-1)^2}{(2K+Q-2)^2}-1\right)\delta(\sigma_1,\sigma_2)\right] \qquad (4.41)\\
=&(2K+Q-2)^2\left[\frac{(K^2+Q-1)^2}{(2K+Q-2)^2}\right]^{\delta(\sigma_1,\sigma_2)} \qquad (4.42)\\
=&(2K+Q-2)^2 K'^{\delta(\sigma_1,\sigma_2)}, \qquad (4.43)
\end{aligned}$$

where Q is the number of states that the spins can take and $K' = (K^2+Q-1)^2/(2K+Q-2)^2$. Using equation 4.43, for a system with magnification 2^p, if the interaction of spins is K_p, then the interaction at a lower magnification 2^{p-1} is

$$K_{p-1} = \left[\frac{K_p^2+Q-1}{2K_p+Q-2}\right]^2 = \phi(K_p), \qquad (4.44)$$

which defines the RG flow map. Equation 4.43 shows that the contribution of each diamond to Z_p is equal to an edge in the next lower magnification 2^{p-1} that contributes to Z_{p-1} with a factor $(2K+Q-2)^2$. Hence, a transformation equation from Z_{p-1} to Z_p can be written as

$$\begin{aligned}
Z_p(K_p) &= [(2K_p+Q-2)^2]^{4^{p-1}} Z_{p-1}(K_{p-1}) \qquad (4.45)\\
\Longrightarrow Z_p(K) &= (2k+Q-2)^{2\times 4^{p-1}} Z_{p-1}[\phi(K)]. \qquad (4.46)
\end{aligned}$$

The extra power of 4^{p-1} is the total number of bonds at magnification 2^{p-1}. The definition of free energy bonds related to the partition function in equation 4.40, along with equation 4.46

is

$$f_p(K) = (-k_B T)\frac{1}{4^p}\ln Z_p(K) \tag{4.47}$$

$$= (-k_B T)\frac{1}{4^p}[2\cdot 4^{p-1}\ln(2K+Q-2) + \ln Z_{p-1}(K')]$$

$$= (-k_B T)\left[\frac{1}{2}\ln(2K+Q-2) + \frac{1}{4}\cdot\frac{1}{4^{p-1}}\ln Z_{p-1}(K')\right]$$

$$= (-k_B T)\frac{1}{2}\ln(2K+Q-2) + \frac{1}{4}f_{p-1}[\phi(K)], \tag{4.48}$$

which is the RG formalism

$$f_p(K) = g(K) + \frac{1}{\mu}f_{p-1}[\phi(K)], \tag{4.49}$$

where $g(K) = 1/2(-k_B T)\ln(2K+Q-2)$ and $\mu = 4$. The RG calculation recovers the functional form of equation 4.27, which indicates that the free energy of an infinite fractal for some microscopic coupling K satisfies equation 4.49. Therefore, the behavior of the free energy close to a critical point K_c follows a power law.

4.3.3 Real and Complex Exponent Solutions

Section 4.3.1 shows that the solution to equation 4.27 close to the critical point $x = 0$ follows the power law

$$F(x) \sim x^m, \tag{4.50}$$

with a real exponent

$$m = \ln\mu/\ln\lambda. \tag{4.51}$$

As $g(x)$ is the non-singular part of equation 4.27, and the proportional relation 4.50 only reflects the singular behavior about the critical point of $F(x)$, the solution to the exponent

m of 4.50 can be derived by a substitution of the singular part on both sides of equation 4.27:

$$\begin{aligned} x^m &= \frac{1}{\mu}(\lambda x)^m \\ \Longrightarrow &\lambda^m/\mu = 1. \end{aligned} \tag{4.52}$$

The expression 4.51 is only one specific solution to the exponent m for real numbers. A general solution to the complex critical exponent m can be deduced by adding a zero term using the identity $\exp(i2\pi n) = 1$. Nothing forces m to actually be a real number [83]. From equation 4.52, it is simple to obtain

$$\begin{aligned} m\ln\lambda &= \ln\mu + \ln 1 \\ \Longrightarrow m_n &= \frac{\ln\mu}{\ln\lambda} + n\frac{2\pi}{\ln\lambda}i \qquad\qquad n \geq 0. \end{aligned} \tag{4.53}$$

If we use the complex expression 4.53 to substitute the exponent in 4.50, then the solution is:

$$F(x) \approx A + x^m \left[x^{\left(\sum_{n\geq 0}\frac{2\pi n}{\ln\lambda}i\right)}\right] \tag{4.54}$$

However, $F(x)$ is real. Therefore, the general solution to $F(x)$ with a complex exponent m only takes the real part of the complex solution in 4.54:

$$F(x) \approx A + Bx^m + x^m \sum_{n>0} C_n \cos\left(2\pi n\Omega \ln x + \Phi_n\right), \tag{4.55}$$

where $m = \ln\mu/\ln\lambda$, $\Omega = 1/\lambda$, and A, B, C_n are parameters. The general solution to $F(x)$ with complex critical exponent in equation 4.55 exhibits a power law associated with log-periodic oscillations.

Chapter 5

Hierarchical Model

The Hierarchical Model (HM) was introduced in Chapter 3, where it was discussed how it is appropriate in modeling the trading behavior in the stock market. This chapter derives the periodic oscillation power law characteristics from the hierarchical model and the construction of the Log-Periodic Power Law (LPPL) model for the prediction of financial crashes.

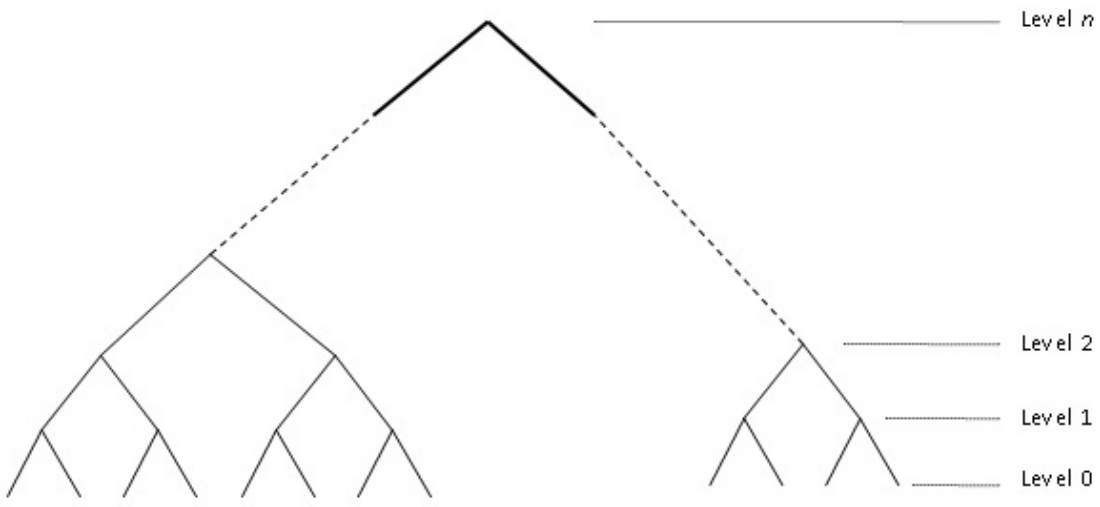

Figure 5.1: Example of Hierarchical Model structure with $n + 1$ levels and group members of 2.

5.1 Model Definition and Structure

Figure 3.7 in Chapter 3 shows an example of hierarchical model. Each vertex in the graph represents a trader in the market. The traders at any levels other than level 0 are considered as trading agents of all its descendants. The purpose of this HM analysis is to find the macroscopic behavior of the traders under the assumption of interaction between traders. Accordingly, the model structure can be simplified to a fractal binary tree, which means each vertex has exactly two children, and the interactions between two siblings are same for all levels.

Suppose a trader i of order 0 has a preferred time t_i to buy the stock with the same utility function σ that measures willingness and timing for buying. Assume t_i has the pdf:

$$p_0(t) = \kappa[\sigma(t)]^\rho \exp\{-\kappa[\sigma(t)]^\rho t\}, \tag{5.1}$$

then the *cdf* is:

$$P_0(t) \equiv \int_0^t p_0(t')dt' = 1 - \exp\left\{-\kappa \int_0^t [\sigma(t')]^\rho dt'\right\} \tag{5.2}$$

and when $\sigma(t')$ is constant, P_0 becomes

$$P_0(t) = 1 - \exp\{-\kappa\sigma^\rho t\} \tag{5.3}$$

This is an exponential distribution with the memoryless property, which means

$$P_0(T > t + s|T > s) = P_0(T > t) \tag{5.4}$$

This property is similar to the Markov property.[1] Consider that each purchase event of trader i changes its state, so the state variable is a jump process. Since $P_0(t)$ is an exponential distribution, this jump process is a Markov process. For a time independent σ, the purchase events of trader i is a Poisson process, as shown in figure 5.2. The mean

[1] Given times $0 < t_1 < t_2 < ... < t_n < s$ and $t > 0$, the Markov property is:

$$P[X(t+s) = y|X(s) = x, X(t_n) = x_n, ..., X(t_1) = x_1] = P[X(t+s) = y|X(s) = x] \tag{5.5}$$

time between purchase events is $(\kappa\sigma^{\rho})^{-1}$. The parameter ρ, called the sensitivity of the time-to-buy on σ, measures the response of the trader to changes in his utility function.

Figure 5.2: Starting from $t = 0$, the trader i makes the first purchase of a stock at time t_{i1}. The time from t_{i1} to the trader's second purchase is t_{i2}.

As assumed in the model structure, each group has two traders at the m^{th} level. There exists an imitation process between the two traders within the group. If one of the two traders buys a stock at time t_1, the utility function for the other trader is affected, from σ to $2^{\beta/\rho}\sigma$, after t_1 until the second trader buys a stock at t_{12}. Therefore, using equation 5.3, the *cdf* of t_{12} becomes:

$$P_0(t_{12}) = 1 - exp\{-\kappa\sigma^{\rho}[t_1 + 2^{\beta}(t_{12} - t_1)]\}, \tag{5.6}$$

where t_{12} is influenced by the first trader from t_2 to t_{12}. This *cdf* is conditional on the first trader buying at time t_1. Without the condition of t_1, the *cdf* of t_2:

$$P_0(t_2) = 1 - exp\{-\kappa\sigma^{\rho}t_2\} \tag{5.7}$$

is equal to equation 5.6. So we have

$$t_1 + 2^{\beta}(t_{12} - t_1) = t_2 \tag{5.8}$$

$$\Longrightarrow t_{12} = t_1 + 2^{-\beta}(t_2 - t_1), \tag{5.9}$$

with $\beta > 0$ an influence exponent measuring the strength of interaction between the two traders. If $\beta \to 0$, the interaction is weak with $t_{12} \to t_2$; if $\beta \to \infty$, the interaction is strong with $t_{12} \to t_1$. Under the assumption of the hierarchical structure, this imitation process is transferred to the next $(m+1)^{\text{th}}$ level when both of the traders at m^{th} level buy the stock. The trader of order $m + 1$ is considered having bought the stock once the two traders at the m^{th} level in its group have done so. With this information, the other trader of order

$m+1$ of the pair changes the time-to-buy from t_{34} to t_{1234}. This process may continue to higher levels and lead to a complex superposition of actions and influences starting at the lowest level of the hierarchy and progressively overlapping as more groups get linked at higher levels.

Suppose there are initially $M = 2^N$ traders in the market at level 0. Each adjacent pair of traders are grouped together viewed as an agent at level 1. Continuing this grouping, every $m = 2$ agents make up of a new agent of the next level in the hierarchical model. As a hierarchical model scale is the same for each level, we can start from the highest order N of the hierarchy. The buy time of the two groups of traders at level $N-1$ are coupled. If the *pdf* of the traders at level $N-1$ is $p_{N-1}(t)$, by equation 5.9, the coupled *pdf* of the buy time of the groups of traders at level N is:

$$\begin{aligned} p_N(t) &= 2\int_0^t dt_1 \int_{t_1}^{\infty} dt_2 p_{N-1}(t_1)p_{N-1}(t_2)\delta[t - t_1 - 2^{-\beta}(t_2 - t_1)] \\ &= \frac{2}{2^{-\beta}} \int_0^t dt_1 p_{N-1}(t_1) p_{N-1}\left(\frac{t - (1-2^{-\beta})t_1}{2^{-\beta}}\right). \end{aligned} \tag{5.10}$$

Equation 5.10 is the renormalization group (RG) equation for the probability that the whole hierarchical system of traders buy a stock at time t. It is the fundamental equation of the analysis of the hierarchical model. Theoretically, as $N \to \infty$ all traders in the stock market place a buy orders at the time t in equation 5.10. At this interval a crash maturing time for the system is signaled:

$$p_N(t) \to p_\infty(t) \equiv \delta(t - t_c) \text{ as } N \to \infty, \tag{5.11}$$

where t_c is the critical crash time.

5.2 Modelling Formulation and Solutions

5.2.1 Special Solution for the Case of $\beta = 1$

As $\beta = 1$, equation 5.10 becomes:

$$p_N(t) = 4\int_0^t dt_1 p_{N-1}(t_1)p_{N-1}(2t - t_1) \tag{5.12}$$

The Fourier transform of $p_N(t)$ is:

$$\begin{aligned}
\hat{p}_N(k) &= 4\int_{-\infty}^{+\infty}\int_0^t p_{N-1}(t_1)p_{N-1}(2t-t_1)e^{-ikt}dt_1dt \\
&= 2\int_{-\infty}^{+\infty}\int_0^{2t} p_{N-1}(t_1)p_{N-1}(2t-t_1)e^{-ikt}dt_1dt, \text{ since it is symmetric by } t_1 = t \\
&= 2\int_{-\infty}^{+\infty}\int_{-\infty}^{+\infty} p_{N-1}(t_1)p_{N-1}(2t-t_1)e^{-ikt}dt_1dt, \\
&\text{since } p_{N-1}(t_1) = 0 \text{ as } t_1 < 0 \text{ and } p_{N-1}(2t-t_1) = 0 \text{ as } t_1 > 2t \\
&= 2\int_{-\infty}^{+\infty} p_{N-1}(t_1)dt_1 \int_{-\infty}^{+\infty} p_{N-1}(2t-t_1)e^{-ikt}dt \\
&= 2\frac{1}{2}\int_{-\infty}^{+\infty} p_{N-1}(t_1)dt_1 \int_{-\infty}^{+\infty} p_{N-1}(u)e^{-iku/2}e^{-ikt_1/2}du \\
&= \int_{-\infty}^{+\infty} p_{N-1}(t_1)e^{-ikt_1/2}dt_1\hat{p}_{N-1}(\frac{k}{2}) \\
&= \hat{p}_{N-1}(\frac{k}{2})\hat{p}_{N-1}(\frac{k}{2})
\end{aligned}$$

The Fourier transform of the *pdf* defines the characteristic function as [95]:

$$\hat{p}_N(k) = \exp\left[\sum_n^{\infty}\frac{c_n^{(N)}}{n!}(ik)^n\right] \tag{5.13}$$

$$\hat{p}_{N-1}(\frac{k}{2})\hat{p}_{N-1}(\frac{k}{2}) = \exp\left[\sum_n^{\infty}\frac{c_n^{(N-1)}}{n!}(i\frac{k}{2})^n\right]\exp\left[\sum_n^{\infty}\frac{c_n^{(N-1)}}{n!}(i\frac{k}{2})^n\right] \tag{5.14}$$

$$= \exp\left[\sum_n^{\infty}\frac{c_n^{(N-1)}}{n!}\frac{(ik)^n}{2^{n-1}}\right] \tag{5.15}$$

Since equations 5.13 and 5.15 are equal, we have the equation for the cumulants of the distributions of two adjacent levels as:

$$c_n^{(N)} = \frac{c_n^{(N-1)}}{2^{n-1}} \tag{5.16}$$

Let t be the average time for all traders M of order 0 to buy a stock. As the *pdf* is completely

determined from the knowledge of its cumulants, the *pdf* of t is:

$$p(t, M, c_1, c_2, c_3, ..., c_n, ...) = p(t', \frac{M}{2}, c_1, \frac{c_2}{2}, \frac{c_3}{2^2}, ..., \frac{c_n}{2^{n-1}}, ...) \tag{5.17}$$

$$= p(t^{(2)}, \frac{M}{2^2}, c_1, \frac{c_2}{2^{2\cdot 1}}, \frac{c_3}{2^{2\cdot 2}}, ..., \frac{c_n}{2^{2(n-1)}}, ...) \tag{5.18}$$

.....

$$= p(t^{(N)}, \frac{M}{2^N}, c_1, \frac{c_2}{2^N}, \frac{c_3}{2^{N\cdot 3}}, ..., \frac{c_n}{2^{N(n-1)}}, ...) \tag{5.19}$$

As $N \to \infty$, all cumulants other than c_1 are all zero, i.e. converging to a Gaussian with variance approaching 0. This is expressed in equation 5.11 for the special case of $\beta = 1$ where the distribution converges to a δ function at $t = t_c$, which is the crash time. Theoretically, this is the time that every trader in the market buys a stock. However, this is not reflected in the real world. Instead, it provides a status that all traders in the market are highly connected and their trading actions are highly simulated. When one of the millions of traders sells a stock, all others follow. It results in a market crash.

5.2.2 Special Solution for the Case of $\beta \to 0$ and $\beta \to \infty$

For the case of $\beta \to 0$, all traders in the market are totally independent. The decision of every trader to buy a stock is not affected by any other traders' decisions. It is apparent that as $\beta \to 0$, then $2^{-\beta}$ approaches 1. equation 5.10 becomes

$$\begin{aligned} p_N(t) &= \frac{2}{1}\int_0^t p_{N-1}(t_1)p_{N-1}(\frac{t-(1-1)t_1}{1}) && \text{as } \beta \to 0 \\ &= 2p_{N-1}(t)\int_0^t p_{N-1}(t_1)dt_1 \\ &= 2p_{N-1}(t)P_{N-1}(t) && \text{where } P_{N-1}(t) \text{ is the } \textit{cdf}. \end{aligned} \tag{5.20}$$

The integral of equation 5.20 is the *cdf* of the distribution, which is:

$$\begin{aligned} P_N(t) &= \int_0^t p_N(\tau)d\tau \\ &= 2\int_0^t p_{N-1}(\tau)P_{N-1}(\tau)d\tau \\ &= P_{N-1}^2(t) \end{aligned} \tag{5.21}$$

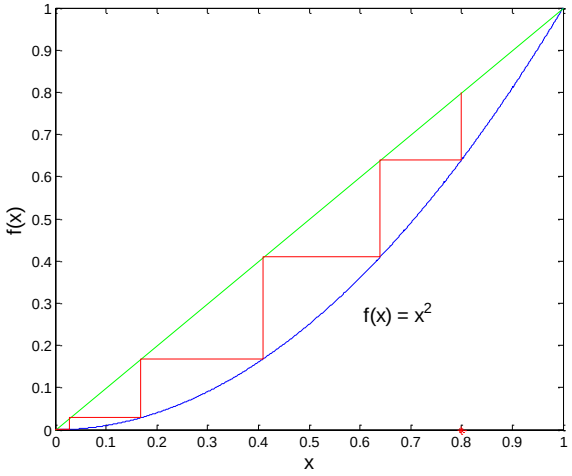

Figure 5.3: Cobweb diagram for the function $f(x) = x^2$ starting from $x_0 = 0.8$.

Since the *cdf* $P_{N-1} \in (0, 1)$, then $P_{N-1}^2 < P_{N-1}$. So we have $0 < P_N < P_{N-1}$. Equation 5.21 is equivalent to a discrete dynamical system defined by the function $f(x) = x^2$ with $0 < x < 1$. The stable equilibrium for the function. Figure 5.3 is a cobweb diagram of the function showing the convergence to . Therefore, equation 5.21 gives that $P_N \to 0$ as $N \to \infty$, i.e. 0 is an attracting fixed point of this discrete dynamical system.

As shown in Figure 5.4, a *cdf* of an exponential distribution is a function starting from zero approaching 1. The *cdf* curve of each level is beneath the *cdf* curve of the adjacent lower level with a later time approaching 1. The *cdf* curve is similar to a step function with the jump at time $t_c = \infty$ as $N \to \infty$. The *pdf* of the distribution is a δ function with the pulse at the time when the *cdf* has the jump. Therefore, the *pdf* of crash times converges to a delta function at the time of infinity when there is no interaction among traders. In this instance the market never crashes.

For the case of $\beta \to \infty$, the traders in the market are fully interacted. In other words, if one of the two traders in a group purchases the stock at time t_1, the other trader in the same group is affected and buys the stock immediately at t_1. The analysis of this case is much more complicated than the previous case of $\beta \to 0$ because the factor of equation 5.10 exhibits unstable properties. Both $\frac{2}{2^{-\beta}}$ and $\frac{t-(1-2^{-\beta})t_1}{2^{-\beta}}$ diverge to infinity as β approaches infinity. As expected, $p_N(t)$ converges to a δ function at $t = 0$ as $N \to \infty$ when the

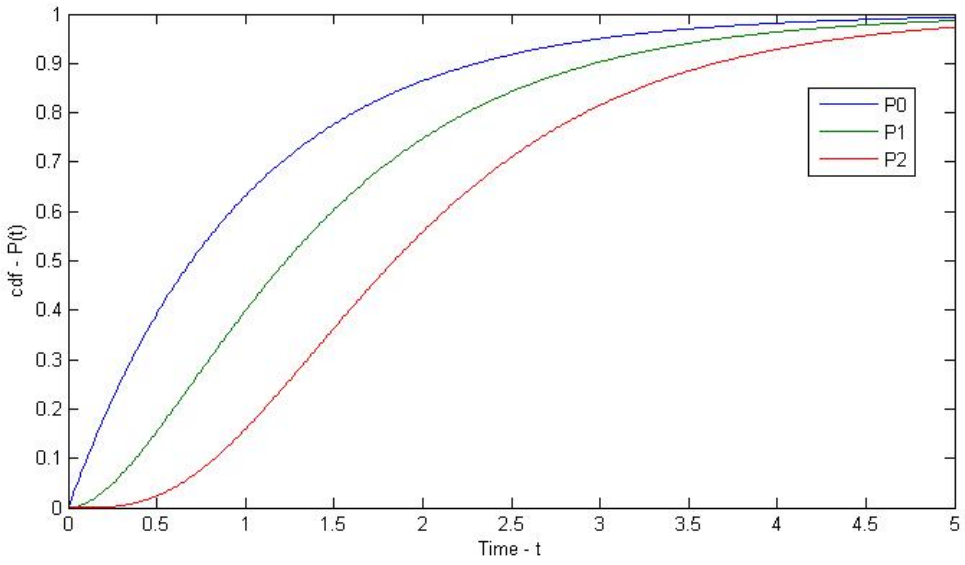

Figure 5.4: The *cdf* curve of each level is beneath the *cdf* curve of the adjacent lower level with a later time approaching 1.

traders are fully interacted. The mathematical proof below shows this behavior from the fundamental equation 5.10 of the hierachical model.

Proof: Defining a function $f_N(t)$, which extending the integral range to $\frac{t}{1-2^{-\beta}}$ of equation 5.10.

$$f_N(t) = \frac{2}{2^{-\beta}} \int_0^{\frac{t}{1-2^{-\beta}}} p_{N-1}(t_1) p_{N-1}\left(\frac{t-(1-2^{-\beta})t_1}{2^{-\beta}}\right) dt_1 \tag{5.22}$$

It is noticed that $p_{N-1}(t_1)p_{N-1}\left(\frac{t-(1-2^{-\beta})t_1}{2^{-\beta}}\right) = 0$ when $t_1 < 0$ or $t_1 > \frac{t}{1-2^{-\beta}}$. The integral range can be further extended as

$$f_N(t) = \frac{2}{2^{-\beta}} \int_{-\infty}^{+\infty} p_{N-1}(t_1) p_{N-1}\left(\frac{t-(1-2^{-\beta})t_1}{2^{-\beta}}\right) dt_1 \tag{5.23}$$

The Fourier transform of $f_N(t)$ is:

$$\begin{aligned}
\hat{f}_N(k) &= \frac{2}{2^{-\beta}} \int_{-\infty}^{+\infty} \int_{-\infty}^{+\infty} p_{N-1}(t_1) p_{N-1}\left(\frac{t-(1-2^{-\beta})t_1}{2^{-\beta}}\right) e^{-ikt} dt_1\, dt \\
&= \frac{2}{2^{-\beta}} \int_{-\infty}^{+\infty} p_{N-1}(t_1) \int_{-\infty}^{+\infty} p_{N-1}\left(\frac{t-(1-2^{-\beta})t_1}{2^{-\beta}}\right) e^{-ikt} dt\, dt_1 \\
&= \frac{2}{2^{-\beta}} 2^{-\beta} \int_{-\infty}^{+\infty} p_{N-1}(t_1) \int_{-\infty}^{+\infty} p_{N-1}(u) e^{-ik2^{-\beta}u} e^{-ik(1-2^{-\beta})t_1} du\, dt_1 \\
&= 2 \int_{-\infty}^{+\infty} p_{N-1}(t_1) e^{-ik(1-2^{-\beta})t_1} dt_1 \hat{p}_{N-1}(2^{-\beta}k) \\
&= 2\hat{p}_{N-1}\left[(1-2^{-\beta})k\right] \hat{p}_{N-1}(2^{-\beta}k)
\end{aligned} \tag{5.24}$$

Let $2^{-\alpha} = 1 - 2^{-\beta}$, equation 5.24 becomes

$$\begin{aligned}
\hat{f}_N(k) &= 2\hat{p}_{N-1}\left[(1-2^{-\beta})k\right] \hat{p}_{N-1}(2^{-\beta}k) \\
&= 2\hat{p}_{N-1}\left[(1-2^{-\alpha})k\right] \hat{p}_{N-1}(2^{-\alpha}k).
\end{aligned} \tag{5.25}$$

Therefore, if there exists an α such that $2^{-\alpha} = 1 - 2^{-\beta}$, then equation 5.25 implies

$$\begin{aligned}
&\frac{2}{2^{-\beta}} \int_0^{\frac{t}{1-2^{-\beta}}} p_{N-1}(t_1) p_{N-1}\left(\frac{t-(1-2^{-\beta})t_1}{2^{-\beta}}\right) dt_1 \\
=&\frac{2}{2^{-\alpha}} \int_0^{\frac{t}{1-2^{-\alpha}}} p_{N-1}(t_1) p_{N-1}\left(\frac{t-(1-2^{-\alpha})t_1}{2^{-\alpha}}\right) dt_1
\end{aligned} \tag{5.26}$$

From equation 5.22, one can show that

$$\begin{aligned}
f_N(t) &= \frac{2}{2^{-\beta}} \int_0^{\frac{t}{1-2^{-\beta}}} p_{N-1}(t_1) p_{N-1}\left(\frac{t-(1-2^{-\beta})t_1}{2^{-\beta}}\right) dt_1 \\
&= \frac{2}{2^{-\beta}} \left[\int_0^t p_{N-1}(t_1) p_{N-1}\left(\frac{t-(1-2^{-\beta})t_1}{2^{-\beta}}\right) dt_1 \right. \\
&\qquad \left. + \int_t^{\frac{t}{1-2^{-\beta}}} p_{N-1}(t_1) p_{N-1}\left(\frac{t-(1-2^{-\beta})t_1}{2^{-\beta}}\right) dt_1 \right]
\end{aligned} \tag{5.27}$$

Using a substitution with $u = \frac{t-(1-2^{-\beta})t_1}{2^{-\beta}}$ on the second term of the right side of equation 5.27, then $t_1 = \frac{t-2^{-\beta}u}{1-2^{-\beta}}$ and $dt_1 = \frac{2^{-\beta}}{2^{-\beta}-1} du$. For the lower and upper limits, $u = t$ as

$t_1 = t$, and $u = 0$ as $t_1 = \frac{t}{1-2^{-\beta}}$. Then the integral becomes

$$\begin{aligned}
&\int_t^{\frac{t}{1-2^{-\beta}}} p_{N-1}(t_1)p_{N-1}\left(\frac{t-(1-2^{-\beta})t_1}{2^{-\beta}}\right)dt_1 \\
=&\frac{2^{-\beta}}{2^{-\beta}-1}\int_t^0 p_{N-1}\left(\frac{t-2^{-\beta}u}{1-2^{-\beta}}\right)p_{N-1}(u)du \\
=&\frac{2^{-\beta}}{1-2^{-\beta}}\int_0^t p_{N-1}(u)p_{N-1}\left(\frac{t-2^{-\beta}u}{1-2^{-\beta}}\right)du
\end{aligned} \tag{5.28}$$

Putting equation 5.28 into equation 5.27, changing the variable to t_1, and writing the second term in terms of α using equation 5.26, the equation appears as

$$\begin{aligned}
f_N(t) &= \frac{2}{2^{-\beta}}\int_0^{\frac{t}{1-2^{-\beta}}} p_{N-1}(t_1)p_{N-1}\left(\frac{t-(1-2^{-\beta})t_1}{2^{-\beta}}\right)dt_1 \\
&= \frac{2}{2^{-\beta}}\int_0^t p_{N-1}(t_1)p_{N-1}\left(\frac{t-(1-2^{-\beta})t_1}{2^{-\beta}}\right)dt_1 \\
&\quad + \frac{2}{1-2^{-\beta}}\int_0^t p_{N-1}(t_1)p_{N-1}\left(\frac{t-2^{-\beta}t_1}{1-2^{-\beta}}\right)dt_1 \\
&= \frac{2}{2^{-\beta}}\int_0^t p_{N-1}(t_1)p_{N-1}\left(\frac{t-(1-2^{-\beta})t_1}{2^{-\beta}}\right)dt_1 \\
&\quad + \frac{2}{2^{-\alpha}}\int_0^t p_{N-1}(t_1)p_{N-1}\left(\frac{t-(1-2^{-\alpha})t_1}{2^{-\alpha}}\right)dt_1
\end{aligned} \tag{5.29}$$

Combining equation 5.29 and 5.26 together, the fundamental equation 5.10 is written as

$$\begin{aligned}
p_N(t) &= \frac{2}{2^{-\beta}}\int_0^t p_{N-1}(t_1)p_{N-1}\left(\frac{t-(1-2^{-\beta})t_1}{2^{-\beta}}\right)dt_1 \\
&= \frac{2}{2^{-\alpha}}\int_0^{\frac{t}{1-2^{-\alpha}}} p_{N-1}(t_1)p_{N-1}\left(\frac{t-(1-2^{-\alpha})t_1}{2^{-\alpha}}\right)dt_1 \\
&\quad - \frac{2}{2^{-\alpha}}\int_0^t p_{N-1}(t_1)p_{N-1}\left(\frac{t-(1-2^{-\alpha})t_1}{2^{-\alpha}}\right)dt_1
\end{aligned} \tag{5.30}$$

Recalling that α satisfies the equation $2^{-\alpha} = 1 - 2^{-\beta}$. As $\beta \to \infty$, $\alpha \to 0$, then $2^{-\alpha}$

approaches to 1. equation 5.30 is simplified as

$$\begin{aligned} p_N(t) &= 2\int_0^\infty p_{N-1}(t_1)p_{N-1}(t)dt_1 - 2\int_0^t p_{N-1}(t_1)p_{N-1}(t)dt_1 \\ &= 2p_{N-1}(t) - 2p_{N-1}(t)P_{N-1}(t), \end{aligned}$$

and the *cdf* is

$$P_N(t) = 2P_{N-1}(t) - P_{N-1}^2(t) \tag{5.31}$$

Rewrite equation 5.31 as

$$P_N(t) = P_{N-1}(t)(2 - P_{N-1}(t)). \tag{5.32}$$

Since the *cdf* $P_{N-1} \in (0,1)$, then $(2 - P_{N-1})$ is greater than 1. So we have $P_N > P_{N-1}$ from equation 5.32. If equation 5.31 is rewritten as

$$P_N(t) = 1 - (1 - P_{N-1}(t))^2, \tag{5.33}$$

it shows that $P_N < 1$ as $P_{N-1} \in (0,1)$.

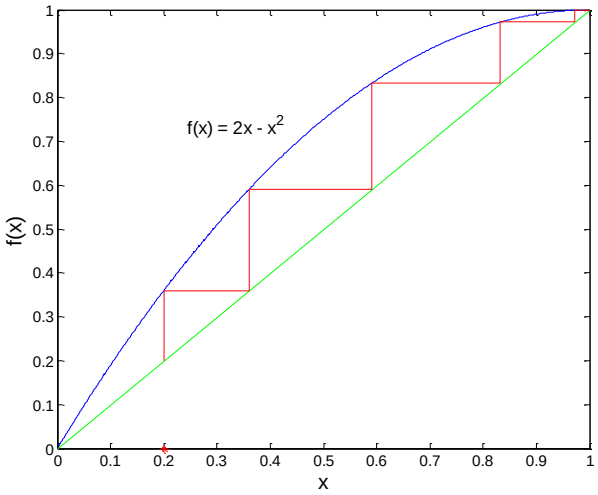

Figure 5.5: Cobweb diagram for the function $f(x) = 2x - x^2$ starting from $x_0 = 0.2$.

Equation 5.31 is equivalent to a discrete dynamical system defined by the function

$f(x) = 2x - x^2$ with $0 < x < 1$. The stable equilibrium for the function. Figure 5.5 is a cobweb diagram of the function showing the convergence to 1. Therefore, equation 5.31 gives that $P_N \to 1$ as $N \to \infty$, i.e. 1 is an attracting fixed point of this discrete dynamical system.

This concludes the proof for the case of β approaching ∞. ■

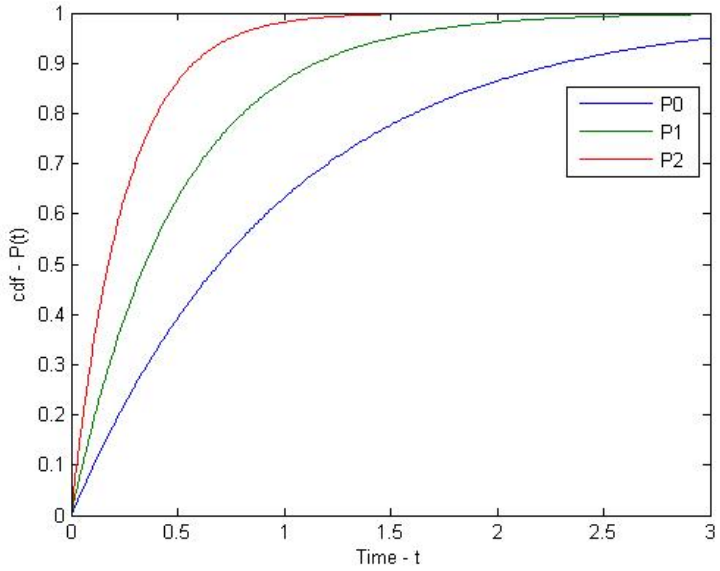

Figure 5.6: The *cdf* curve of each level is over the *cdf* curve of the adjacent lower level with a later time approaching 0.

As shown in Figure 5.6 the result from equation 5.31 implies that $P_N(t)$ converges to a step function at $t_c = 0$ as $N \to \infty$. Similarly, with a step function at $t_c = 0$ being the *cdf*, the *pdf* of the distribution has to be the δ function at $t_c = 0$. Whenever one of the two traders at a level in a group of the hierarchical model buys a stock, the other trader buys it immediately. This leads to a crash time of zero, where one trader buying a stock triggers all traders in the market buying stocks simultaneously.

5.2.3 General Solution

Assume p_{N-1} is a rectangle, then

$$p_{N-1}(t) = \begin{cases} \frac{1}{\varepsilon}, & t \in \left[t_c - \frac{\varepsilon}{2}, t_c + \frac{\varepsilon}{2}\right] \\ 0, & otherwise \end{cases} \tag{5.34}$$

which converges to the δ function as $\varepsilon \to 0$. Putting equation 5.34 into equation 5.10, $p_N(t)$ can be written as:

$$p_N(t) = \begin{cases} 0 & t \in \left[0, t_c - \frac{\varepsilon}{2}\right] \\ \frac{2}{2^{-\beta}\varepsilon} \int_{t_c - \frac{\varepsilon}{2}}^{t} p_{N-1}\left(\frac{t-(1-2^{-\beta})t_1}{2^{-\beta}}\right) dt_1 & t \in \left[t_c - \frac{\varepsilon}{2}, t_c + \frac{\varepsilon}{2}\right] \\ 0 & t \in \left[t_c + \frac{\varepsilon}{2}, \infty\right] \end{cases} \tag{5.35}$$

For $t < t_c - \frac{\varepsilon}{2}$, it is apparent that $p_{N-1}(t_1)$ in equation 5.10 is zero in $[0, t]$. For $t > t_c + \frac{\varepsilon}{2}$, we have

$$\begin{aligned} \frac{t-(1-2^{-\beta})t_1}{2^{-\beta}} &> \frac{t-(1-2^{-\beta})t}{2^{-\beta}} \\ &= \frac{2^{-\beta}t}{2^{-\beta}} \\ &> t_c + \frac{\varepsilon}{2} \end{aligned}$$

which means $p_{N-1}\left(\frac{t-(1-2^{-\beta})t_1}{2^{-\beta}}\right) = 0$ in $[0, t]$.

To find the solution for $t \in \left[t_c - \frac{\varepsilon}{2}, t_c + \frac{\varepsilon}{2}\right]$, we let $u = \frac{t-(1-2^{-\beta})t_1}{2^{-\beta}}$, then

$$p_N(t) = \frac{2}{\cancel{2}^{-\beta}\varepsilon} \frac{\cancel{2}^{-\beta}}{2^{-\beta} - 1} \int_{\frac{t-(1-2^{-\beta})(t_c - \frac{\varepsilon}{2})}{2^{-\beta}}}^{t} p_{N-1}(u)du, \qquad t \in \left[t_c - \frac{\varepsilon}{2}, t_c + \frac{\varepsilon}{2}\right] \tag{5.36}$$

As p_{N-1} is only defined when u is in $\left[t_c - \frac{\varepsilon}{2}, t_c + \frac{\varepsilon}{2}\right]$, both limits of the integral should be in this interval. It is easy to show when $u = t_c - \frac{\varepsilon}{2}$, $t = t_c - \frac{\varepsilon}{2}$; and when $u = t_c + \frac{\varepsilon}{2}$, $t = t_c - \frac{\varepsilon}{2} + 2^{-\beta}\varepsilon$. For $\beta > 0$, $2^{-\beta}\varepsilon$ is smaller than ε, then $t_c - \frac{\varepsilon}{2} + 2^{-\beta}\varepsilon < t_c + \frac{\varepsilon}{2}$. As a

result, equation 5.36 is separated into two integrals:

$$p_N(t) = \begin{cases} \frac{2}{\varepsilon(2^{-\beta}-1)} \int_{\frac{t-(1-2^{-\beta})(t_c-\frac{\varepsilon}{2})}{2^{-\beta}}}^{t} p_{N-1}(u)du, & t \in \left[t_c - \frac{\varepsilon}{2}, t_c - \frac{\varepsilon}{2} + 2^{-\beta}\varepsilon\right] \\ \frac{2}{\varepsilon(2^{-\beta}-1)} \int_{t_c+\frac{\varepsilon}{2}}^{t} p_{N-1}(u)du, & t \in \left[t_c - \frac{\varepsilon}{2} + 2^{-\beta}\varepsilon, t_c + \frac{\varepsilon}{2}\right] \end{cases} \tag{5.37}$$

$$= \begin{cases} \frac{2}{\varepsilon^2(2^{-\beta}-1)}(t - \frac{t-(1-2^{-\beta})(t_c-\frac{\varepsilon}{2})}{2^{-\beta}}), & t \in \left[t_c - \frac{\varepsilon}{2}, t_c - \frac{\varepsilon}{2} + 2^{-\beta}\varepsilon\right] \\ \frac{2}{\varepsilon^2(2^{-\beta}-1)}(t - (t_c + \frac{\varepsilon}{2})), & t \in \left[t_c - \frac{\varepsilon}{2} + 2^{-\beta}\varepsilon, t_c + \frac{\varepsilon}{2}\right] \end{cases} \tag{5.38}$$

$$= \begin{cases} \frac{2}{\varepsilon^2}\frac{t-t_c+\frac{\varepsilon}{2}}{2^{-\beta}}, & t \in \left[t_c - \frac{\varepsilon}{2}, t_c - \frac{\varepsilon}{2} + 2^{-\beta}\varepsilon\right] \\ \frac{2}{\varepsilon^2}\frac{t_c-t+\frac{\varepsilon}{2}}{1-2^{-\beta}}, & t \in \left[t_c - \frac{\varepsilon}{2} + 2^{-\beta}\varepsilon, t_c + \frac{\varepsilon}{2}\right] \end{cases} \tag{5.39}$$

This process of p_{N-1} to p_N changes the shape of the *pdf* from a rectangle to a triangle within the same scale, which satisfies the requirement of normalization. With $\varepsilon \to 0$, both p_{N-1} and p_N approach the δ function at the fixed point t_c. The value of the critical point t_c depends on the intrinsic distribution for the time the traders buy a stock . Next, we need to find the general renormalization group equation.

Since $p_N(t)$ approaches to the fixed point *pdf*, which is a δ function, as $N \to \infty$, we can express the *pdf* $p_{N-1}(t)$ as the fixed point distribution with a normalization constant plus a function of their difference $\Delta p_{N-1}(t)$. This is written as:

$$p_{N-1}(t) = Cp_\infty(t) + \Delta p_{N-1}(t). \tag{5.40}$$

To find the constant C, we integrate on both sides.

$$\int_0^\infty p_{N-1}(t)dt = C\int_0^\infty p_\infty(t)dt + \int_0^\infty \Delta p_{N-1}(t)dt \tag{5.41}$$

As both $p_{N-1}(t)$ and $p_\infty(t)$ are normalized *pdf*s, and their integrals are 1, then equation 5.41 becomes:

$$1 = C + \int_0^\infty \Delta p_{N-1}(t)dt \tag{5.42}$$

$$\Rightarrow C = 1 - \int_0^\infty \Delta p_{N-1}(t)dt \tag{5.43}$$

Let $\Delta_{N-1} \equiv \int_0^\infty \Delta p_{N-1}(t)dt$, then equation 5.40 becomes

$$p_{N-1}(t) = (1 - \Delta_{N-1})p_\infty(t) + \Delta p_{N-1}(t) \tag{5.44}$$

Putting it into equation 5.10, we have:

$$\begin{aligned}
p_N(t) = \frac{2}{2^{-\beta}} \int_0^t & [(1 - \Delta_{N-1})p_\infty(t_1) + \Delta p_{N-1}(t_1)] \\
& \left[(1 - \Delta_{N-1})p_\infty(\frac{t - (1 - 2^{-\beta})t_1}{2^{-\beta}}) + \Delta p_{N-1}(\frac{t - (1 - 2^{-\beta})t_1}{2^{-\beta}})\right] dt_1 && \text{(5.45a)} \\
= \frac{2}{2^{-\beta}} \Bigg[& \int_0^t (1 - \Delta_{N-1})(1 - \Delta_{N-1})p_\infty(t_1)p_\infty(\frac{t - (1 - 2^{-\beta})t_1}{2^{-\beta}})dt_1 && \text{(5.45b)} \\
& + \int_0^t (1 - \Delta_{N-1})\Delta p_{N-1}\left(\frac{t - (1 - 2^{-\beta})t_1}{2^{-\beta}}\right) p_\infty(t_1)dt_1 && \text{(5.45c)} \\
& + \int_0^t (1 - \Delta_{N-1})\Delta p_{N-1}(t_1)p_\infty\left(\frac{t - (1 - 2^{-\beta})t_1}{2^{-\beta}}\right) dt_1 && \text{(5.45d)} \\
& + \int_0^t \Delta p_{N-1}(t_1)\Delta p_{N-1}\left(\frac{t - (1 - 2^{-\beta})t_1}{2^{-\beta}}\right) dt_1 \Bigg] && \text{(5.45e)}
\end{aligned}$$

By dropping all the second or higher order in Δ, it becomes:

$$\begin{aligned}
= \frac{2}{2^{-\beta}} \Bigg[& \int_0^t (1 - 2\Delta_{N-1})p_\infty(t_1)p_\infty(\frac{t - (1 - 2^{-\beta})t_1}{2^{-\beta}})dt_1 && \text{(5.45f)} \\
& + \int_0^t \Delta p_{N-1}\left(\frac{t - (1 - 2^{-\beta})t_1}{2^{-\beta}}\right) p_\infty(t_1)dt_1 && \text{(5.45g)} \\
& + \int_0^t \Delta p_{N-1}(t_1)p_\infty\left(\frac{t - (1 - 2^{-\beta})t_1}{2^{-\beta}}\right) dt_1 && \text{(5.45h)} \\
& + 0] && \text{(5.45i)}
\end{aligned}$$

Also, as $\varepsilon \to 0$, $p_\infty(t)$ can be written as a δ function centered at t_c:

$$\begin{aligned}
= \frac{2}{2^{-\beta}} \Bigg[& \int_0^t (1 - 2\Delta_{N-1})\delta(t_1 - t_c)\delta(t_c - \frac{t - (1 - 2^{-\beta})t_1}{2^{-\beta}})dt_1 && \text{(5.45j)} \\
& + \int_0^t \Delta p_{N-1}\left(\frac{t - (1 - 2^{-\beta})t_1}{2^{-\beta}}\right) \delta(t_1 - t_c)dt_1 && \text{(5.45k)} \\
& + \int_0^t \Delta p_{N-1}(t_1)\delta\left(t_c - \frac{t - (1 - 2^{-\beta})t_1}{2^{-\beta}}\right) dt_1 && \text{(5.45l)} \\
& + 0] && \text{(5.45m)}
\end{aligned}$$

After above simplification, we need to solve the three integrals (5.45j, 5.45k, 5.45l) one by one.

Integral 5.45j: Since $(1-2\Delta_{N-1})$ is a constant, it can be removed from the integral. We now need to prove:

$$\int_0^t \delta(t_1 - t_c)\delta(t_c - \frac{t-(1-2^{-\beta})t_1}{2^{-\beta}})dt_1 = \frac{2^{-\beta}}{2}\delta(t-t_c) \tag{5.46}$$

Proof: To prove this, we show that the integral of the product of an arbitrary continuous function $f(t)$ and the left side is equal to the the product of $f(t)$ and the right side:

$$\int_0^\infty \int_0^t \delta(t_1 - t_c)\delta(t_c - \frac{t-(1-2^{-\beta})t_1}{2^{-\beta}})dt_1 f(t)dt = \int_0^\infty \frac{2^{-\beta}}{2}\delta(t-t_c)f(t)dt \tag{5.47}$$

RHS of equation 5.47:

$$\int_0^\infty \frac{2^{-\beta}}{2}\delta(t-t_c)f(t)dt = \frac{2^{-\beta}}{2}f(t_c) \tag{5.48}$$

LHS of equation 5.47:

$$\begin{aligned}
&\int_0^\infty \int_0^t \delta(t_1 - t_c)\delta(t_c - \frac{t-(1-2^{-\beta})t_1}{2^{-\beta}})f(t)dt_1 dt \\
=&\int_0^\infty \delta(t_1 - t_c)\int_{t_1}^\infty \delta(t_c - \frac{t-(1-2^{-\beta})t_1}{2^{-\beta}})f(t)dtdt1 \\
=&2^{-\beta}\int_0^\infty \delta(t_1 - t_c)\int_{t_1}^\infty \delta(2^{-\beta}t_c + (1-2^{-\beta})t_1 - t)f(t)dtdt1 \\
=&2^{-\beta}\int_{t_c}^\infty \delta(2^{-\beta}t_c + (1-2^{-\beta})t_c - t)f(t)dt \\
=&2^{-\beta}\int_{t_c}^\infty \delta(t_c - t)f(t)dt \\
=&\frac{2^{-\beta}}{2}f(t_c)
\end{aligned} \tag{5.49}$$

Since the LHS and the RHS of equation 5.47 are equal, this completes the proof of equation 5.46. ■

In the last step of above proof, the result of the integral from t_c to ∞ is half of the

integral from 0 to ∞. To show this, we can define a function $\delta_\varepsilon(t)$, such that

$$\lim_{\varepsilon \to 0} \delta_\varepsilon(t) = \delta(t),$$

which can be defined as:

$$\delta_\varepsilon(t) = \begin{cases} \frac{1}{\varepsilon} & t \in \left[\frac{-\varepsilon}{2}, \frac{\varepsilon}{2}\right] \\ 0 & \text{otherwise} \end{cases} \tag{5.50}$$

So the integral in the last step of equation 5.49 becomes:

$$\begin{aligned} \int_{t_c}^{\infty} \delta(t_c - t) f(t) dt &= \lim_{\varepsilon \to 0} \int_{t_c}^{\infty} \delta_\varepsilon(t_c - t) f(t) dt \\ &= \lim_{\varepsilon \to 0} \int_{t_c}^{t_c + \frac{\varepsilon}{2}} \delta_\varepsilon(t_c - t) f(t) dt \end{aligned}$$

Using the Mean Value Theorem, there exists a $t_\varepsilon \in [t_c, t_c + \frac{\varepsilon}{2}]$, such that

$$\begin{aligned} \lim_{\varepsilon \to 0} \int_{t_c}^{t_c + \frac{\varepsilon}{2}} \delta_\varepsilon(t_c - t) f(t) dt &= \lim_{\varepsilon \to 0} f(t_\varepsilon) \int_{t_c}^{t_c + \frac{\varepsilon}{2}} \delta_\varepsilon(t_c - t) dt \\ &= \lim_{\varepsilon \to 0} f(t_\varepsilon) \frac{1}{\varepsilon} (t_c + \varepsilon/2 - t_c) \\ &= \frac{1}{2} \lim_{\varepsilon \to 0} f(t_\varepsilon) \\ &= \frac{1}{2} f(t_c) \end{aligned}$$

Integral 5.45k: As $t < t_c$, the values of $\delta(t_1 - t_c)$ for t_1 from 0 to t are 0. The integral is then zero when $t < t_c$. For $t = t_c$, similar the proof above, the integral is equal to $\frac{1}{2}\Delta p_{N-1}(t_c)$. This can be dropped because it is comparably small to the integral of the term 5.45j, which is a δ function at t_c. The only non-zero and valid part of the integral is when $t > t_c$. In conclusion, the integral 5.45k can be written as

$$\int_0^t \Delta p_{N-1}\left(\frac{t - (1 - 2^{-\beta})t_1}{2^{-\beta}}\right) \delta(t_1 - t_c) dt_1 = \begin{cases} 0, & t \le t_c \\ \Delta p_{N-1}\left(\frac{t - (1-2^{-\beta})t_c}{2^{-\beta}}\right), & t > t_c \end{cases} \tag{5.51}$$

Integral 5.45l: This integral is the compensation of integral 5.45k. It is zero for $t > t_c$ and is dropped for $t = t_c$. For $t < t_c$, it is solved by a substitution of $u = \frac{t-(1-2^{-\beta})t_1}{2^{-\beta}}$, then

$$\begin{aligned}
&\int_0^t \Delta p_{N-1}(t_1)\delta\left(t_c - \frac{t-(1-2^{-\beta})t_1}{2^{-\beta}}\right)dt_1 \\
=&\int_t^{+\infty} \Delta p_{N-1}\left(\frac{t-2^{-\beta}u}{1-2^{-\beta}}\right)\delta(t_c-u)\frac{2^{-\beta}}{1-2^{-\beta}}du \\
=&\frac{2^{-\beta}}{1-2^{-\beta}}\Delta p_{N-1}\left(\frac{t-2^{-\beta}t_c}{1-2^{-\beta}}\right)
\end{aligned}$$

Therefore, the solution to the integral of 5.45l is

$$\begin{aligned}
&\int_0^t \Delta p_{N-1}\left(\frac{t-(1-2^{-\beta})t_1}{2^{-\beta}}\right)\delta(t_1-t_c)dt_1 \\
=&\begin{cases} \frac{2^{-\beta}}{1-2^{-\beta}}\Delta p_{N-1}\left(\frac{t-2^{-\beta}t_c}{1-2^{-\beta}}\right), & t < t_c \\ 0, & t \geq t_c \end{cases}
\end{aligned} \tag{5.52}$$

Combining the results of equations 5.46, 5.51, and 5.52, the solution to equation 5.45 is

$$p_N(t) = \begin{cases} \frac{2}{1-2^{-\beta}}\Delta p_{N-1}\left(\frac{t-2^{-\beta}t_c}{1-2^{-\beta}}\right), & t < t_c \\ (1-2\Delta_{N-1})\delta(t-t_c), & t = t_c \\ \frac{2}{2^{-\beta}}\Delta p_{N-1}\left(\frac{t-(1-2^{-\beta})t_c}{2^{-\beta}}\right), & t > t_c \end{cases} \tag{5.53}$$

This can be re-written as one single equation

$$p_N(t) = (1-2\Delta_{N-1})\delta(t-t_c) + \Delta p_N(t) \tag{5.54}$$

$$= (1-2\Delta_{N-1})p_\infty(t) + \Delta p_N(t), \tag{5.55}$$

where

$$\Delta p_N(t) = \frac{2}{1-2^{-\beta}}\Delta p_{N-1}\left(\frac{t-2^{-\beta}t_c}{1-2^{-\beta}}\right), \qquad t < t_c$$

$$\Delta p_N(t) = \frac{2}{2^{-\beta}}\Delta p_{N-1}\left(\frac{t-(1-2^{-\beta})t_c}{2^{-\beta}}\right), \qquad t > t_c$$

Shifting the fixed point t_c to zero by changing the variable to $\tau = t - t_c$, equation 5.55 is re-written as

$$p_N(\tau) = (1 - 2\Delta_{N-1})p_\infty(\tau) + \Delta p_N(\tau), \tag{5.56}$$

where
$$\Delta p_N(\tau) = \frac{2}{1-2^{-\beta}}\Delta p_{N-1}\left(\frac{\tau}{1-2^{-\beta}}\right), \qquad \tau < 0 \tag{5.57}$$

$$\Delta p_N(\tau) = \frac{2}{2^{-\beta}}\Delta p_{N-1}\left(\frac{\tau}{2^{-\beta}}\right), \qquad \tau > 0 \tag{5.58}$$

equations 5.57 and 5.58 are in the renormalization group formalism with $\tau = 0$ as the fixed point and β as the exponent determining the re-scaling factor to τ. Let $\phi(\tau) = \frac{\tau}{1-2^{-\beta}}$ and $\phi(\tau) = \frac{\tau}{2^{-\beta}}$, respectively, which is the RG flow map, and $\mu = \frac{1-2^{-\beta}}{2}$ and $\mu = \frac{2^{-\beta}}{2}$, respectively, which is the re-scaling factor corresponding to the RG flow map. equation 5.57 and 5.58 are re-written as

$$\Delta p_N(\tau) = \frac{1}{\mu}\Delta p_{N-1}(\phi(\tau)) = \frac{1}{\mu^N}\Delta p_0(\phi^{(N)}(\tau)) \tag{5.59}$$

where the superscript (N) denotes the N^{th} composition.

The solution to an equation in the form of a renormalization group close to the critical points is expressed in a power law: [95]

$$\Delta p_N(\tau) \sim \tau^\kappa. \tag{5.60}$$

The critical points correspond to the unstable fixed points of the RG flow map $\phi(\tau)$ when the absolute value of the derivative of ϕ with respect to τ becomes greater than 1. Defining this value as $\lambda = d\phi/d\tau|_{\tau=\phi(\tau)}$, the k^{th} derivative of $\Delta p_N(\tau)$ is proportional to $(\lambda^k/\mu)^N$. Since $\lambda > 1$, the singular behavior emerges for a sufficiently large k, such that $(\lambda^k/\mu)^N$ is greater than the unit radius of convergence. Therefore, the solution to $\Delta p_N(\tau)$ close to the critical point is proportional to τ^κ with $\lambda^\kappa/\mu = 1$. This gives a solution to κ:

$$\kappa = \frac{\ln \mu}{\ln \lambda} \tag{5.61}$$

Using equation 5.61, for $\tau < 0$,

$$\begin{aligned}
\lambda_- &= \frac{1}{1-2^{-\beta}} \\
\mu_- &= \frac{1-2^{-\beta}}{2} \\
\kappa_- &= \frac{\ln \mu}{\ln \lambda} \\
&= \frac{\ln(1-2^{-\beta}) - \ln 2}{-\ln(1-2^{-\beta})} \\
&= \frac{\ln 2}{\ln(1-2^{-\beta})} - 1, \qquad \tau < 0.
\end{aligned} \tag{5.62}$$

Similar to equation 5.61

$$\kappa_+ = -\frac{1}{\beta} - 1, \qquad \tau > 0. \tag{5.63}$$

equations 5.62 and 5.63 are the real exponents of the power law in 5.60, which is just a special solution, denoted by $\Delta p_N^0(\tau) \sim \tau^\kappa$. For a more general solution with periodicity, $\Delta p_N(\tau) \sim \tau^{\kappa_n}$ considering κ being a complex number, it can be derived as

$$\begin{aligned}
&\lambda^{\kappa_n} = \mu \\
\Rightarrow &\kappa_n \ln \lambda = \ln \mu + \ln 1 = \ln \mu + \ln e^{i2\pi n} \\
\Rightarrow &\kappa_n = \frac{\ln \mu}{\ln \lambda} + i\frac{2\pi n}{\ln \lambda}
\end{aligned} \tag{5.64}$$

Substituting κ_n in τ^{κ_n} with equation 5.64, it gives

$$\begin{aligned}
\tau^{\kappa_n} &= \tau^{\frac{\ln \mu}{\ln \lambda} + i\frac{2\pi n}{\ln \lambda}} \\
&= \tau^\kappa \tau^{i\frac{2\pi n}{\ln \lambda}} \\
&= \tau^\kappa e^{i\frac{2\pi n}{\ln \lambda} \ln \tau}
\end{aligned} \tag{5.65}$$

The additional term $\ln 1$ in equation 5.64 is a zero term, thus an infinite number of such terms can be added to the equation and n is an arbitrary integer. Considering this and

taking the real part of equation 5.65, a more general form is then:

$$\tau^{\kappa_n} = \tau^{\kappa}[a_0 + \sum_{n=1}^{\infty} a_n \cos(n\Omega \ln \tau + \phi_n)], \tag{5.66}$$

where $\Omega = \frac{2\pi}{\ln \lambda}$. equation 5.66 shows that the general singular solution $\Delta p_N(\tau)$ and the special solution $\Delta p_N^0(\tau)$ are related by a periodic function $p(\tau)$:

$$\Delta p_N(\tau) = \Delta p_N^0(\tau) p(\ln \Delta p_N^0(\tau)) \tag{5.67}$$

The periodic function $p(\tau)$ satisfies the periodicity requirement with a period $\ln \mu$, where μ is as defined in equation 5.59. This is expressed as

$$p(\ln \mu + \ln \Delta p_{N-1}^0(\tau)) = p(\ln \Delta p_N^0(\tau)) \tag{5.68}$$

Thus, the general solution to the hierarchical model of stock markets is an asymptotic power law associated with log-periodic oscillations, which is consistent with findings in Bree and Joseph [11], Sornette [87], and Zhou and Sornette [123].

If the *pdf* of the number of traders at level n buying stock is $p_n(t)$, then the proportion of the total traders at level n buying the stock at time t is $P_n(t) = \int_0^t p_n(\tau) d\tau$. This *cdf* is under the assumption that the traders at the same level are independent individuals without any interactions. For example, $P_0(t)$ is the *cdf* for level 0 traders without interactions, and likewise, $P_1(t)$ is the *cdf* for level 1 traders without interactions, and so forth. However, $P_1(t)$ is determined by the distribution of level 0 traders and the strength of interactions between traders at level 0. Therefore, the fraction of traders at level 0 buying the stock with interactions is:

$$F_0(t) \approx P_0(t) + [1 - P_0(t)]P_1(t) + [1 - P_0(t)][1 - P_1(t)]P_2(t) + ... \tag{5.69}$$

The renormalization group recursion equation of $p_n(t)$ derived above has log-periodic oscillations as t closes to the crash time t_c, and the *cdf*s of $P_n(t)$ also exhibit such oscillations, as does $F_0(t)$.

5.2.4 Simulation of General Solutions

Two general solutions of the model are not mathematically proved from section 5.2.1 to section 5.2.2. One is the general solution to crash time t_c as a function of traders interaction strength β, with the characteristic of approaching to infinity as $\beta \to 0$ and converging to zero as β increases to infinity. The other is the general solution to $F_0(t)$, which is a power law distribution associated with log-periodic oscillations. However, both of their properties are presented by numerical simulations.

Crash Time t_c

The derivation in Section 5.2.1 and Section 5.2.2 shows the crash time t_c for three special cases of β:

β	0	1	∞
t_c	∞	$\bar{t}$	0

Table 5.1: Relationship of interaction strength β vs. crash time t_c.

The greater the interaction exists between traders, the faster the market crashes. The results shown in Table 5.2.4 and the definition of β indicate that the crash time t_c is monotonically decreasing as β increases. equation 5.3 indicates that the simulation starts by defining the *pdf* $p_0(t)$ with numerical values from 0 to t, for level zero. By the fundamental equation 5.10, the *pdf* values of each level (i.e., $p_1(t), p_2(t), \cdots$) are calculated. The analysis in Section 5.2.3 shows that the *pdf* $p_n(t)$ converges to a δ function as $N \to \infty$. The calculation for $p_N(t)$ in the simulation is terminated when the maximum value of the *pdf* is greater than a large number, such as 100. The time t where the maximum *pdf* is obtained is approximately the crash time as we defined. Thus, for each β, the crash time can be calculated. The plot of crash time t_c to the interaction parameter β is shown in Figure 5.7. The MatLab program for the simulation is in Appendix A.

Figure 5.7 demonstrates a power law relationship between the crash time t_c and the interaction strength β. The relationship is expressed as:

$$t_c(\beta) \sim \frac{\bar{t}}{\beta^{\mu}} \tag{5.70}$$

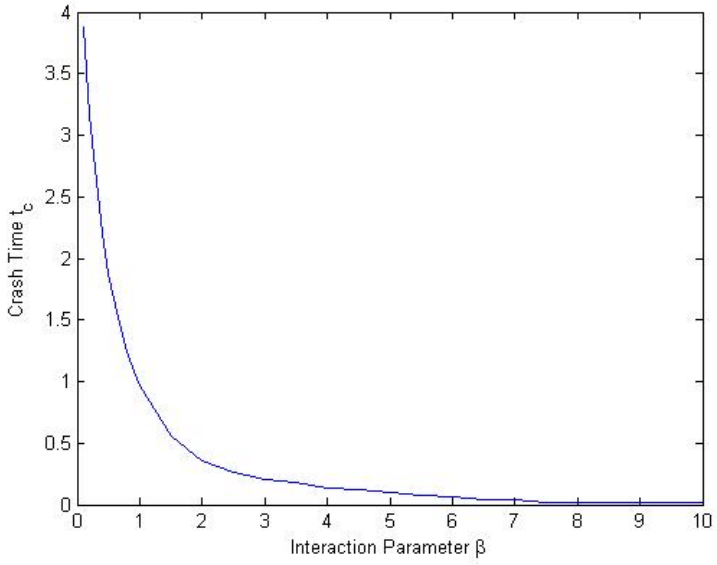

Figure 5.7: Plot for the relationship between the crash time and the interaction strength between traders. The initial distribution $p_0(t)$ is exponential with $\lambda = 1$. The fit to the power law of expression 5.70 gives the estimated values $\bar{t} = 0.9602$ and $\mu = 0.6685$ with the coefficient of determination of $R^2 = 0.9349$.

where $\bar{t}$ is the original mean of buying times of all traders without interactions, and μ is the parameter that depends on the buying time distribution.

Fraction of Traders Buying Stocks $F_0(t)$

The simulation of $F_0(t)$ is more complicated than that of t_c. As the derivation of equation 5.69 is an approximation, it smooths the oscillation characteristics. Furthermore, the truncation on the *pdf* in the numerical simulation and the precision of the *pdf* as n gets large and approaches a δ function prevents the appearance of the expected log-periodic oscillations. Based on equation 5.10 and 5.69 the log-periodic oscillations are not observable in the simulation experiments.

This hierarchical model for stock market crashes is analogous to the hierarchical fiber rupture model in Sornette [95] or the hierarchical failure model to precursory seismic activation in Newman [77]. The time of traders buying the stock is the rupture or failure time, and the effects of one trader after buying the stock on the other in the same group is the stress transfer. To illustrate the log-periodic behavior, the simulation analysis starts from

equation 5.9.

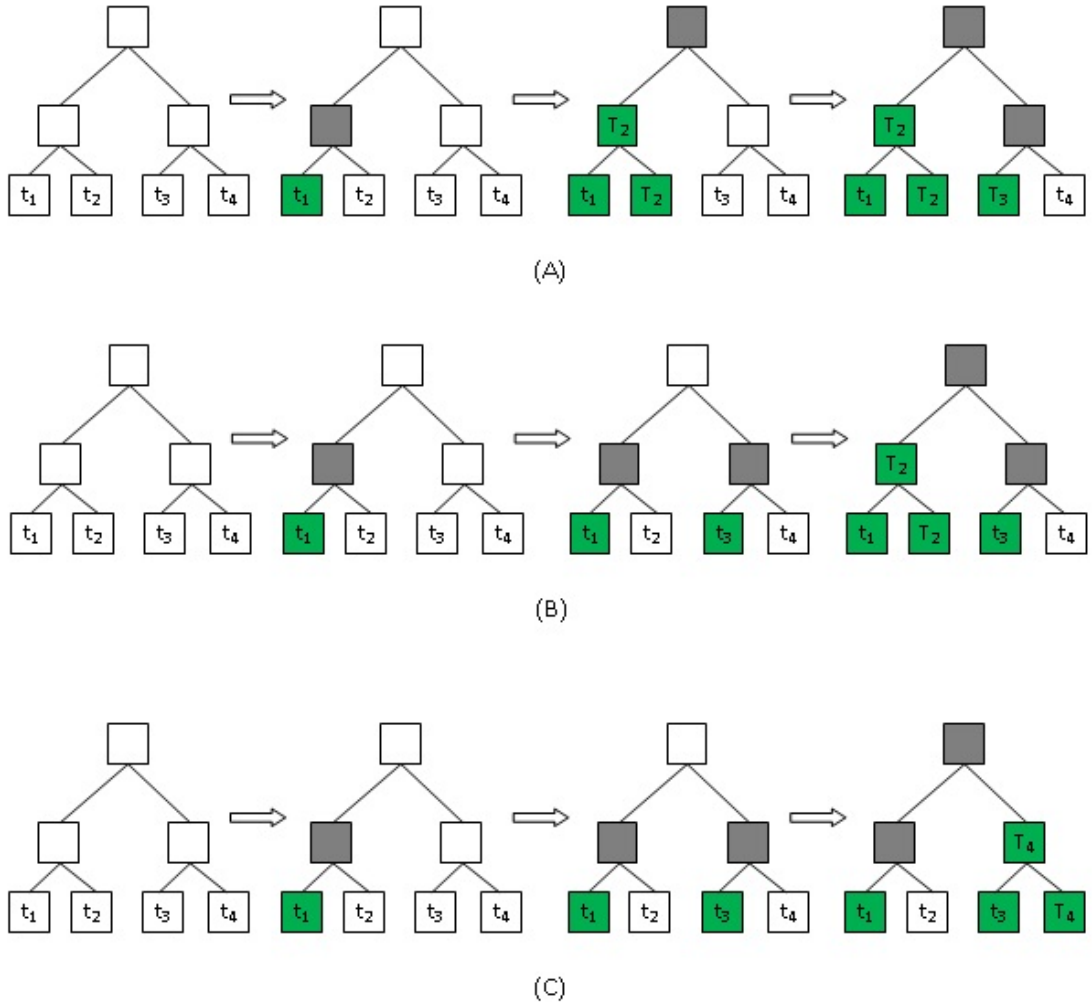

Figure 5.8: Examples of the evolution of traders buying stock in the hierarchical model.

Figures 5.8 are three examples of the evolution of traders buying stock with interactive effects in the hierarchical model [77]. The box in white with a notation t_i stands for the time at which the agent is expected to buy the stock. The box in green represents the agent buying the stock at that time. The box in grey is the agent influencing its descendants on the expected time of buying the stock. This implies that the impact is on the descendants who have not bought the stock (white boxes).

Initially, both cases (A) and (B) have the same time assigned when traders of level 0

buy the stock with the relation $t_1 < t_3 < t_2 < t_4$. The difference between these two cases is that they have different interaction parameters, $\beta_a > \beta_b$. At time t_1, the first trader at level 0 buys the stock in both cases. As discussed in Section 5.1, when one of the agents in the same group buys a stock, this information transfers to the other agent and influences its buying time with the relation as equation 5.9: $t_{12} = t_1 + 2^{-\beta}(t_2 - t_1)$. Accordingly, under the effect of the first trader at level 0 through the first agent at level 1, the buy time of the second trader at level 0 becomes T_2, but with different values for the two cases. In case (B) with smaller interaction parameter β_b, supposing T_2 is still greater than t_3, the third trader buys the stock at its original time t_3 and then the second trader buys at T_2. In contrast, case (A) has larger interaction between traders. Supposing T_2 is less than t_3, the second trader buys the stock prior to the third. After the second trader buys the stock, the first agent at level 1 also buys the stock at time T_2, and it affects its neighbour and the neighbour's children who have not bought the stock yet through the top agent. Consequently, the buy time of the third agent is changed to T_3 instead of t_3. Eventually, the fourth trader is under the effects of the preceding three traders, which significantly shortens the buy time.

In case (C), the assigned buy time is $t_1 < t_3 < t_4 < t_2$. The first trader buys at t_1. The second trader buy time is initially t_2. It changes to T_2 calculated using equation 5.9. Supposing $t_3 < T_2$, then the third trader buys of the second order at t_3. With the influence of the third trader, the buy time of the fourth trader becomes T_4. Again, supposing $T_4 < T_2$, then the fourth trader buys at T_4. After time T_4, the second trader is affected from the second agent at level 1 through the top agent besides the first trader at level 0. Its buy time should be changed again.

In the interpretation above, the calculation of the evolution of traders buying the stock is different depending on the initial buying time and the interactive parameter. In case (A) illustrated in Figure 5.8, the actual buy time of the second trader is $T_2 = t_1 + 2^{-\beta_a}(t_2 - t_1)$. The buy time of the third trader is affected by the first agent at T_2, and its actual buy time is:

$$\begin{aligned} T_3 &= T_2 + 2^{-\beta_a}(t_3 - T_2) \\ &= t_1(1 - 2^{-\beta_a})^2 + t_2(1 - 2^{-\beta_a})2^{-\beta_a} + 2^{-\beta_a}t_3 \end{aligned} \tag{5.71}$$

The fourth trader, at time T_3, receives the same amount of effects as the third trader. When the third trader buys the stock, the fourth trader is further influenced from the third. The actual buy time of the fourth trader is:

$$\begin{aligned} T_4 &= T_3 + 2^{-\beta_a}[T_2 + 2^{-\beta_a}(t_4 - T_2) - T_3] \\ &= t_1(1 - 2^{-\beta_a})^2 + (t_2 + t_3)(1 - 2^{-\beta_a})2^{-\beta_a} + t_4 2^{-2\beta_a} \end{aligned} \tag{5.72}$$

Using the same analysis for case (B) and case (C), the actual buy times are:

Case (B)

$$T_2 = t_1 + 2^{-\beta_b}(t_2 - t_1) \tag{5.73}$$

$$\begin{aligned} T_4 &= T_2 + 2^{-\beta_b}[t_3 + 2^{-\beta_b}(t_4 - t_3) - T_2] \\ &= t_1(1 - 2^{-\beta_b})^2 + (t_2 + t_3)(1 - 2^{-\beta_b})2^{-\beta_b} + t_4 2^{-2\beta_b} \end{aligned} \tag{5.74}$$

Case (C)

$$T_4 = t_3 + 2^{-\beta}(t_4 - t_3) \tag{5.75}$$

$$\begin{aligned} T_2 &= T_4 + 2^{-\beta}[t_1 + 2^{-\beta}(t_2 - t_1) - T_4] \\ &= t_3(1 - 2^{-\beta})^2 + (t_4 + t_1)(1 - 2^{-\beta})2^{-\beta} + t_2 2^{-2\beta} \end{aligned} \tag{5.76}$$

The analysis shows that the calculations are not identical for different cases. The situation is much more complicated when the number of traders is getting larger. Based on the algorithm provided in Newman et al. [76] for the hazard rate, the algorithm below is applied to the programming using recursion methods in the simulation.

We use the mathematical literature instead in the interpretation of the algorithm. Each trader/agent in the model is a node. The nodes are connected by edges. Two nodes in the same group are neighbours of each other. They are both connected to the same node, which is their parent, and they are both children of this parent. The nodes at the bottom level have no children and the top node has no parent. Each node has a time value representing the buy time of the stock, and has a property with 'bought' or 'un-bought' status indicating whether the trader/agent has bought the stock or not. If a node with a positive time value has 'un-bought' status, the time value is the expected buy time. It is finalized as the actual buy time only if the status of the node is 'bought', and the time value of the node is not

changed. If the time value of a non-zero level node is -1, it indicates that the status of both of its children are 'un-bought'.

Algorithm for the simulation of the number of traders who have bought the stock:

1. Assign initial expected buy times to the lowest level (level 0) nodes associated with a certain distribution (e.g., exponential and power law).

2. Set the buy time of all other nodes (other than level 0) as -1.

3. Set the status of all nodes as 'un-bought'.

4. Compare the buy time of all nodes with the 'un-bought' status and the buy time greater or equal to zero. Then find the node whose buy time is minimal (called 'node C' below).

5. Set the status of node C and its children with the 'un-bought' status as 'bought', and set the buy time of those children to the same as node C.

6. Check the status of the neighbour of node C.

7. If the status of the neighbour is 'bought', set the status of its parent as 'bought', set the buy time of its parent as node C, and set the parent node as node C and return to step 6.

8. If the status of the neighbour is 'un-bought', find all its descendents at level zero with an 'un-bought' status, and recalculate their time value with equation:

$$T = t + 2^{-\beta}(T - t), \tag{5.77}$$

   where T is the time value of the 'un-bought' child being calculated, and t is the time value of node C. The time value of 'un-bought' children is updated by the new value.

9. Repeat step 4 to step 8 until the status of the top node is 'bought'.

Figure 5.9 is a plot of the simulation experiments that illustrates the existence of log-periodic oscillation and power law relationship. The simulation experiments show that

the initial distribution of time that traders buy the stock has no apparent effects on the characteristics of the convergence. It is the interaction strength parameter in the control of convergent speed and the amplitude of the oscillation. Figure 5.10 is the log-log plot of five simulations with same parameter values in figure 5.9. The MatLab source code that applies the algorithm above is detailed in Appendix B.

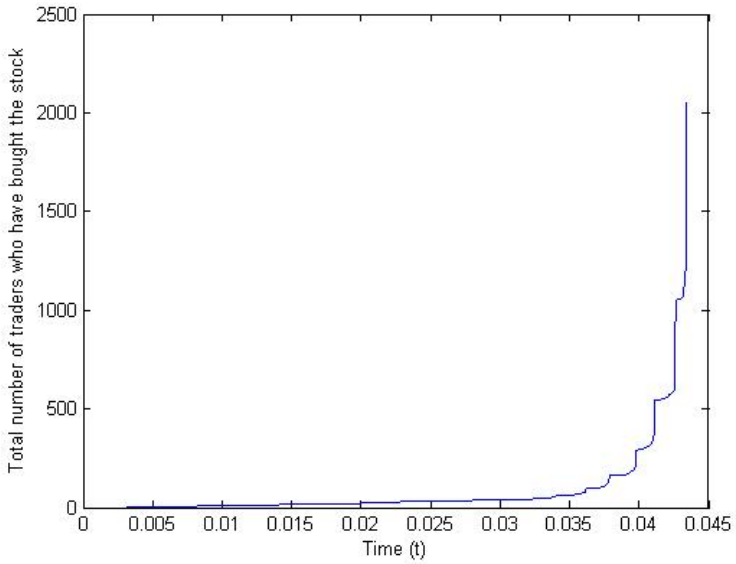

Figure 5.9: Total number of traders who have bought the stock as a function of time with an interaction parameter of 5 and an exponential initial distribution.

5.3 Construction of the Power-Law Regression Model

The Hierarchical Model shows the characteristics of a power-law distribution associated with log-period oscillation in the behavior of financial market traders placing buy orders over time. Theoretically, it explains that the imitation and herding behavior of market traders is the intrinsic reason for financial crashes. The extreme scenario is that the stock market collapses when all traders have bought the stock, which means that there are no active traders in the market. It describes the phase transition of the system in the context of critical phenomena in science. This is not going to happen in a real financial market. Moreover, the solution to the hierarchical model of the crash time t_c depends on the distribution of

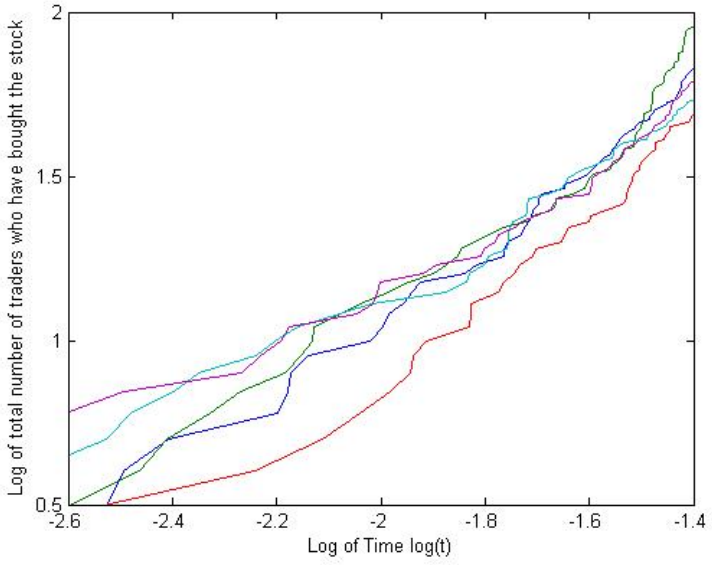

Figure 5.10: Log-Log plot of five simulation runs of total number of traders who have bought the stock over time with an interaction parameter of 5 and an exponential initial distribution.

original time when traders plan to buy the stock and on the interaction exponent β. Neither of them is measurable in any financial market. Hence, the hierarchical model is not directly applicable to the prediction of a financial market crash time.

An applicable model for the prediction of crash time ought to have similar characteristics to the hierarchical model with measurable variables as a function of time. For the stock market example, the stock price is the most accessible data variable over time. The stock price increases when more traders put in buy orders. Consequently, the stock price has the trajectory of a power-law associated with log-periodic oscillations, which is consistent with most observable stock market price patterns. This characteristic of the stock price trajectory is similar to the trader behavior of buying the stock in the hierarchical model, which indicates that a model based on the stock price over time is feasible for the prediction of the stock market crash time.

Johansen et al. [51] first constructed a non-linear regression model suitable for the prediction of crash time in both microscopic and macroscopic modelling. The model was further developed and discussed in many papers [48, 87, 49, 50]. It is widely used in a lot of studies in the prediction of many regional and global crashes by fitting the power-law

regression model to real data.

The risk-driven model, the model such named in Sornette [87], characterizes the occurrence of a crash by the hazard rate $h(t)$. All the traders/agents in the world are organized into a network and they influence each other locally through this network. The model assumes that agents tend to imitate the opinions of their connections. The imitation process is described by the hazard rate $h(t)$ with a power law [87].

$$\frac{\mathrm{d}h}{\mathrm{d}t} = Ch^{\delta}, \qquad \text{with } \delta > 1, \tag{5.78}$$

where C is a positive constant. The hazard rate $h(t)$ is the collective result of the interactions between traders. It has an unstable fixed point at zero with power law increase or decrease with the hazard rate. The exponent δ quantifies the number of interactions $\delta - 1$ felt by a trader. Integrating equation 5.78, we get

$$h(t) = \frac{B}{(t_c - t)^{\alpha}}, \qquad \text{with } \alpha \equiv \frac{1}{\delta - 1} \tag{5.79}$$

The critical time t_c, at which the bubble ends, is determined by the initial conditions at the origin of time. In order to get a finite stock price close to t_c, we have $0 < \alpha < 1$, and correspondingly $2 < \delta < +\infty$. By that means an agent has at least one interaction with other agents. The hazard rate reaches infinity in a finite critical time t_c, called the finite-time singularity.

The derivation from the Ising Model provides an intuitive description to the equations 5.78 and 5.79. The Ising model is defined by the equation

$$s_i = \mathrm{sign}(K \sum_{j \in N_{(i)}} s_j + \sigma\varepsilon_i + G), \qquad \text{with } K > 0, \varepsilon_i \sim N(0,1) \tag{5.80}$$

- s_i: the buy$(+1)$ or sell(-1) decision of the trader i at time t.
- $N_{(i)}$: the number of relatives with whom the trader i interacts significantly.
- K: called coupling strength, governs the tendency of traders towards imitation, proportional to time.
- σ: governs the tendency towards idiosyncratic behavior, the degree that agents buy/sell

decision is influenced by market noise.

- G: global influence term, tends to favor state $+1(-1)$ if $G > 0 (< 0)$.

When $K < K_c$, a critical point determining the properties of the system, the imitation between traders is weak. The traders are not self-organized and are in disorder regimes. Since K is a proportion of time t, K increases and approaches K_c at time t_c. When K gets close to K_c, the imitation between traders becomes strong and propagates over long distances. The traders self-organize into order regimes. However, either t_c for the hazard rate or K_c in the Ising model does not indicate that a crash must occur at the critical point. It may happen at any point before t_c or K_c. The critical point just signals the death of the speculative bubble. Even after the critical point, there exists a finite probability $1 - \int_{t_0}^{t_c} h(t)dt > 0$ of ending a bubble without crash. We can also define the traders average decision (buy/sell) as $M = \frac{1}{I}\sum_{i=1}^{I} s_i$. When $G = 0$, the expected value of M is $\langle M \rangle = 0$. The susceptibility (χ) of the system is defined as

$$\chi = \left. \frac{d(< M >)}{dG} \right|_{G=0}, \tag{5.81}$$

which quantifies the chance that a large group of traders finds themselves suddenly at the same decision. The dynamics of the stock price is given by

$$dp = \mu(t)p(t)dt - \kappa[p(t) - p_1]dj, \tag{5.82}$$

where $\kappa \in (0, 1)$ is the percentage of the price drops of the price increased above a reference value p_1, $\mu(t)$ denotes the return rate, and j is zero before a price jump and one afterwards. One assumption of this model is that a fair game condition holds, which is equivalent to the Martingale hypothesis.[2]

$$E_t[p(t')] = p(t), \qquad \text{with } \forall t' > t, \tag{5.83}$$

where $p(t)$ denotes the price of the asset at time t and $E_t[.]$ denotes the expectation conditional on information up to time t. When the fair game condition holds, we have $dp = 0$.

[2]A process $y_t; t = 1, ..., T$ is a Martingale if and only if $E_t(y_{t+1}) = y_t$, where E_t is the conditional expectation given the information $y_0, ..., y_t$.

Then equation 5.82 becomes

$$0 = \mu(t)p(t)dt - \kappa[p(t) - p_1]dj \tag{5.84}$$

$$\Longrightarrow \mu(t)p(t) = \kappa[p(t) - p_1]\frac{dj}{dt} \tag{5.85}$$

Taking the expectation on both sides, we get

$$\mu(t)p(t) = \kappa[p(t) - p_1]E_t(\frac{dj}{dt}) \tag{5.86}$$

Since $E_t(\frac{dj}{dt}) = h(t)$, this yields [87]:

$$\mu(t)p(t) = \kappa[p(t) - p_1]h(t) \tag{5.87}$$

This means that the hazard rate increases as the return rate increases. By equation 5.87 and 5.82, we find the solution to the price $p(t)$ for $|p(t) - p(t_0)| < |p(t_0) - p_1|$:

$$p(t) \approx p(t_0) + \kappa[p(t_0) - p_1]\int_{t_0}^{t} h(t')dt' \quad \text{with } t < t_0 \text{ (before the crash) and } t \to t_0 \tag{5.88}$$

Proof: By taking the integral of both sides of equation 5.87, we have

$$\int_{t_0}^{t} \mu(t')p(t')dt' = \int_{t_0}^{t} \kappa[p(t') - p_1]h(t')dt' \tag{5.89}$$

Under the condition of before crash, $\frac{dj}{dt} = 0$, equation 5.82 leads to:

$$\frac{dp}{dt} = \mu(t)p(t) \tag{5.90}$$

$$\Longrightarrow p(t) - p(t_0) = \int_{t_0}^{t} \mu(t')p(t')dt' = \int_{t_0}^{t} \kappa[p(t') - p_1]h(t')dt' \tag{5.91}$$

Let

$$g(t) = \int_{t_0}^{t} \kappa[p(t') - p_1]h(t')dt' - \kappa[p(t_0) - p_1]\int_{t_0}^{t} h(t')dt' \tag{5.92}$$

$$\Longrightarrow g(t_0) = 0 \tag{5.93}$$

$$\Longrightarrow g'(t_0) = \kappa[p(t_0) - p_1]h(t_0) - \kappa[p(t_0) - p_1]h(t_0) = 0 \tag{5.94}$$

By the Taylor series expansion

$$g(t) = g(t_0) + g'(t_0)(t - t_0) + \frac{g''(t_0)}{2!}(t - t_0)^2 + \mathcal{O}[(t - t_0)^3] \approx 0 \tag{5.95}$$

$$\Longrightarrow \int_{t_0}^{t} \kappa[p(t') - p_1]h(t')dt' \approx \kappa[p(t_0) - p_1] \int_{t_0}^{t} h(t')dt' \tag{5.96}$$

$$\Longrightarrow p(t) \approx p(t_0) + \kappa[p(t_0) - p_1] \int_{t_0}^{t} h(t')dt' \tag{5.97}$$

■

If $\kappa \in (0, 1)$ is the percentage drop of the price instead, then we have the following:

$$dp = \mu(t)p(t)dt - \kappa p(t)dj \tag{5.98}$$

$$\Longrightarrow E_t[dp] = \mu(t)p(t)dt - \kappa p(t)h(t)dt = 0 \tag{5.99}$$

$$\Longrightarrow \mu(t) = \kappa h(t) \tag{5.100}$$

$$\Longrightarrow \log\left[\frac{p(t)}{p(t_0)}\right] = \kappa \int_{t_0}^{t} h(t')dt' \qquad \text{before the crash} \tag{5.101}$$

Substituting $h(t')$ in equation 5.88 with equation 5.79, letting $t_0 = t_c$ and $p(t_0) = p_c$, the following is given:

$$p(t) \approx p_c + \kappa(p_c - p_1) \int_{t_c}^{t} \frac{B}{(t_c - t')^{\alpha}} dt' \qquad \text{with } \alpha \in (0, 1) \tag{5.102}$$

$$= p_c + \kappa(p_c - p_1) \frac{B}{\alpha - 1} \, (t_c - t')^{1-\alpha} \Big|_{t_c}^{t} \tag{5.103}$$

$$= p_c - \frac{\kappa B}{1 - \alpha}(p_c - p_1)(t_c - t)^{1-\alpha} \tag{5.104}$$

Let $z = 1 - \alpha$ and κ denotes the actual amount of price drop instead,which is $\kappa(p_c - p_1)$ in equation 5.104, then we have

$$p(t) \approx p_c - \frac{\kappa B}{z} \times (t_c - t)^z, \qquad \text{before the crash with } z \in (0, 1) \tag{5.105}$$

This equation shows that the price before the crash follows a power law. Since the price evolves with log-periodic oscillations, the regression equation of the price before the crash

becomes:

$$p(t) \approx p_c - \frac{\kappa}{z}\{B_0(t_c - t)^z + B_1(t_c - t)^z \cos[\omega \ln(t_c - t) - \phi]\} \tag{5.106}$$

This non-linear regression model is also applicable using the log-price instead, which is:

$$\ln[p(t)] \approx \ln(p_c) - \frac{\kappa}{z}\{B_0(t_c - t)^z + B_1(t_c - t)^z \cos[\omega \ln(t_c - t) - \phi]\} \tag{5.107}$$

5.4 General Form

The derivative of the non-linear regression model in Section 5.3 gives the power law regression equation 5.105. The log-periodic property in equation 5.106 and 5.107 is an add-in term according to the analysis of the hierarchical model in Section 5.2. equation 5.107 is a log-periodic power law formula, which has been used for modeling physical quantities with observable singular behavior at time t_c of rupture [3, 53, 88, 90]. The price or index in financial markets has similar physical behavior, which becomes scale-invariant at the critical point. The trajectory of the fitting is often not satisfactorily accurate because of the variant oscillation behavior in financial markets, with a single angular log-frequency ω. The analogous study of the discrete renormalization group equations show that a more general form for expanding equation 5.107 with higher order terms of log-periodicities can account for more complex alternation of increases and decreases of financial market prices. This section shows the derivative of equation 5.106 and 5.107 using RG formalism inspired by Sornette and Zhou [91, 95, 123].

Rewriting the log-period power law formula 5.107 by combining and re-labeling the parameters, it becomes:

$$\ln[p(t)] \approx A + B(t_c - t)^\alpha + C(t_c - t)^\alpha \cos[\omega \ln(t_c - t) - \phi] \tag{5.108}$$

First, a scale invariance renormalization group equation is necessary for the use of RG formalism analysis. Defining a factor $1/\gamma = e^{2\pi/\omega}$ relating to the prices at two time scales,

let $\mu = \gamma^{\alpha}$. After a substitution of t by $t_c - (t_c - t)/\gamma$, equation 5.108 becomes:

$$\ln p\left[t_c - \frac{t_c - t}{\gamma}\right] = A + B\left(\frac{t_c - t}{\gamma}\right)^{\alpha} + C\left(\frac{t_c - t}{\gamma}\right)^{\alpha} \cos[\omega(\ln(t_c - t) - \ln\gamma) - \phi]$$

As $\gamma = e^{2\pi/\omega}$, $\omega \ln\gamma$ is then a multiple of 2π, which can be removed.

$$\begin{aligned}
&\Longrightarrow \ln p\left[t_c - \frac{t_c - t}{\gamma}\right] = A + B\frac{(t_c - t)^{\alpha}}{\mu} + C\frac{(t_c - t)^{\alpha}}{\mu}\cos[\omega\log(t_c - t) - \phi] \\
&\Longrightarrow \mu \ln p\left[t_c - \frac{t_c - t}{\gamma}\right] = \mu A - A + A + B[(t_c - t)^{\alpha}] + C[(t_c - t)^{\alpha}]\cos[\omega\log(t_c - t) - \phi] \\
&\Longrightarrow \mu \ln p\left[t_c - \frac{t_c - t}{\gamma}\right] = \mu A - A + \ln p(t) \\
&\Longrightarrow \ln p\left[\frac{t_c - t}{\gamma}\right] = \frac{\mu - 1}{\mu}A + \frac{1}{\mu}\ln p(t_c - t) \qquad (5.109)
\end{aligned}$$

equation 5.109 is an RG equation with μ describing the rescaling of the price upon the rescaling the length of time to the critical time. It implies that the market price p at a given time t is related to that at another time t'. According to this relationship, constructing an RG formalism equation as a function of variable x is:

$$F(x) = \ln p(t_c) - \ln p(t), \text{with } x = |t_c - t| \qquad (5.110)$$

The corresponding variable for another time t' related to t is:

$$x' = R(x) = \gamma x, \qquad (5.111)$$

where $R(x)$ is the RG flow map with the approximation by taking its first order linearized transformation. Then $F(x)$ in equation 5.110 can be re-written to describe the corresponding correlation transformation in RG formalism:

$$F(x) = G(x) + \frac{1}{\mu}F[R(x)] \qquad (5.112)$$

This equation is in the same form as in Section 4.3, where $G(x)$ represents the non-singular part of the function $F(x)$ and μ describes the scaling of $F(x)$ upon a rescaling of $R(x)$. As shown in section 4.3, with $R(x) = \gamma x$ as the flow map, solving equation 5.112 recursively

gives

$$F(x) = \sum_{n=0}^{\infty} \frac{1}{\mu^n} G\left[R^{(n)}(x)\right] = \sum_{n=0}^{\infty} \frac{1}{\mu^n} G\left[\gamma^n(x)\right] \tag{5.113}$$

In the mathematical literature, a Weierstrass function is originally defined as [41]:

$$f(x) = \sum_{n=0}^{\infty} a^n \cos(b^n \pi x), \tag{5.114}$$

where $0 < a < 1, ab > 1 + \frac{3}{2}\pi$, and b is an odd integer. Or, in a special case with $a = b^{-\alpha}$, the Weierstrass function is

$$W_\alpha(x) = \sum_{n=0}^{\infty} b^{-n\alpha} \cos(b^n x), \tag{5.115}$$

corresponding to equation 5.113 with $\gamma = b, \mu = \gamma^\alpha$, and $G(x) = \cos x$. Then equation 5.113 becomes

$$F(x) = \sum_{n=0}^{\infty} \frac{1}{\mu} G\left[\gamma^n(x)\right] = \sum_{n=0}^{\infty} \gamma^{-n\alpha} \cos(\gamma^n x) \tag{5.116}$$

a Weierstrass function. With the condition of equation 5.114, an important property of the Weiestrass function, found by Weierstrass in 1876, is 'continuous everywhere, but differentiable nowhere' [61]. This property makes it exhibit self-similarity, like fractals. The geometrical concept of fractals is generalized by the symmetry of scale invariance. A hallmark of scale invariance is the power law distribution. Following Gluzman and Sornette[38] and Saleur and Sornette [84], a power law series of equation 5.113 is obtained by applying Mellin transform.

The *Mellin transform* is defined as [30]:

$$\mathcal{M}\{f(x); s\} = \tilde{f}(s) = \int_0^\infty x^{s-1} f(x) dx, \tag{5.117}$$

and the inverse of the *Mellin transform*

$$f(x) = \frac{1}{2\pi i}\int_{c-i\infty}^{c+i\infty} x^{-s}\tilde{f}(s)ds. \tag{5.118}$$

The Mellin transform is related to the two-sided *Laplace transform* of $f(x)$ by:

$$\tilde{f}(s) = \mathcal{L}\{f(e^{-x}); s\} + \mathcal{L}\{f(e^{x}); -s\}. \tag{5.119}$$

Following these definitions, the Mellin transform of equation 5.113 is

$$\begin{aligned}
\tilde{F}(s) &= \int_0^\infty \sum_{n=0}^{\infty} \frac{1}{\mu^n} x^{s-1} G[\gamma^n x]dx \\
&= \sum_{n=0}^{\infty} \frac{1}{\mu^n}\int_0^\infty x^{s-1} G[\gamma^n x]dx \\
&= \sum_{n=0}^{\infty} \frac{1}{\mu^n\gamma^{ns}}\int_0^\infty (\gamma^n x)^{s-1} G[\gamma^n x]\frac{d(\gamma^n x)}{\gamma^n} \\
&= \sum_{n=0}^{\infty} \frac{1}{\mu^n\gamma^{ns}}\tilde{G}(s) \\
&= \frac{\mu\gamma^s}{\mu\gamma^s - 1}\tilde{G}(s),
\end{aligned} \tag{5.120}$$

where $\tilde{G}(s)$ is the Mellin transform of $G(x)$. The inverse of the Mellin transform $\tilde{F}(s)$ in equation 5.120 is equivalent to $F(x)$ in equation 5.113. We split the function $F(x)$ into a singular part and a regular part:

$$F(x) = F_s(x) + F_r(x), \tag{5.121}$$

where $F_s(x)$ is the series expansion in singular and $F_r(x)$ is the regular power law of x for the property of self-similarity. Given the definition of Mellin transform, the inverse of $\tilde{F}(s)$ is

$$\begin{aligned}
F(x) &= \frac{1}{2\pi i}\int_{c-i\infty}^{c+i\infty} x^{-s}\tilde{F}(s)ds \\
&= \frac{1}{2\pi i}\int_{c-i\infty}^{c+i\infty} \frac{\mu\gamma^s}{\mu\gamma^s - 1} x^{-s}\tilde{G}(s)ds
\end{aligned} \tag{5.122}$$

The poles[3] of equation 5.122 are in $\tilde{G}(s)$ contributing to the regular part $F_r(x)$, and the term $\frac{\mu\gamma^s}{\mu\gamma^s-1}$ from the infinite sum over successive embeddings of scales contributing to the singular part $F_s(x)$ [38]. The poles of the latter one are at $s = s_n$ such that

$$\begin{aligned} &\mu\gamma^{s_n} - 1 = 0 \\ \Longrightarrow &\gamma^{s_n} = \frac{1}{\mu} \\ \Longrightarrow &s_n \ln\gamma = -\ln\mu + \ln 1 \\ \Longrightarrow &s_n = -m + i\frac{2\pi}{\ln\gamma}n \end{aligned} \tag{5.123}$$

where $m = \frac{\ln\mu}{\ln\gamma}$. Cauchy's Residue Theorem[4] indicates that $F(x)$ can be expanded as the sum of its residue at the poles of both the singular part and the regular part. The residue[5] of $\tilde{F}(s)$ at s_n with $\lim_{s\to s_n}\mu\gamma^s = 1$ is

$$\begin{aligned} Res(\tilde{F}(s), s_n) &= \lim_{s\to s_n}(s - s_n)\frac{\mu\gamma^s}{\mu\gamma^s - 1}\tilde{G}(s) \\ &= \lim_{s\to s_n}\frac{s - s_n}{\mu\gamma^s - 1}\tilde{G}(s) \\ &= \lim_{s\to s_n}\frac{1}{\mu\gamma^s\ln\gamma}\tilde{G}(s) \\ &= \frac{\tilde{G}(s_n)}{\ln\gamma} \end{aligned} \tag{5.124}$$

Using the method of contour integral,

$$\int_{c-i\infty}^{c+i\infty} x^{-s}\tilde{F}(s)ds = \oint_C x^{-s}\tilde{F}(s)ds - \int_{Arc} x^{-s}\tilde{F}(s)ds \tag{5.125}$$

The path of the arc length integral is a half circle from $c + i\infty$ to $c - i\infty$, so $|s|$ along the path approaches infinity. Given the power term x^{-s}, the arc length integral on the right hand side of the second term of equation 5.125 approaches zero. Therefore, according to

[3]In simple words, a pole of a function $f(z)$ on an open subset D of the complex plane is a point z_0 such that $f(z)$ approaches infinity as z approaches z_0

[4]Cauchy's residue theorem is stated for the equation $\oint_C f(z)dz = 2\pi i\sum_{k=1}^{n} Res(f(z))$, for detail statement of the theorem, see Ref. [12].

[5]Residue Res(f, z_0) is the R such that $(f(z) - R)/(z - z_0)$ has an analytic antiderivative in a punctured disk. The residue is given by $Res(f, z_0) = \lim_{z\to z_0}(z - z_0)f(z)$ at a simple pole z_0.

Cauchy's Residue Theorem, $F(x)$ can be expressed in a sum series as:

$$\begin{aligned} F(x) &= \frac{1}{2\pi i}\int_{c-i\infty}^{c+i\infty} x^{-s}\tilde{F}(s)ds \\ &= \frac{1}{2\pi i}\oint_C x^{-s}\tilde{F}(s)ds \\ &= \sum_{n=0}^{\infty} Res(x^{-s}\tilde{F}(s), s_n) \\ &= \sum_{n=0}^{\infty} \frac{\tilde{G}(s_n)}{\ln\gamma} x^{-s_n} \end{aligned} \tag{5.126}$$

As justified in Gluzman and Sornette [38], $\tilde{G}(s_n)$ is expressed as the product of an exponential decay by a power prefactor and a phase as $n \to \infty$:

$$\tilde{G}(s_n) = \frac{1}{n^p} e^{-\kappa n} e^{i\psi_n}, \tag{5.127}$$

where $p, \kappa \geq 0$ and ψ_n are determined by $G(x)$, μ and γ. For the case of the proposed form of $G(x) = \cos(x)$, the parameters are found to be

$$\begin{aligned} p &= m + 0.5, \\ \kappa &= 0, \\ \psi_n &= \omega n \ln(\omega n), \end{aligned}$$

giving its Mellin transform to be

$$\tilde{G}(s) = n^{-m-0.5} e^{\omega n \ln(\omega n)}, \qquad \text{for large } n. \tag{5.128}$$

Plugging equation 5.128 into 5.126, the general form of the log-periodic power-law regression formula is generated as

$$F(x) = A + Bx^m + C\sum_{n=1}^{N} n^{-m-0.5} e^{\omega n \ln(\omega n)} x^{-m+i\frac{2\pi}{\ln\gamma}n} \tag{5.129}$$

As a more general formula for fitting the market price, the equation used for the model fit

is

$$\ln[p(t)] = A + B(t_c - t)^m + C\Re\left(\sum_{n=1}^{N} n^{-m-0.5} e^{\omega n \ln(\omega n)} (t_c - t)^{-m+i\omega n}\right) \tag{5.130}$$

The first three terms of the equation 5.130 are the same as equation 5.107.

Chapter 6

Data Analysis

This chapter applies the model to FTSE 100 index as an example to illustrate the data analysis for the prediction of the crash and for possible investment strategies. The Log-Periodic Power Law (LPPL) model has been used in past research to predict crash times, and the trends of bubble and anti-bubble regimes in variant stock markets, real estate markets, option markets, and exchange markets [11, 47, 52, 96, 68, 69, 124, 125, 123, 126, 127, 128]. Some of the research describes the fitting procedure in the data analysis [11, 47, 68, 123, 125]. As the LPPL model formula is a non-linear regression function with a combination of both linear parameters and non-linear parameters, there is no statistical analysis guaranteeing a best fit with least square errors. The fitting procedures in those papers are slightly different, but substantively the same. The term "non-linear" here refers to the form non-linearizable with any kinds of mathematical transforms.

6.1 Fitting Procedure

The basic method for fitting procedure separates the estimation of the parameters into linear parameters and non-linear parameters by rewriting equation 5.130 as:

$$h(f,g) = A + Bf(x;\Phi) + \sum_{n=1}^{N} C_n g_n(x;\Phi), \tag{6.1}$$

where the variable x is the time to the crash $t_c - t$ instead of time t, and Φ denotes all non-linear parameters, including m and ω. Considering the functions $f(x)$ and $g_n(x)$ as

variables of the function h, then the parameters A, B, and C_n are linear parameters. Using the linear estimation technique of least squares, the estimations of the linear parameters with the best fit satisfying the sum of least square is found. Hence, the estimation of A, B, and C_n are slaved to the estimation of the non-linear parameters. For the estimation of non-linear parameters, the methods and techniques, such as Taboo search[47, 123], Nelder-Mead Simplex search [11], Harmony search [34], etc., are variants for the optimization of the fit of the model. We use the Taboo search to limit the search range of global optima of the non-linear parameters, then the Quasi-Newton method with line search is employed to find the estimation of the non-linear parameters.

6.1.1 Least Square Estimations.

Given data set $\{(f_j, g_{1j}, g_{2j}, \cdots, g_{nj}, h_j) : j = 1, 2, \cdots, J\}$ for the linear regression model 6.1, with the assumption of normal error, the function can be written as [64]:

$$h_j = A + Bf_j + C_1 g_{1j} + \cdots + C_n g_{nj} + \varepsilon_j, \qquad j = 1, \cdots, J \tag{6.2}$$

where ε_j is the normal error. It can be expressed in a matrix system as defined below:

$$\begin{bmatrix} h_1 \\ h_2 \\ \vdots \\ h_j \end{bmatrix} = \begin{bmatrix} 1 & f_1 & g_{11} & g_{21} & \cdots & g_{n1} \\ 1 & f_2 & g_{12} & g_{22} & \cdots & g_{n2} \\ \vdots & \vdots & \vdots & \vdots & \ddots & \vdots \\ 1 & f_j & g_{1j} & g_{2j} & \cdots & g_{nj} \end{bmatrix} \begin{bmatrix} A \\ B \\ C_1 \\ C_2 \\ \vdots \\ C_n \end{bmatrix} + \begin{bmatrix} \varepsilon_1 \\ \varepsilon_2 \\ \vdots \\ \varepsilon_j \end{bmatrix}$$

$$\uparrow \qquad\qquad \uparrow \qquad\qquad \uparrow \qquad\qquad \uparrow$$

$$\boldsymbol{H} = \qquad\qquad \boldsymbol{X} \qquad\qquad \boldsymbol{\beta} + \boldsymbol{\epsilon} \tag{6.3}$$

Using the method of least squares [64], in a matrix notation, the quantity to be minimized is

$$\begin{aligned} Q &= (\boldsymbol{H} - \boldsymbol{X\beta})^{\boldsymbol{T}}(\boldsymbol{H} - \boldsymbol{X\beta}) \\ &= \boldsymbol{H^T H} - \boldsymbol{\beta^T X^T H} - \boldsymbol{H^T X\beta} + \boldsymbol{\beta^T X^T X\beta} \\ &= \boldsymbol{H^T H} - (\boldsymbol{H^T X\beta})^{\boldsymbol{T}} - \boldsymbol{H^T X\beta} + \boldsymbol{\beta^T X^T X\beta} \\ &= \boldsymbol{H^T H} - \boldsymbol{2H^T X\beta} + \boldsymbol{\beta^T X^T X\beta}. \end{aligned} \tag{6.4}$$

So the values of $\boldsymbol{\beta}$ at which minimizing Q are the roots of $\boldsymbol{\beta}$ to the the derivative of equation 6.4 with respect to $\boldsymbol{\beta}$ equating to zero.

$$\frac{\partial Q}{\partial \boldsymbol{\beta}} = -2\boldsymbol{X^T H} + 2\boldsymbol{X^T X\beta} = 0 \tag{6.5}$$

The estimations for $\boldsymbol{\beta}$ are then

$$\boldsymbol{b} = (\boldsymbol{X^T X})^{-1}\boldsymbol{X^T H} \tag{6.6}$$

For each set of estimated non-linear parameters, the linear parameters are estimated by equation 6.6 for a best fit with least square sum. A stochastic search method (i.e., Taboo search) can be employed to determine the solutions to the non-linear parameters by an ensuing line search procedure combined with the quasi-Newton method.

In the search for non-linear parameters, the optimal estimated value is measured by the Sum of Squared Error (SSE). The SSE is defined as:

$$SSE = \sum_{i=1}^{n}(y_i - f(x_i))^2. \tag{6.7}$$

6.1.2 Taboo Search

Taboo Search (TS), or Tabu Search, was first introduced by Fred Glover in 1986 [36] as a device for implementing the oscillating assignment strategy [37]. The use of the Taboo search was extended and a more efficient algorithm was developed to provide simple and effective procedures for solving a wide range of global optimization problems, including

discrete functions, mix-integer problems, continuous functions, and graph theory problems [79, 54]. The Taboo search is a meta-heuristic procedure starting from an initial solution, moving to the best neighbour of the current solution without cycling by 'Tabu'.

The TS was modified in researches for different purposes. The core of the TS does not change: quicken the search to the attractor by the tabu of re-visit and enhance the searching movement around the attractor. The flow chart in Figure 6.1 illustrates the process and algorithm employed in this LPPL model fitting procedure. The step of 'Initialization' predefines several key variables and some structures.

Dimension: The dimension d in the TS is the number of non-linear parameters to be estimated.

Range & Interval: The values of each parameter are empirically limited in a certain range. Within the range, the possible values of the i^{th} parameter are evenly or unevenly divided into p_i intervals.

Cells: The sample points for the possible values of the estimated parameters are stored in many cells. The total number of cells to be structured is the product of the number of intervals of each parameter, which is $N = p_1 \cdot p_2 \cdots p_d$.

Sample points: Sample values are taken from each interval of the estimated parameters. A combination of the parameter sample values is a sample point. There are m sample points defined in each cell with values in the intervals pre-assigned.

Address: Each cell has a distinct address to exclusively represent the combination of the intervals for every parameter.

Taboo list: A taboo list is a structure storing an address list to record the most recently visited cells. This is the key element to avoid cycling in the TS. The length of the taboo list is set in the initialization as TL. The larger the TL, the longer the memory of the TS process.

Elite list: The Elite list is also an key element in the TS. It is a structure storing the information, including the value, address and solution to the sample point, of the first EL^{th} cells with the best values. The list encourages more searching movements in the

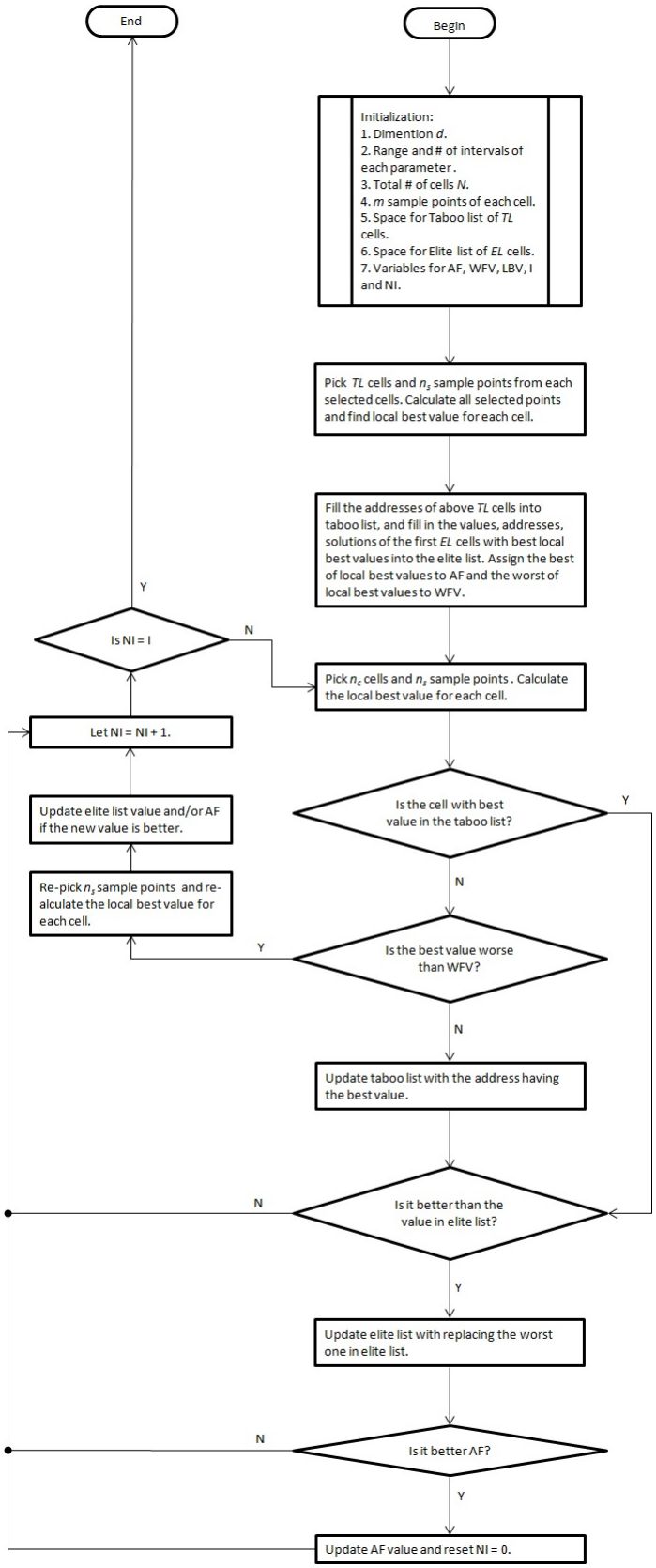

Figure 6.1: Taboo Search Process.

cells with current best values, which have more opportunities to contain the optima, so that it enhances the move to the attractor more quickly.

Aspiration Function (AF): AF memorizes the current best value in the elite list.

Worst Function Value (WFV): The opposite of the AF, WFV memorizes the current worst value in the elite list.

Local Best Value (LBV): There are m points in each cell. For each search, n_s sample points are selected and calculated. LBV stores the local best value of those sample points.

No Improvement (NI) count and Stopping Criteria (I) For each successful search, NI is reset to zero when a new AF is updated, and NI is increased by 1 when the improvement is on the elite list only. I is initialized at the beginning and the TS stops after I iterations with no improvement.

As shown in Figure 6.1, the fitting procedure starts with the initialization as described above. The first step after initialization is to assign initial values to the taboo list and elite list. To do this, we pick the number of TL cells and pick n_s sample points from each cell. The addresses of the TL cells are assigned to the taboo list. For each sample point, we calculate the Sum Square Error (SSE) of the fit. The point with the minimum SSE among those n_s sample points in each cell is the local best value (LBV). Comparing the TL local best values, the smallest LBV is assigned to AF, the greatest LBV is assigned to WFV, and the information of the first EL^{th} smallest LBV, involving the sample point values, cell addresses, and the SSEs, fill up the elite list. Practically, this is considered the end of the initialization.

The searching procedure is implemented in two loops, with one embedded in the other. The outer loop begins with picking n_c cells and n_s sample points in each of these cells. The LBVs are calculated and compared them, and we get the address of the cell with the best value of the LBVs. The inner loop is to scans all the n_c cells one by one. For each cell, its LBV is first compared with the WFV. If it is worse than the WFV, the LBV is dropped. However, before scanning the next cell, one cell from the elite list is randomly selected and re-sampled to enhance its LBV, or to enhance the AF. This is the step of enhancing move

to the attractor. Conversely, if the comparison with the WFV shows the current LBV is better than the WFV, the enhancement process stops. Instead, the taboo list, and the elite list, as well as the WFV, are updated by this cell. Notwithstanding, if the current cell is already in the taboo list the step of comparing the LBV to the WFV is skipped. Next, if the cell is not in the taboo list or the LBV is better than the WFV, the LBV is checked against the AF. If the current LBV is better than the AF, the AF and the elite list are updated. Furthermore, the NI is reset to zero whenever the AF is updated. Then the process is repeated in the next cell. When all the n_c cells are checked, the process stops in the inner loop and proceeds to the outer loop. Let NI increase by 1, and jump out of the loop when NI is equal to the predefined I. This represents I consecutive no improvement searches. Then the global optima is considered to be in one of the cells in the elite list. A line search procedure in conjunction with a quasi-Newton method is employed to find the global optima.

6.1.3 Quasi-Newton Method with Line Search

The Newton method [103] for optima is based on the iterative use of the quadratic approximation, which is the second order Taylor series expansion, to a function $f(\boldsymbol{X}) : R^n \rightarrow R$ around an iteration,

$$f(\boldsymbol{X}_{k+1}) \approx f(\boldsymbol{X}_k) + \nabla f(\boldsymbol{X}_k)^T \Delta \boldsymbol{X} + \frac{1}{2} \Delta \boldsymbol{X}^T \nabla^2 f(\boldsymbol{X}_k) \Delta \boldsymbol{X}, \tag{6.8}$$

where $\boldsymbol{X}_{k+1} = \boldsymbol{X}_k + \Delta \boldsymbol{X}$. The gradient of $f(\boldsymbol{X}_{k+1})$ with respect to $\Delta \boldsymbol{X}$ is

$$\nabla f(\boldsymbol{X}_{k+1}) = \nabla f(\boldsymbol{X}_k) + \nabla^2 f(\boldsymbol{X}_k) \Delta \boldsymbol{X}, \tag{6.9}$$

which is close to zero with the optimization of f. By optimizing equation 6.8, equation 6.9 yields Newton's formula:

$$\Delta \boldsymbol{X} = -\boldsymbol{H}_k^{-1} \nabla f(\boldsymbol{X}_k) \tag{6.10}$$

or

$$\boldsymbol{X}_{k+1} = \boldsymbol{X}_k - \boldsymbol{H}_k^{-1} \nabla f(\boldsymbol{X}_k), \tag{6.11}$$

where $\boldsymbol{H}_k = \nabla^2 f(\boldsymbol{X}_k)$ is the Hessian matrix.

The Newton method gives a fast convergent iteration to the optimization with the calculated Hessian matrix. Notwithstanding, for a lot of non-linear problems, it is difficult to evaluate the Hessian matrix. The Quasi-Newton method [103] is a method providing a similar convergent quality without actually calculating the Hessian matrix. Instead, a series of Hessian approximations are generated by the gradient of f. For the Quasi-Newton method, the Hessian matrix in equation 6.10 and 6.11 is usually replaced by $\boldsymbol{B}_k$ denoting the approximate Hessian matrix of $f(\boldsymbol{X}_k)$,

$$\Delta \boldsymbol{X} = -\boldsymbol{B}_k^{-1} \nabla f(\boldsymbol{X}_k) \tag{6.12}$$

or

$$\boldsymbol{X}_{k+1} = \boldsymbol{X}_k - \boldsymbol{B}_k^{-1} \nabla f(\boldsymbol{X}_k), \tag{6.13}$$

In equation 6.12 and 6.13, to approximate $\boldsymbol{B}_k$, the next step $\boldsymbol{X}_{k+1}$ or the step size $\Delta \boldsymbol{X}_k$ needs to be determined. The line search [103] is a method to find the suitable step direction and step size for $\boldsymbol{X}_k$ in multivariable optimization algorithms. The purpose of the line search is to find the α^* such that

$$\alpha^* = \arg\min_{\alpha > 0} f(\boldsymbol{X}_k + \alpha \Delta \boldsymbol{X}), \tag{6.14}$$

where $\Delta \boldsymbol{X}$ is in decent direction for $f(\boldsymbol{X}_k)$. $\Delta \boldsymbol{X}$ is obtained by equation 6.12 with the current approximated Hessian matrix: $\Delta \boldsymbol{X} = -\boldsymbol{B}_k^{-1} \nabla f(\boldsymbol{X}_k)$. Many other choices for the descendent direction are valid only if its dot product with the gradient of f is less than 0. If α^* is "good enough," the function value of next step f_{k+1} is reduced compared to the current step f_k:

$$f(\boldsymbol{X}_k + \alpha \Delta \boldsymbol{X}) < f(\boldsymbol{X}_k)$$

.

There are several options for the approach of α^*. In the LPPL fitting case, we employ the Quadratic Interpolation Method. This method approximates $f(\boldsymbol{X}_k + \alpha \Delta \boldsymbol{X})$ by fitting a quadratic polynomial in α to known data. The steps of the procedure are:

Step 1 Initially, let $\alpha = 1$.

Step 2 Calculate and compare $f(\boldsymbol{X}_k + \alpha\Delta\boldsymbol{X})$ and $f(\boldsymbol{X}_k)$. If $f(\boldsymbol{X}_k + \alpha\Delta\boldsymbol{X}) < f(\boldsymbol{X}_k)$, then $\alpha^* = \alpha$ and the search ends. If not move to *Step 3*.

Step 3 Fit $q(\alpha) = a + b\alpha + c\alpha^2$ with

$$\begin{cases} q(0) = f(\boldsymbol{X}_k) \\ q(\alpha) = f(\boldsymbol{X}_k + \alpha\Delta\boldsymbol{X}) \\ q'(0) = \nabla f(\boldsymbol{X}_k)^T \Delta\boldsymbol{X} \end{cases}$$

Step 4 With computed values for a, b and c, find

$$\tilde{\alpha} = \arg \min_{0<\alpha<1} q(\alpha).$$

Step 5 Let $\alpha = \tilde{\alpha}$, and repeat at *Step 2*.

Once a "good enough" step size is found, the next approximation of the Hessian matrix is updated. One direct method to update $\boldsymbol{B}$ is by Newton's method in equation 6.9 with

$$\boldsymbol{B}_{k+1} = \frac{\nabla f(\boldsymbol{X}_{k+1}) - \nabla f(\boldsymbol{X}_k)}{\boldsymbol{X}_{k+1} - \boldsymbol{X}_k}.$$

However, the BFGS update[1] method is more preferable as it often works well in conjunction with some line searches with lower accuracy. Let $\boldsymbol{Y}_k = \nabla f(\boldsymbol{X}_{k+1}) - \nabla f(\boldsymbol{X}_k)$, then by the BFGS update, the new approximate to the Hessian matrix is:

$$\boldsymbol{B}_{k+1} = \boldsymbol{B}_k + \frac{\boldsymbol{Y}_k \boldsymbol{Y}_k^T}{\boldsymbol{Y}_k^T \Delta\boldsymbol{X}_k} + \frac{\boldsymbol{B}_k \Delta\boldsymbol{X}_k (\boldsymbol{B}_k \Delta\boldsymbol{X}_k)^T}{\Delta\boldsymbol{X}_k^T \boldsymbol{B}_k \Delta\boldsymbol{X}_k} \tag{6.15}$$

Summarizing the procedures above, the algorithm using the quasi-Newton method with a line search for local optima of a cell in the elite list from the taboo search is:

Step 1 Given n number of parameters to be estimated, choose one point $\boldsymbol{X}_0 \in R^n$ from a cell in the elite list, $\boldsymbol{B}_0 = I \in R^{n\times n}$, $0 < \varepsilon < 1$, and $k = 0$.

Step 2 If $\|\nabla f(\boldsymbol{X}_k)\| < \varepsilon$, *STOP*.

[1]The BFGS update was discovered independently by Broyden, Fletcher, Goldfarb and Shanno in 1970 [103].

Step 3 Compute $\Delta \boldsymbol{X}_k = -\boldsymbol{B}_k^{-1} \nabla f(\boldsymbol{X}_k)$.

Step 4 Find a step size $\alpha_k^* > 0$ using a *line search* such that $f(\boldsymbol{X}_k + \alpha_k^* \Delta \boldsymbol{X}) < f(\boldsymbol{X}_k)$, and then set $\boldsymbol{X}_{k+1} = \boldsymbol{X}_k + \alpha_k^* \Delta \boldsymbol{X}_k$.

Step 5 Update $\boldsymbol{B}_{k+1}$ using the BFGS update with equation 6.15.

Step 6 Let $k = k + 1$ and return to *Step 2*.

The $\boldsymbol{X}_k$ found by this algorithm is the local minimum in the given cell of the elite list. Repeat this procedure for each cell in the elite list generated by the Taboo search. The minimum of all the local minima is considered the global minimum.

6.2 Bubble vs. Anti-Bubble

A bubble is a well-known term in financial markets, especially in stock markets. A bubble in a market, usually called a financial bubble, an economic bubble, or a price bubble, refers to the inflated market price of a product, such as a stock or a property, where it is above its intrinsic value without being realized by most of traders. It is originally a metaphor for an over speculative market. The inflation of a bubble is based on nothing, but speculation. A bubble eventually bursts when it is expanded beyond a certain point. The same thing happens to the price of a market: if the price of a product rises rapidly, departing from its fundamental price because of mania only, it is fragile and open to a sudden drop. That is why a bubble is usually followed by a crash. Examples include the US stock market in the late 20^{th} century and the housing market during 2005 - 2006. They are considered bubbles and were followed by a large crash. An attribute of a large crash in the stock market is its considerable financial impact. Hence, by definition, bubbles and crashes are of profound importance to risk management of investment portfolios [56]. Accordingly, the existence of a bubble is usually related to potential financial crisis.

By the bubble definition, the question of identifying a bubble is what the inherent value is and how to measure it. Therefore, whether or not a bubble exists in a market is always debatable. For instance, there is no consensus opinion of the existence of bubbles in the Greater Vancouver real estate market. The reason is that the fundamental value of a product, especially in financial markets, is based on a collection of various factors. No

one is able to master all the information of these determination factors. For example, the goodwill of a company can be realized only if a large portion, or all, of its shares are traded in one transaction. Bubbles can be absolutely confirmed in hindsight only after a crash occurs. Moreover, even if a bubble is identified, it is obvious that a substantial contraction will be induced preempting the bubble, which is an outcome that all researchers are trying to avoid. Nonetheless, a crash is always induced by the bursting of accumulated bubbles. For the purpose of data analysis in crash prediction, the LPPL model is valid if the price trajectory is in a bubble regime. Following the LPPL model definition, a bubble regime is defined as a transient regime where the increasing price trajectory is self-reinforcing and faster-than-exponential, created by positive price-to-price feedbacks feeding an overall sense of optimism effect market strengthened by interpersonal interactions [119]. Mathematically, it is characterized by a power law increase of the price time series with accelerating log-periodic oscillations created by the imitation and herding behavior of market traders [122].

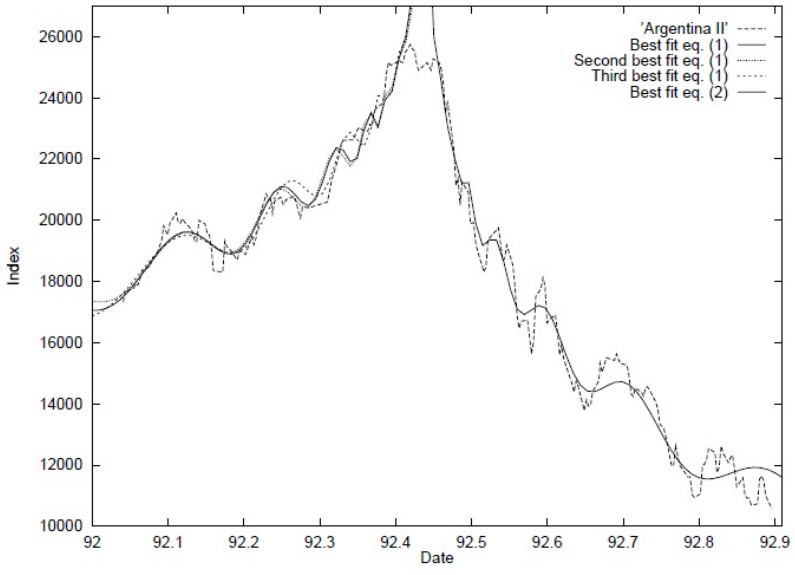

Figure 6.2: The Argentinian stock market bubble and anti-bubble of 1992. Reprinted from [52].

The mechanics of an anti-bubble regime is the inverse of a bubble regime. It is a result of herding reverse behavior of market traders. More and more traders make the buy/sell decisions on their own without being influenced by others. From this point of

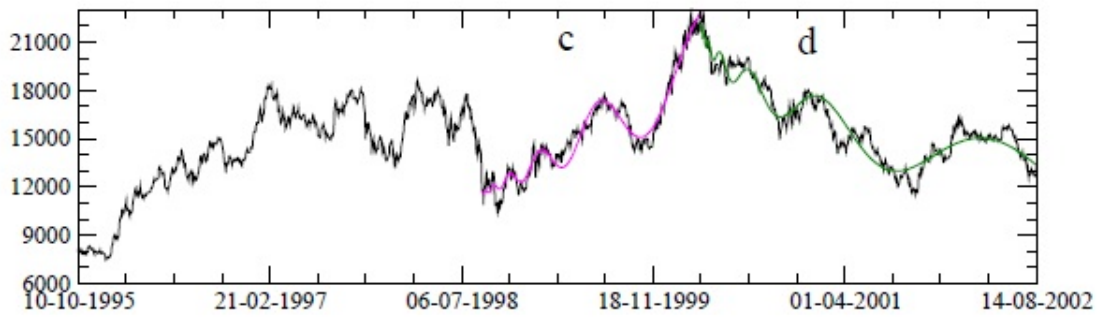

Figure 6.3: The Polish stock market bullish anti-bubble of 1998-2000. Reprinted from [39].

view, an anti-bubble regime should be mathematically defined as a price trajectory in the form of decreasing power law with decelerating log-periodic oscillations [122]. An anti-bubble regime is in an overall downward price trajectory with longer and longer periodic oscillations. Although a bubble regime often leads to a crash, it can lead to an anti-bubble regime. The bubble is gradually squeezed out in an anti-bubble regime. The anti-bubble regime above is applicable to this case. Figure 6.2 is an example of such anti-bubble regime following a bubble regime. However, a new regime was identified in Zhou and Sornette [122], and Gnaciński and Makowiec [39]. This regime still has the characteristic of expanding log-periodic oscillations, but it is generally increasing. P. Gnaciński and D. Makowiec identified it in the Polish stock market and named it as the "inverted bubble regime". W.X. Zhou and D. Sornette identified it in the stock markets of other six countries and named it the "bullish anti-bubble regime". To distinguish it, they renamed the "common" anti-bubble regime, as previously defined, to the "bearish anti-bubble regime". The section *c* of Figure 6.3 is an example of the "bullish anti-bubble regime".

This thesis incorporates the conventions of Zhou and Sornette [122]. A "bullish anti-bubble regime" is then defined as a price trajectory in the form of increasing power law with decelerating log-periodic oscillations. Therefore, an anti-bubble regime is identified by the expanding log-periodic oscillations. If a bubble leads to a crash, depending on the size of the crash and other factors, the market may enter any one of the three regimes: the bubble regime, the normal regime, or the anti-bubble regime. It is easy to notice that a bullish anti-bubble regime only occurs after a big crash, but a bearish anti-bubble regime

follows a bubble regime with or without a crash. A bearish anti-bubble regime is considered a process of market correction to an overvalued market price. On the contrary, a bullish anti-bubble regime is a process of market correction to an under-valued market price. This usually occurs after a deep crash such that the market is over-corrected to a price under the fundamental price.

The RG analysis of HM in Chapter 5, in equation 5.108 or equation 5.130 with harmonics, is applicable for the model fitting in a bubble regime. Since the anti-bubble regime is the inverse of the bubble regime, the RG analysis is applicable to anti-bubble regime studies, and similar equations can be deduced for anti-bubble regimes as:

$$\ln[p(t)] \approx A + B(t - t_c)^{\alpha} + C(t - t_c)^{\alpha} \cos[\omega \ln(t - t_c) - \phi], \tag{6.16}$$

or the general form

$$\ln[p(t)] = A + B(t - t_c)^{m} + C\Re\left(\sum_{n=1}^{N} n^{-m-0.5} e^{\omega n \ln(\omega n)} (t - t_c)^{-m+i\omega n}\right). \tag{6.17}$$

The fitting equations with harmonic terms in equation 5.130 and 6.17 are supposed to have a better fit. However, there are more parameters to estimate, which increases the computation time. The most important aspect of the prediction in the bubble regime is the crash time t_c. Accordingly, equation 5.107 may provide a "good fit" to bubble regimes. On the other hand, in the anti-bubble regime, the prediction has more concerns on the length and the amplitude of the anti-bubble process. A more accurate fitting is required, and equation 6.17 may be more applicable. This will be tested in the next section.

6.3 Results Discussion

This section uses FTSE 100 Index as an example to illustrate how to implement the LPPL to the data and how to interpret the fitting results. It is used as a tool to predict possible market crashes and trends to prevent the investment large losses from investment.

Figure 6.4 shows the FTSE 100 index daily closing from Apr. 4, 1984 to Jan. 20, 2012. During this period, three faster than exponential increasing segments, A, B and C, are identified, which implies a bubble price is more or less generated. After each of

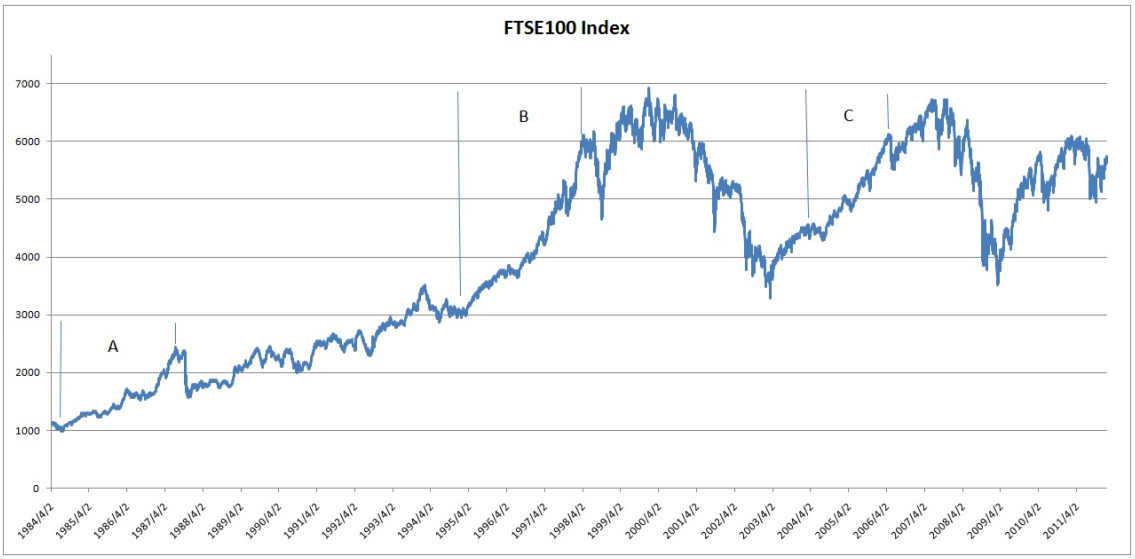

Figure 6.4: FTSE 100 index daily closing from Apr. 4, 1984 to Jan. 20, 2012.

these three increases, a significant drop follows. Depending on the depth and the speed of the downward trend these significant drops are classified as either crashes or significant corrections. In financial markets, a crash is generally defined as more than a 10% decrease over several days. Nonetheless, there is no unified definition for it. The definition is diverse for different purposes of analysis, different market categories, and different market regions. For example, Sergio Albeverio *et al.* [1], defined a crash as "a drop of more than 15% in less than two weeks". Also, some markets may have a larger fluctuation amplitude on average. To distinguish a crash from a significant correction or a bearish anti-bubble regime, we apply a relatively strict definition: a drop of more than 10% within two days, more than a 20% drop within a week, or more than a 30% drop within two weeks. According to this rule, the accelerating growth of trajectories A and C leads to a crash on Oct. 15, 1987 and Oct. 6, 2008, respectively.

6.3.1 Analysis of Crash Prediction in 1987

Figure 6.5 is a magnification of segment A in Figure 6.4. In Figure 6.6 the fitted line is shown of the LPPL model of equation 5.108 to the FTSE 100 index daily closing. The predicted crash time from the LPPL model is April 15, 1988, which is about half a year

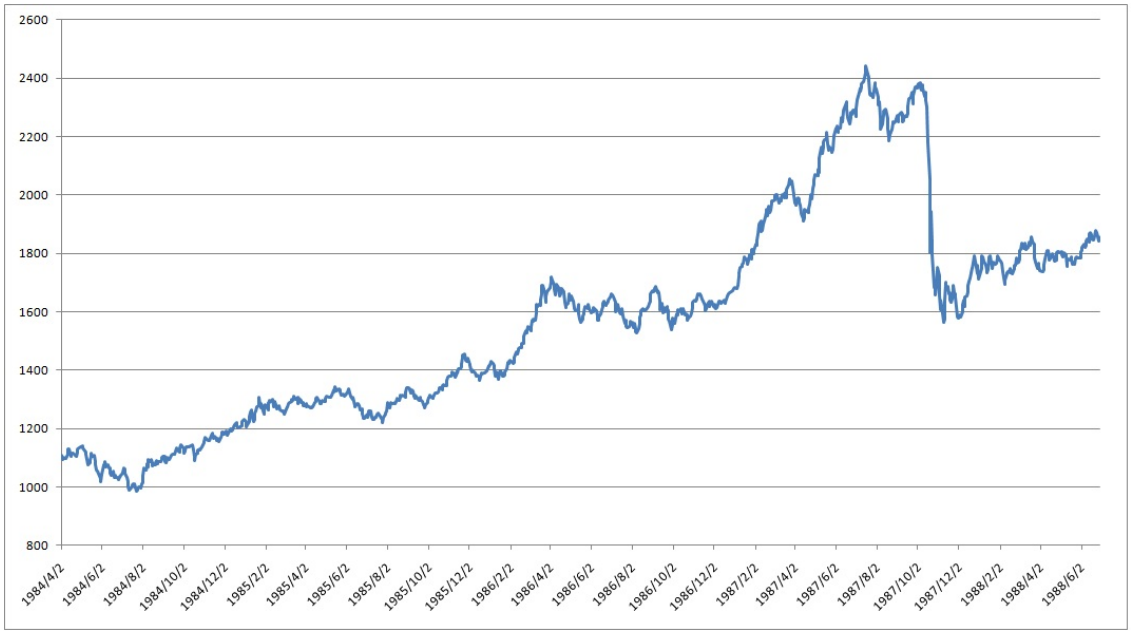

Figure 6.5: FTSE 100 index daily closing from Apr. 4, 1984 to Jun. 28, 1988.

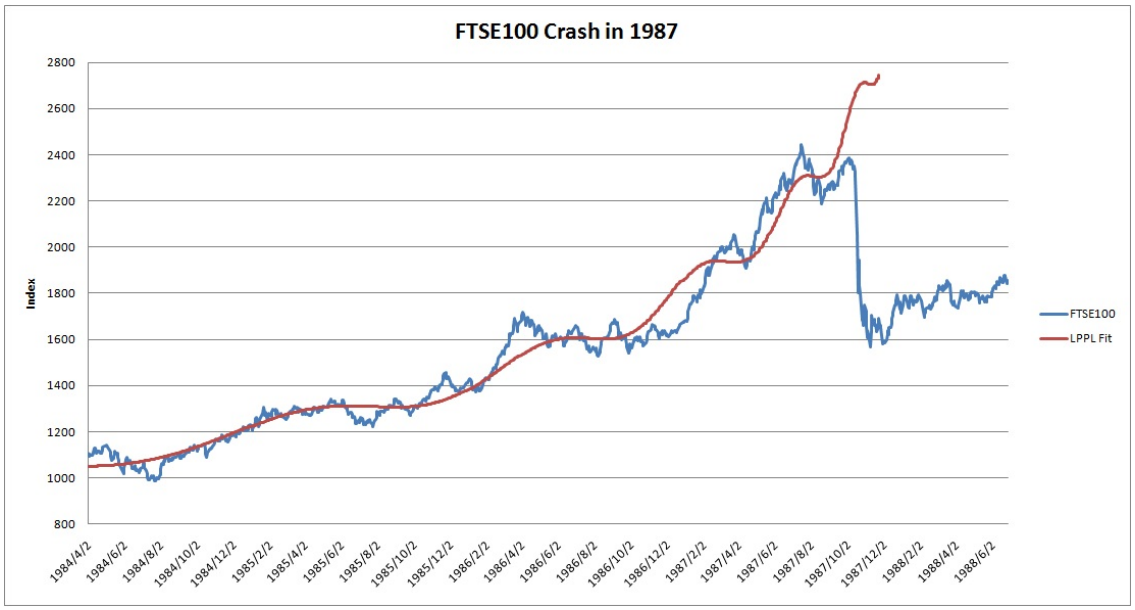

Figure 6.6: Fitting LPPL to the data of FTSE 100 index daily closing for the 1987 crash.

behind the actual crash date.

Data	t_c	α	ω	ϕ	A	B	C	MSE
Origin	1988/4/15	0.17215	13.806	0.68671	9.8800	-0.87757	-0.012823	0.0016549
Smoothed	1988/3/18	0.18488	12.665	5.2531	9.5838	-0.72311	-0.010683	0.0013454

Table 6.1: Estimated parameters of the LPPL fitted by unsmoothed and smoothed data.

Outliers among the data should be considered, as the existence of noise in the stock market impacts the price,. A process of smoothing the data can eliminate the effects of noise on the stock market volatility, and may assist in finding a better model fit to the data with more accurate crash time prediction. Figure 6.7 shows the difference between the original data and the smoothed data in two plots. As shown in Table 6.1, fitting the LPPL model to the smoothed data gives a slightly better prediction on the crash time t_c and smaller MSE. However, there is still a big gap between the actual and predicted crash time.

6.3.2 Prediction Comparison of Bubble Regimes

Fitted Data	Section A	Section B		Section C	
Estimated Crash Time	1988/3/18	1998/11/27	2000/3/30	2006/7/31	2008/5/30
Start of Drop Time	1987/10/16	1998/7/20	2000/4/11	2006/5/11	2008/6/6
Estimated Index at Crash	14527	15540	6543	7831	6796
Time Elapsed of the Drop	18 Days	38 Days	705 Days	8 Days	195 Days
Time Elapsed to Recover	438 Days	117 Days	1185 Days	100 Days	>800 Days
Drop % of Increased	65.49%	38.97%	89.59%	25.25%	108.64%
Estimated Exponent (α)	0.18488	0.25753	1.45311	0.38703	1.48788

Table 6.2: Comparison of estimations by the LPPL model of the three bubble regimes.

Comparing the fitting results of different bubble regime data helps discover whether or not the LPPL model provides reliable predictions. We fit the LPPL model to the data of section B and C in Figure 6.4. The estimated results are as shown in Table 6.2. The second columns of section B and C use the data for the higher peak after the drops of B and C respectively. For descriptive purposes, we name the columns as 'A, B1, B2, C1, C2'. The row called "Start of Drop Time" is the actual crash time or the reversal time of bullish to

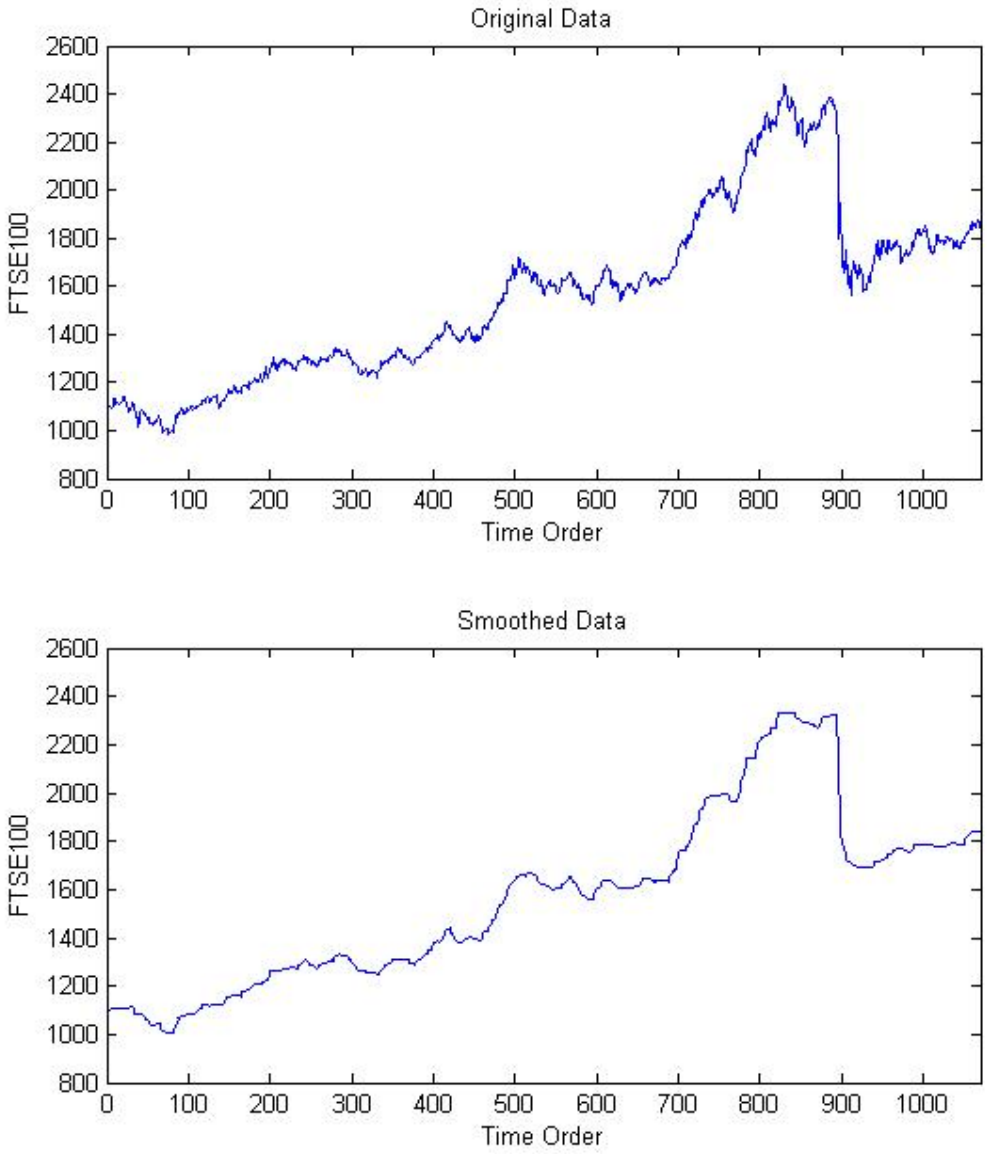

Figure 6.7: Comparison of the unsmoothed and smoothed data plots.

bearish. Each of them is within 6 months prior or posterior to the estimated crash time of the model.

First, the table indicates a crash in 'A' and 'C1', and a significant drop 'B1'. They all occur before the estimated crash time. Ideally, if the stock traders tend to imitate the trading behavior of others and herd to have the same trading behavior, the stock index converges to the estimated index value close to the crash time. However, in the real world, there is a lot of information which may change trading decisions instead of simple imitations. When a bubble regime appears in the market, it suggests that the traders start herding. While some of those herded traders make selling actions based on some market information, the remaining in the herded group follow. It leads to an earlier, but smaller crash than expected as the un-herded traders do not follow those selling behaviors. After the drops of 'B1' and 'C1', most of the herded traders do not lose their confidence in following others as their loss is not large. They are still highly connected. When some of the traders in the herded group start buying stocks, it does not take long for others to imitate those buying behaviors. This pushes the index back to the increasing trajectory quickly (117 days and 100 days, respectively). The drop of 'A' produces a 65.49% loss of the total index increase in the uptrend. This relatively big drop breaks most connections among the herded traders. The system goes back to the state where traders are not connected. Therefore, it a takes longer for the index to reach the peak value of 'A' before the crash (438 days). Viewing these drops from the point of chartists, 'B1' and 'C1' are considered big corrections of the bullish market as the percentages of the drops over the index increase are less than 50% according to the Dow theory. The uptrend directions are not changed thereafter. The index increases immediately after the drops. The index losses from the drops are recovered soon. Thereafter, the drop of 'A' is not considered a correction because it is more than 50%. The time elapsed to recover the losses is much longer.

Second, the drops of 'B1' and 'C1' are viewed as outliers in the power law increases. They make the index deviate from the expected power law trajectory. Even though the index comes back to the same value much faster as compared to a big crash like 'A', some imitation connections are broken. To a certain extent, the time elapsed for the recovery relaxes the tension of the bubbles in the market, or looses the degree of imitation behaviors among traders. This makes the system have less likely to reach the critical point, which

means an expected large crash is less likely to occur. When the stock index deviates from the predicted trajectory, the effects of the herding behavior are released. The phase transition from the bullish market to the bearish market becomes a first order transition through the phase curve instead of a critical point.

Third, the estimated exponent parameters α in 'B2' and 'C2' are both greater than 1 and the actual index drop time is later than the critical time. From Chapter 5 we know that the increasing index is supposed to have an acceleration close to the critical point and the exponent α should be less than 1. An exponent greater than 1 represents a deceleration close to the critical point. In this case, in 'B2' and 'C2', a crash does not occur. Instead, there is a long deep downtrend reversal bearish market. This is a result of the traders not all herded together, and the negative market information and bubbles in the market are interpreted differently by traders. The index is corrected to the fundamental value in a bearish regime.

According to the analysis results of this experiment, we observe the following in these three cases:

1. Fitting the model to the data of bubble regimes before a crash, we observe that the exponent α is less than 1 and the predicted crash time is within 6 months after the actual crash time.

2. Fitting the model to the data of bubble regimes followed by a bearish regime, we observe that the exponent α is greater than 1 and the predicted crash time is within 3 months before the actual crash time.

3. A crash or a drop with less loss is recovered faster.

6.3.3 Fitted Data Selection

This experiment investigates the influence of the fitted data selection on the estimated crash time. We fit the LPPL model to the FTSE 100 index data for the crash of 1987. The end date of the fitted data is fixed on September 15^{th}, 1987. The start date of the first fit is April 2^{nd}, 1984. We fit the model for other 29 time intervals. For each fit, the start date is changed to ten trading days after the previous fit. The estimated crash time t_c and exponent α, and the MSE are shown in Table 6.3. The difference of the 30 estimated crash

	Start Date	Crash Time (t_c)	Exponent (α)	MSE
1	1984/4/2	1988/3/30	0.182433118	0.001347094
2	1984/4/16	1988/3/21	0.235738023	0.001339332
3	1984/5/1	1988/3/17	0.236238927	0.001330794
4	1984/5/17	1988/3/7	0.296874373	0.001274485
5	1984/6/4	1988/2/24	0.301489466	0.001253046
6	1984/6/18	1988/2/17	0.37820528	0.001317338
7	1984/7/2	1988/2/19	0.402719857	0.001326867
8	1984/7/16	1988/2/24	0.407552321	0.001347968
9	1984/7/30	1988/3/9	0.321206044	0.001314963
10	1984/8/13	1988/2/24	0.295420051	0.001199494
11	1984/8/28	1988/2/25	0.266146652	0.001272485
12	1984/9/11	1988/2/24	0.262105913	0.001284701
13	1984/9/25	1988/2/29	0.219542164	0.001294597
14	1984/10/9	1988/1/26	0.102446099	0.001279831
15	1984/10/23	1988/3/1	0.109153643	0.001293101
16	1984/11/6	1988/4/27	0.104298623	0.001223542
17	1984/11/20	1988/5/31	0.10340906	0.001192343
18	1984/12/4	1987/11/26	0.117938908	0.001103518
19	1984/12/18	1987/11/25	0.163055232	0.001016401
20	1985/1/4	1987/12/3	0.124898678	0.000996585
21	1985/1/18	1987/12/2	0.1307454	0.000972989
22	1985/2/1	1987/12/11	0.107437736	0.001007242
23	1985/2/15	1987/11/30	0.135003068	0.000999824
24	1985/3/1	1987/11/26	0.133263826	0.001017643
25	1985/3/15	1987/12/11	0.12332109	0.001043232
26	1985/3/29	1987/12/3	0.121554009	0.001068174
27	1985/4/16	1987/11/30	0.15961844	0.001080545
28	1985/4/30	1987/11/23	0.25666129	0.001130043
29	1985/5/15	1988/5/26	0.103939557	0.001057986
30	1985/5/30	1988/4/29	0.10769114	0.000884669

Table 6.3: Fitting results of fitted data with different start dates. The end date is on September 15^{th}, 1987.

times is between '1987/11/23' and '1988/5/26'. It means that the start date of the data selection has significant effects on the accuracy of the estimated crash time. The actual crash time is October 11^{th}, 1987. From the 18^{th} fit to the 28^{th} fit, the estimated crash time is closer to the actual crash time. Also, these fits have smaller MSE than those before the 18^{th} fit. Therefore, to fit the crash of 1987, the start time of the bubble regime should be around '1984/12/4'.

	End Date	Crash Time (t_c)	Exponent (α)	MSE
1	1986/7/23	1988/5/3	1.484784931	0.000428073
2	1986/8/6	1988/9/1	1.384789979	0.000455443
3	1986/8/20	1988/11/7	1.495917775	0.000441328
4	1986/9/4	1987/9/30	1.453348814	0.000439849
5	1986/9/18	1988/8/30	1.40293958	0.000426439
6	1986/10/2	1989/2/8	1.461537507	0.000429573
7	1986/10/16	1989/4/10	1.181633799	0.00039795
8	1986/10/30	1989/3/28	1.350925476	0.000384138
9	1986/11/13	1989/3/23	1.495535725	0.000377618
10	1986/11/27	1989/4/12	1.263370913	0.000415845
11	1986/12/11	1989/4/11	1.421976455	0.000439906
12	1986/12/29	1989/2/27	1.494008423	0.000377547
13	1987/1/13	1989/4/6	1.492027678	0.000452758
14	1987/1/27	1989/3/21	1.497612331	0.000488167
15	1987/2/10	1989/4/11	1.49314106	0.000479557
16	1987/2/24	1989/4/6	1.339593241	0.000551335
17	1987/3/10	1989/4/5	0.90992444	0.000611878
18	1987/3/24	1989/4/5	0.321873484	0.000638905
19	1987/4/7	1989/4/7	0.343823597	0.000616065
20	1987/4/23	1989/4/10	0.368128702	0.000615077
21	1987/5/8	1989/4/11	0.126095922	0.000618263
22	1987/5/22	1987/7/15	0.135300287	0.000624672
23	1987/6/8	1987/7/22	0.150558536	0.000655556
24	1987/6/22	1987/7/21	0.173425401	0.000699345
25	1987/7/6	1987/7/31	0.147063092	0.000713049
26	1987/7/20	1987/8/10	0.159536988	0.000738745
27	1987/8/3	1987/9/10	0.177866273	0.00078871
28	1987/8/17	1987/10/5	0.162561332	0.000872845
29	1987/9/1	1987/10/28	0.128773786	0.00095274
30	1987/9/15	1987/11/18	0.184915091	0.001097953

Table 6.4: Fitting results of fitted data with different end dates. The start date is on December 4^{th}, 1984.

Next, we fit the LPPL model with to the FTSE 100 index data with the fixed start date on December 4^{th}, 1984, but with different end dates from '1986/7/23' to '1987/9/15'. The fitting results are shown in Table 6.4. The estimated exponents α from the 1^{st} to the 16^{th} are greater than 1. This suggests a low risk of a crash. Furthermore, the estimated crash time is far away from the end date until the 22^{nd} fit with the end date of '1987/7/15'. The result of the 22^{nd} fit provides a strong signal of the existence of bubbles and the high risk of a crash. Suppose a stock trader uses the LPPL model periodically. If he buys the stocks around April 2^{nd}, 1984 when the market is still in the fundamental regime, and sells it around May 22^{nd}, 1987 when the crash time within 6 months is predicted, the total return rate is 96.3%. In such a case, the trader misses the increase to the peak on July 16, 1987, which is about 15% more in the return rate. However, he may not avoid the crash if he continues holding the stocks. Eventually, his total return rate is down to about 50%.

This experiment shows that the LPPL model is able to provide early indications of the existence of bubbles in the market and a strong selling signal when the risk of a crash is high. However, the choice of the start date for fitted data has influence on the predicted crash time, and the users of the model should check their start date choice periodically.

Chapter 7

Conclusion

Merits and weaknesses of LPPL model

The LPPL model is a non-linear regression model of market price/index over time. The fitting techniques used to estimate its parameters are somewhat complicated. but the users do not need to know about those techniques. The use of computer programs of the model provides a simple implementation for the users with price/index data. The LPPL model is categorized as a macroscopic model. A macroscopic model is usually constructed based on historical patterns. In contrast to other macroscopic models, the LPPL model is derived from a microscopic model - the hierarchical model. Hence, it is a macroscopic model with strong microscopic foundation. In addition, as the expected time to crash in the LPPL model is always finite, a market crash or recession is inevitable.

On the contrary, the simplicity of the LPPL model is also a disadvantage for users. The model asserts that the crash is the result of the herding behaviors of market traders that leads to a critical point. Hence, the time to crash can be estimated by fitting the critical phenomena approaching the critical point. It does not account for the effects of any other market factors. However, the financial market is a complex system which is not isolated. The LPPL model assumes that the financial market is isolated or the negative and positive effects of other market factors cancel the effects of each other. Therefore, further study in the LPPL model may involve corrections responding to the effects of large market events.

Use of RG in financial market modelling

The Renormalization Group (RG) is a mathematical apparatus that allows the decomposition of a macroscopic problem viewed at different scales. It is a crucial tool in the analysis of physical systems exhibiting critical behavior. It is applicable to the physical modelling of microscopic interactions and macroscopic phase transitions. The financial market price or index movement is a manifestation of the actions and interactions of stock traders. The similarity of the fractal structure of price movements suggests the modelling of the interactions among stock traders with fractal structures, such as the hierarchical model. Thus, the systematic investigation of the interactions viewed at different scales is possible. The RG is applicable to the financial market modelling considering financial crashes as critical phenomena and the reversals of market trends as phase transitions.

Finding the RG flow is the crucial step in RG analysis. The RG analysis of the Hierarchical Model (HM) finds that the time to the critical point of a system is a function of the interaction degree of stock traders in power law. The RG formalism of the HM deduces that the fraction of all stock traders putting buy orders over time follows a power law coupled with log-periodic oscillations. Based on the RG analysis results of the HM, a Log-Periodic Power Law (LPPL) model is derived by constructing an RG formalism from the risk-driven model.

Meaning of the LPPL model

Financial market traders expect a model to provide accurate information of market movements, such as the exact crash time and the exact price peaks and troughs. Sornette [94] states the paradox of a financial model giving accurate predictions.

The total money in a financial market does not increase from transactions. For example, assume a stock market with only one stock of 100 shares is initially sold at $1 per share. The total money invested in this market is $100. If a transaction of one share at the price of $10 is made, the total money in the market becomes $109. However, as the price is changed to $10 per share, it seems that the total stock value becomes $1000. Using simulation terminology, suppose a financial market is an isolated physical system, and the money invested in the market is the energy in the system. According to the law of conservation of energy in physics, the total amount of energy remains constant in an isolated system if

there is no energy transferred into or out of the system. It implies that the form or location of the energy may change, but the total amount does not change. Therefore, excluding the company profits and the transaction fees and taxes, the total amount of money in a financial market is equal to the total investments from the traders. When a trader has gains, some traders must have losses. The money is transferred from one trader to another. Therefore, no model can ensure that every investor has gains in the financial market. The purpose of modelling a financial market is similar to the study of critical phenomena in natural sciences, to avoid the occurrence of critical phenomena or reduce loss in an extreme event.

Many recent studies show that it is possible to model the price trajectory of financial markets and predict the time of crashes. However, no model trained by the data of a market can be validated by other markets or by other crashes of the same market. The LPPL model requires case by case training with data and self-validation by comparing the results of different ranges of training dates for the prediction. Even though the exact crash time is unpredictable in the LPPL model, the uncertainty makes it possible for the market to avoid a crash if some, or even all, traders believe the model predictions. The fitting analysis in Section 6.3 shows the actual time to a crash or a big price drop is within 6 months of the estimated critical time when the estimated exponent and MSE agree. It implies that if a trader holding stocks sells them as soon as the model signals a crash he can definitely avoid the losses from a crash. However, he may miss an increasing trend to a higher price. The traders have different investment risk tolerance. These diversities in risk tolerance induce stock holders to sell their stocks at different times. The conservative investors may sell their stocks immediately after a bubble signal. The aggressive investors may continue holding their stocks until they believe the price is at the peak. To some extent, it prevents traders from further herding behavior. Then the price trajectory deviates from the original power-law trajectory. This process is like an invisible intervention leading the market phase transition through the transition curve instead of the critical point, which implies a sudden crash.

Further study

The financial market price or index movements possess similar characteristics of random walks and fractals. As a result, some other models with fractal structure, such as lattice models and cellular automata (CA) models, are applicable to the microscopic financial market modelling. The RG formalism is a useful tool for solving these models because the systematic decomposition of the models at different scales is possible. Levin and Nave [66] show a simple real space RG technique for 2D lattice models in physics. The behavior of the traders structured in these models is worth investigating.

The behaviors of the traders in financial markets are social behaviors. Therefore, some modelling techniques of social systems are probably applicable to financial market modelling. For example, the fuzzy cognitive map (FCM) may help include other market information into the LPPL model such that the model provides a more accurate estimation of crash time or a better prediction of price trends.

Appendix A

Convergent Time Vs. Interaction Parameter

This MATLAB code is used to simulate the general solution to crash time t_c as a function of traders interaction strength β and plot the resulting diagram. The detailed simulation method is described in Section 5.2.4.

```
clc; clear;

%initial parameters
kapa = 1;
zigma = 1;
rou = 4;
ts = .02; %time step for the simulation
et = 5; %truncated distribution end point
tp = et / ts + 1; %number of points used in the simulation

time(1:28)=0; %array for convergent time
bt(1:28)=0; %array for beta
t = 0:ts:et; %array for time points
p(1, 1:tp) = pzero(t,kapa,zigma,rou); %array for pdf
%separate into two loops for better result of the graph
for b = .1:.1:1
    bn = round((b-.1)*10+1); %beta index in 'bt'
    for i = 1:10
        pcov(i, 1:tp, 1:tp) = pconver(p(i,:), t, b, tp, ts);
```

```
        p1(1:tp) = p(i,:);
        p2(1:tp, 1:tp) = pcov(i,:,:);
        p(i+1, 1:tp) = pnext(p1, p2, t, b, tp, ts ); %pdf of convolution
        [pmax, tau] = max(p(i+1, 1:tp));
        if (pmax > 10) %break the loop if converged enough
            time(bn) = (tau - 1) * ts;
            bt(bn) = b;
            break;
        end
    end
    %assign beta and convergent time to the arrays
    if (bt(bn) == 0)
        time(bn) = (tau - 1) * ts;
        bt(bn) = b;
    end
end
for b = 1.5:.5:10
    bn = round((b-1)/.5+10);
    for i = 1:10
        pcov(i, 1:tp, 1:tp) = pconver(p(i,:), t, b, tp, ts);
        p1(1:tp) = p(i,:);
        p2(1:tp, 1:tp) = pcov(i,:,:);
        p(i+1, 1:tp) = pnext(p1, p2, t, b, tp, ts ); %pdf of convolution
        [pmax, tau] = max(p(i+1, 1:tp));
        if (pmax > 10) %break the loop if converged enough
            time(bn) = (tau - 1) * ts;
            bt(bn) = b;
            break;
        end
    end
    %assign beta and convergent time to the arrays
    if (bt(bn) == 0)
        time(bn) = (tau - 1) * ts;
        bt(bn) = b;
    end
end
```

```
plot(bt,time);
```

Appendix B

Simulation of the Hierarchical Model

This MATLAB code is used to compute the fraction of all traders in the market buying stocks over time and plot the resulting diagram. The detailed simulation method is described in Section 5.2.4.

```
clc; clear;

N = 12; %number of levels
m = 2^N - 1; %number of nodes
M = 2^(N - 1); %number of first level nodes
miu = .03125; %mean of the exponential distribution

%Hierarchy initialization
global hmtree;
hmtree = struct('time', ones(1,m) * (-1), ...
                'parent', zeros(1,m), ...
                'child', zeros(1,m), ...
                'neighbor', zeros(1,m), ...
                'level', zeros(1,m), ...
                'broken', zeros(1,m), ...
                'alpha', miu);

%hmtree.time(1:M) = random('gp', 2, 1, 0, 1, M);    %pareto
%hmtree.time(1:M) = random('logn', 0, 1, 1, M);     %log-normal
```

```
hmtree.time(1:M) = random('exp', 2, 1, M);         %exponential
%hmtree.time(1:M) = random('wbl', 1, 2, 1, M);       %weibull
ubase = 0;
lbase = 0;
for i = 1:N
    prvlbase = lbase;
    lbase = ubase + 1; %start node number of current level
    ubase = 2^(N-i) + ubase; %end node number of current level
    hmtree.level(lbase : ubase) = i;
    for j = lbase : ubase
        if i < N
            hmtree.parent(j) = ceil((j - lbase + 1) / 2) + ubase;
            if mod(j, 2) == 0
                hmtree.neighbor(j) = j - 1;
            else
                hmtree.neighbor(j) = j + 1;
            end
        end
        if i>1
            hmtree.child(j) = (j - lbase) * 2 + prvlbase;
        end
    end
end

cnt = 0;

%continue the calculation till the top node
while hmtree.broken(m) == 0

    %1. Find the min unbroken node
    mintime = 999;
    minnode = 0;
    for i = 1:m
        %do not compare nodes with broken status of '2'
        if (hmtree.broken(i) == 0) && (hmtree.time(i) >= 0)
            if hmtree.time(i) < mintime
```

```
                mintime = hmtree.time(i);
                minnode = i;
            end
        end
    end

    %2. Set the min node and its childre broken and the time
    hmtree.broken(minnode) = 1; %the node is broken
    if hmtree.level(minnode) > 1;
        unbnode = minnode;
        for i = 1 : hmtree.level(minnode) - 1
            if hmtree.broken(hmtree.child(unbnode)) == 2
                unbnode = hmtree.child(unbnode);
            else
                unbnode = hmtree.child(unbnode) + 1;
            end
            hmtree.broken(unbnode) = 1;
        end
    end

    %3. main calculation of the tree of the neighbor of the current node.
    caltree(minnode, mintime);

    %A control of jumping out of the loop in case of not going up to
    %the top of the tree of any errors
    cnt = cnt + 1;
    if cnt > 3*m
        break;
    end
end

A(1,1:M) = sort(hmtree.time(1:M));
A(2,1:M) = 1:M;
plot(A(1,:), A(2,:));
xlabel('Time (t)');
ylabel('Total number of traders who have bought the stock');
```

```
%%%%%%%%%%%%%%%%%%%%%%%%%%%%%%%%%%%%%%%%%%%%%%%%%%%%

function caltree( minnode, mintime )
%CALTREE Summary of this function goes here
%   1. This function calculates the subtree with 'minnode' as the top node
%   under the effect of its neighbor at 'mintime'. The calculation does all
%   necessary updates of broken time and broken status.
%
%   2. If the neighbor has been broken, which means it has been fully
%   calculated, the calculation continues to its parent by recursion.
global hmtree;

if hmtree.parent(minnode) ~= 0 %not the top node
    if hmtree.broken(hmtree.neighbor(minnode)) == 1
        %if the neighbor node has been broken, their parent node should be
        %broken with the broken time of curren node.
        minnode = hmtree.parent(minnode);
        hmtree.time(minnode) = mintime;
        hmtree.broken(minnode) = 1;
        caltree(minnode, mintime); %calculate neighbor of the parent node.
    else
        %if the neighbor node has not been broken, the broken of current
        %node will have immediate impact on all the nodes of its neighbor

        %calculate the neighbor's new broken time under its effect by
        %calculating the broken time of the neighbor's children and taking
        %the greater one as its broken time
        udttime = calchild(hmtree.neighbor(minnode), mintime);

        %if an expected broken time of the neighbor node has been
        %calculated, that time also becomes the broken time of its parent.
        %The status of the neighbor node is set to 2, in which case the
        %node will not be used in searching the minimum unbroken node.
        if hmtree.time(hmtree.neighbor(minnode)) >= 0
            node = hmtree.neighbor(minnode);
```

```
            hmtree.time(node) = udttime;
            hmtree.broken(node) = 2; %Set the broken status of the neighbor
            hmtree.time(hmtree.parent(node)) = udttime;
        end
    end
end
end

%%%%%%%%%%%%%%%%%%%%%%%%%%%%%%%%%%%%%%%%%%%%%%%%%%%%%%%%%%%%

function udttime = calchild( node, time )
%CALCHILD Summary of this function goes here
%   This function calculates the expected broken time of a node with the
%   impact at 'time'. The calculation is on the lowest level nodes only and
%   the parent's expected broken time is updated by the greater childs
%   expected broken time. It traces down to the lowest level node by
%   recursion.

global hmtree;

if hmtree.broken(node) ~= 1 %only for unbroken nodes
    if hmtree.level(node) == 1
        %the calculation runs only when the node is at the lowest lever.
        hmtree.time(node) = time + hmtree.alpha * (hmtree.time(node) - time);
        udttime = hmtree.time(node);
    else
        if hmtree.time(node) > 0
            %if an expected broken time has been calculated, only one of its
            %child must be broken, then the calculation will only traces
            %down on the unbroken one. The newly calculated one is always
            %greater than its neighbor.
            if hmtree.broken(hmtree.child(node)) == 1
                udttime = calchild( hmtree.child(node) + 1, time);
            else
                udttime = calchild( hmtree.child(node), time);
            end
```

```
            hmtree.time(node) = udttime;
        else
            %if no expected broken time is calculated, both children's
            %expected broken time should be calculated, but not need to
            %update the node's expected broken time.
            udttime = calchild( hmtree.child(node), time);
            udttime = calchild( hmtree.child(node) + 1, time);
        end
    end
else
    udttime = time; %A fake operation of assigning the return variable
end
end
```

Bibliography

[1] Sergio Albeverio, V. Jentsch, and Holger Kantz. *Extreme events in nature and society.* Springer, New York, 2006.

[2] Andrew and Clark. Evidence of log-periodicity in corporate bond spreads. *Physica A: Statistical Mechanics and its Applications*, 338(3-4):585 – 595, 2004.

[3] J.-C. Anifrani, C. Le Floc'h, D. Sornette, and B. Souillard. Universal log-periodic correction to renormalization group scaling for rupture stress prediction from acoustic emissions. *Journal de Physique I*, 5:631–638, June 1995.

[4] P. Bak, M. Paczuski, and M. Shubik. Price variations in a stock market with many agents. *Physica A: Statistical Mechanics and its Applications*, 246:430–453, February 1997.

[5] Anthony Barcellos. The fractal geometry of mandelbrot. *The College Mathematics Journal*, 15(2):98–114, 1984.

[6] David S. Bates. The crash of '87: Was it expected? the evidence from options markets. *Journal of Finance*, 46(3):1009–1044, 1991.

[7] Yehuda Ben-Zion. Collective behavior of earthquakes and faults: Continuum-discrete transitions, progressive evolutionary changes, and different dynamic regimes. *Reviews of Geophysics*, 46(4):RG4006, 2008.

[8] George W. Bishop. *Charles H. Dow and the Dow theory.* New York :Appleton-Century-Crofts, 1960.

[9] S. Bornholdt. Expectation bubbles in a spin model of markets. *International Journal of Modern Physics C*, 12:667–674, 2001.

[10] J. . Bouchaud and R. Cont. A Langevin approach to stock market fluctuations and crashes. *The European Physical Journal B*, 6(4):543–550, 1998.

[11] D. S. Bree and N. Lael Joseph. Fitting the log periodic power law to financial crashes: a critical analysis. *ArXiv e-prints*, February 2010.

[12] James W. Brown and Ruel V. Churchill. *Complex variables and applications.* McGraw-Hill Higher Education, Boston, 2004.

[13] Filippo Castiglione and Dietrich Stauffer. Multi-scaling in the Cont-Bouchaud microscopic stock market model. *Physica A: Statistical Mechanics and its Applications*, 300(3):531–538, 2001.

[14] D. Challet and Y.-C. Zhang. Emergence of cooperation and organization in an evolutionary game. In *eprint ArXiv:adap-org/9708006*, page 8006, August 1997.

[15] Iksoo Chang and Dietrich Stauffer. Fundamental judgement in Cont-Bouchaud herding model of market fluctuations. *Physica A: Statistical Mechanics and its Applications*, 264(1):294–298, 1999.

[16] Iksoo Chang and Dietrich Stauffer. Time-reversal asymmetry in Cont-Bouchaud stock market model. *Physica A: Statistical Mechanics and its Applications*, 299(3):547–550, 2001.

[17] Youngna Choi and Raphael Douady. Chaos and Bifurcation in 2007-08 Financial Crisis. *SSRN eLibrary*, 2009.

[18] Rama Cont and Jean-Philipe Bouchaud. Herd behavior and aggregate fluctuations in financial markets. *Macroeconomic Dynamics*, 4(2):170–196, 2000.

[19] Ian Copsey. *Harmonic Elliott Wave: the case for modification of R. N. Elliott's impulsive wave structure*. John Wiley & Sons (Asia) Pte. Ltd, Singapore, 2011.

[20] Djurdje Cvijović and Jacek Klinowski. Taboo search: An approach to the multiple minima problem. *Science*, 267(5198):pp. 664–666, 1995.

[21] Hui-Hui Dai and Alan Jeffrey. *Handbook of mathematical formulas and integrals*. Elsevier Academic Press, Boston, 2008.

[22] Anirban DasGupta. *Asymptotic theory of statistics and probability*. Springer, New York, 2008.

[23] Howard B. Degenholtz and Mamta Bhatnagar. Introduction to hierarchical modeling. *Journal of palliative medicine*, 12(7):631–638, 2009.

[24] B. Derrida, L. de Seze, and C. Itzykson. Fractal structure of zeros in hierarchical models. *Journal of Statistical Physics*, 33:559–569, December 1983.

[25] Robert D. (Robert Davis) Edwards, John Magee, and W. H. C. Bassetti. *Technical analysis of stock trends*. CRC Press, New York, 2007.

[26] E. Egenter, T. Lux, and D. Stauffer. Finite-size effects in monte carlo simulations of two stock market models. *Physica A: Statistical Mechanics and its Applications*, 268(12):250 – 256, 1999.

[27] Víctor M. Eguíluz and Martín G. Zimmermann. Transmission of information and herd behavior: an application to financial markets. *Physical review letters*, 85(26 Pt 1):5659, 2000.

[28] Ferruh Erdogdu. *Optimization in Food Engineering*. CRC Press, Inc., Boca Raton, FL, USA, 2008.

[29] J. A. Feigenbaum and P. G. O. Freund. Discrete scale invariance in stock markets before crashes. *International Journal of Modern Physics B*, 10:3737–3745, 1996.

[30] George J. Fikioris. *Mellin-transform method for integral evaluation*, volume 13. Morgan & Claypool Publishers, San Rafael, Calif., 2007.

[31] A. J. Frost and Robert R. Prechter. *Elliott wave principle: key to market behavior.* New Classics Library, Gainesville, Georgia, 1995.

[32] S. Galam. Rational group decision making: a random field Ising model at T = 0. *Physica A: Statistical Mechanics and its Applications*, 238:66–80, February 1997.

[33] Edward Gately. *Neural networks for financial forecasting.* Wiley, New York, 1996.

[34] Zong W. Geem. Parameter estimation of the nonlinear muskingum model using parameter-setting-free harmony search. *Journal of Hydrologic Engineering*, 2010.

[35] Ramazan Gençay and Nikola Gradojevic. Crash of '87 – was it expected? aggregate market fears and long range dependence. *Journal of Empirical Finance*, 17(2):270, 2010.

[36] F. Glover. Future paths for integer programming and links to artificial intelligence. *Computers & Operations Research*, 13(5):533–549, 1986.

[37] Fred Glover. Heuristics for integer programming using surrogate constraints. *Decision Sciences*, 8(1):156–166, 1977.

[38] S. Gluzman and D. Sornette. Log-periodic route to fractal functions. *Phys. Ref. E*, 65(3):036142–+, March 2002.

[39] P. Gnaciński and D. Makowiec. Another type of log-periodic oscillations on Polish stock market. *Physica A: Statistical Mechanics and its Applications*, 344:322–325, December 2004.

[40] William P. Hamilton. *The stock market barometer : a study of its forecast value based on Charles H. Dow's theory of the price movement. With an analysis of the market and its history since 1897.* 1960.

[41] G. H. Hardy. Weierstrass's non-differentiable function. *Transactions of the American Mathematical Society*, 17(3):301–325, 1916.

[42] Trevor Hastie, Robert Tibshirani, and J. H. (Jerome H.) Friedman. *The elements of statistical learning: data mining, inference, and prediction.* Springer, New York, 2001.

[43] P. C. Hohenberg and B. I. Halperin. Theory of dynamic critical phenomena. *Rev. Mod. Phys.*, 49(3):435–479, Jul 1977.

[44] Yurij Holovatch. *Order, disorder and criticality: advanced problems of phase transition theory.* World Scientific, River Edge, NJ, 2004.

[45] Mark Hulbert. Tracking the dow theory. *Forbes*, 151(5):138, 1993.

[46] G. Iori. Avalanche dynamics and trading friction effects on stock market returns. *Int. J. Modern Phys. C*, 10:1149–1162, 1999.

[47] Z.-Q. Jiang, W.-X. Zhou, D. Sornette, R. Woodard, K. Bastiaensen, and P. Cauwels. Bubble diagnosis and prediction of the 2005-2007 and 2008-2009 chinese stock market bubbles. *ArXiv e-prints*, September 2009.

[48] A. Johansen and D. Sornette. Critical crashes. *ArXiv Condensed Matter e-prints*, January 1999.

[49] A. Johansen and D. Sornette. Modeling the stock market prior to large crashes. *The European Physical Journal B - Condensed Matter and Complex Systems*, 9:167–174, 1999. 10.1007/s100510050752.

[50] A. Johansen and D. Sornette. The NASDAQ crash of april 2000: Yet another example of log-periodicity in a speculative bubble ending in a crash. *The European Physical Journal B - Condensed Matter and Complex Systems*, 17:319–328, 2000. 10.1007/s100510070147.

[51] Anders Johansen, Olivier Ledoit, and Didier Sornette. Crashes as critical points. *International Journal of Theoretical & Applied Finance*, 1, 2000.

[52] Anders Johansen and Didier Sornette. Bubbles and anti-bubbles in latin-american, asian and western stock markets: An empirical study. *International Journal of Theoretical & Applied Finance*, 4(6):853, 2001.

[53] Anders Johansen, Didier Sornette, Hiroshi Wakita, Urumu Tsunogai, William I. Newman, and Hubert Saleur. Discrete scaling in earthquake precursory phenomena: evidence in the Kobe earthquake, Japan. *Japan, J. Phys. I*, 6:1391–1402, 1996.

[54] Johannes Wilhelm Joubert. *An integrated and intelligent metaheuristic for constrained vehicle routing*. PhD thesis, Pretoria, South Africa, South Africa, 2007. AAI0819509.

[55] Taisei Kaizoji. Speculative bubbles and crashes in stock markets: an interacting-agent model of speculative activity. *Physica A: Statistical Mechanics and its Applications*, 287(3-4):493–506, 2000.

[56] Kasimir Kaliva and Lasse Koskinen. Stock market bubbles, inflation and investment risk. *International Review of Financial Analysis*, 17(3):592–603, June 2008.

[57] Maurice G. Kendall, Anthony O'Hagan, and Jonathan Forster. *Kendall's advanced theory of statistics*, volume 2B. Arnold, London, 2004.

[58] Alan Kirman. The economy as an evolving network. *Journal of Evolutionary Economics*, 7(4):339–353, 1997.

[59] Ken Kiyono, Zbigniew R. Struzik, and Yoshiharu Yamamoto. Criticality and phase transition in stock-price fluctuations. *Physical Review Letters*, 96(6):068701, 2006.

[60] Ulrich Köbler and Andreas Hoser. *Renormalization group theory: impact on experimental magnetism*, volume 127. Springer, Heidelberg, 2010.

[61] Kiran M. Kolwankar and Anil D. Gangal. Fractional differentiability of nowhere differentiable functions and dimensions. *CHAOS*, 6:505, 1996.

[62] Peter Kopietz, L. Bartosch, and F. Schütz. *Introduction to the functional renormalization group*, volume 798. Springer, Berlin, 2010.

[63] V. Kushnir and B. Rosenstein. Renormalization group transformations of the decimation type in more than one dimension. *Eprint ArXiv:cond-mat/9506060*, June 1995.

[64] Michael H. Kutner. *Applied linear statistical models*. McGraw-Hill Irwin, Boston, 2005.

[65] Mario Lefebvre. *Basic probability theory with applications*. Springer, Dordrecht, 2009.

[66] M. Levin and C. P. Nave. Tensor renormalization group approach to two-dimensional classical lattice models. *Physical Review Letters*, 99(12):120601, September 2007.

[67] P. Lévy. *Théorie de l'addition des variables aléatoires*. Monographies des probabilités. Gauthier-Villars, 1954.

[68] V. Liberatore. Computational LPPL fit to financial bubbles. *ArXiv e-prints*, March 2010.

[69] V. Liberatore. Financial LPPL bubbles with mean-reverting noise in the frequency domain. *ArXiv e-prints*, September 2010.

[70] E. Lukacs. *Developments in characteristic function theory*. Macmillan, 1983.

[71] Thomas Lux. Time variation of second moments from a noise trader/infection model. *Journal of Economic Dynamics and Control*, 22(1):1–38, 1997.

[72] Thomas Lux. The socio-economic dynamics of speculative markets: interacting agents, chaos, and the fat tails of return distributions. *Journal of Economic Behavior and Organization*, 33(2):143–165, 1998.

[73] Shanggeng Ma. *Modern theory of critical phenomena*, volume no. 46. Benjamin, Reading, Mass, 1976.

[74] Benoit B. Mandelbrot. *The fractal geometry of nature*. W.H. Freeman, San Francisco, 1982.

[75] Michele Marchesi. Scaling and criticality in a stochastic multi-agent model of a financial market. *Nature*, 397(6719):498–500, 1999.

[76] W. Newman, T. Durand, A. Gabrielov, S. Phoenix, and D. Turcotte. An exact renormalization model for earthquakes and material failure statics and dynamics. *Physica D: Nonlinear Phenomena*, 77(1-3):200–216, 1994.

[77] W. I. Newman, D. L. Turcotte, and A. M. Gabrielov. Log-periodic behavior of a hierarchical failure model with applications to precursory seismic activation. *Phys. Rev . E*, 52:4827–4835, November 1995.

[78] Bo Qian and Khaled Rasheed. Hurst exponent and financial market predictability. In *IASTED conference on "Financial Engineering and Applications"(FEA 2004)*, 2004.

[79] J. Rajesh, V.K. Jayaraman, and B.D. Kulkarni. Taboo search algorithm for continuous function optimization. *Chemical Engineering Research and Design*, 78(6):845 – 848, 2000.

[80] Jochen Rau. Statistical mechanics in a nutshell. *Spring*, page 23, 1998.

[81] Pál Révész. *Random walk in random and non-random environments*. World Scientific, Hackensack, N.J, 2005.

[82] Joseph A. Rudnick and George D. Gaspari. *Elements of the random walk: an introduction for advanced students and researchers*. Cambridge University Press, New York, 2004.

[83] H. Saleur, C. G. Sammis, and D. Sornette. Discrete scale invariance, complex fractal dimensions, and log-periodic fluctuations in seismicity. *Journal of Geophysical Research*, 101(B8):17661–17677, 1996.

[84] H. Saleur and D. Sornette. Complex exponents and log-periodic corrections in frustrated systems. *Journal de Physique I*, 6:327–355, March 1996.

[85] Jack D. Schwager. *Fundamental Analysis*. Wiley, New York, 1995.

[86] D. Sornette. A hierarchical model of financial crashes. *Physica A: Statistical and Theoretical Physics*, 261(3-4):581–598, 1998.

[87] D. Sornette. Critical market crashes. *Physics Reports*, 378(1):1–98, 2003.

[88] D. Sornette and K. Ide. Theory of self-similar oscillatory finite-time singularities in finance, population and rupture. *International Journal of Modern Physics C*, 14:267, 2002.

[89] D. Sornette and A. Johansen. Large financial crashes. *Physica A: Statistical and Theoretical Physics*, 245(3-4):411–422, 1997.

[90] D. Sornette and C. G. Sammis. Complex critical exponents from renormalization group theory of earthquakes: Implications for earthquake predictions. *Journal de Physique I*, 5:607–619, May 1995.

[91] D. Sornette and W. X. Zhou. The us 2000-2002 market descent: How much longer and deeper? *Quantitative Finance*, 2:468, 2002.

[92] Didier Sornette. Stock market crashes, precursors and replicas. *J. Phys. I France*, 6:167–175, 1996.

[93] Didier Sornette. Discrete-scale invariance and complex dimensions. *Physics Reports*, 297(5):239–270, 1998.

[94] Didier Sornette. *Why Stock Markets Crash: Critical Events in Complex Financial Systems*. Cambridge University Press: Cambridge, New York, 2003.

[95] Didier Sornette. *Critical phenomena in natural sciences: chaos, fractals, self-organization and disorder : concepts and tools*. Springer, New York, 2004.

[96] Didier Sornette and Anders Johansen. Significance of log-periodic precursors to financial crashes. *Quantitative Finance*, 1(4):452 – 471, 2001.

[97] D. Stauffer and N. Jan. Sharp peaks in the percolation model for stock markets. *Physica A: Statistical Mechanics and its Applications*, 277(1):215–219, 2000.

[98] D. Stauffer and T. Penna. Crossover in the contbouchaud percolation model for market fluctuations1. *Physica A: Statistical and Theoretical Physics*, 256(1-2):284–290, 1998.

[99] Dietrich Stauffer. Can percolation theory be applied to the stock market? *Annalen der Physik*, 7(5-6):529–538, 1998.

[100] Dietrich Stauffer and Amnon Aharony. *Introduction to percolation theory*. Taylor & Francis, London, 1992.

[101] Dietrich Stauffer and Didier Sornette. Self-organized percolation model for stock market fluctuations. *Physica A: Statistical Mechanics and its Applications*, 271(3):496–506, 1999.

[102] M. Stone. Cross-validatory choice and assessment of statistical predictions (with discussion). *Royal Statistical Society, Journal; Series B; Methodological*, 36(2):111–147, 1974.

[103] Wenyu Sun and Ya-xiang Yuan. *Optimization theory and methods: nonlinear programming*, volume 98. Springer, New York, 2006.

[104] Richard Swannell. Can Elliott waves predict market moves? *Futures*, 31(14):42, 2002.

[105] Richard Swannell. Refining the Elliott wave principle with wave analysis. *Futures*, 31(15):48, 2002.

[106] Tetsuya Takaishi. Simulations of financial markets in a Potts-like model. Quantitative Finance Papers cond-mat/0503156, ArXiv.org, March 2005.

[107] L.-H. Tang and G.-S. Tian. Reaction-diffusion-branching models of stock price fluctuations. *Eprint ArXiv:cond-mat/9811114*, November 1998.

[108] Stephen J. Taylor. *Modelling financial time series*. World Scientific, New Jersey, 2008.

[109] Alejandro Tejedor, Javier B. Gómez, and Amalio F. Pacheco. Hierarchical model for distributed seismicity. *Physical review. E, Statistical, nonlinear, and soft matter physics*, 82(1 Pt 2):016118, 2010.

[110] András Telcs. *The art of random walks*, volume 1885. Springer, New York, 2006.

[111] N. Vandewalle, P. Boveroux, A. Minguet, and M. Ausloos. The crash of October 1987 seen as a phase transition: amplitude and universality. *Physica A: Statistical and Theoretical Physics*, 255(1-2):201–210, 1998.

[112] A. N. Vasil'ev. *The field theoretic renormalization group in critical behavior theory and stochastic dynamics*. CRC Press, Boca Raton, 2004.

[113] Bing-Hong Wang, Jie Wang, Chun-Xia Yang, Pei-Ling Zhou, Tao Zhou, and Ying-Di Jin. Evolutionary percolation model of stock market with variable agent number. *Physica A: Statistical Mechanics and its Applications*, 354:505–517, 2005.

[114] Edward C. Waymire and R. N. Bhattacharya. *A basic course in probability theory.* Springer, New York, 2007.

[115] C. Wiecko and E. Roman. Renormalization-group decimation technique for spectra, wave functions, and density of states. *Phys. Rev. B*, 30:1603–1605, Aug 1984.

[116] K.G. Wilson. Problems in physics with many scales of length. *Scientific American*, 241:158–179, August 1979.

[117] Yan-Bo Xie, Bing-Hong Wang, Bo Hu, and Tao Zhou. Power law distribution of wealth in population based on a modified Equíluz-Zimmermann model. *Physical review. E, Statistical, nonlinear, and soft matter physics*, 71(4 Pt 2):046135, 2005.

[118] Rossitsa Yalamova and Bill McKelvey. Explaining what leads up to stock market crashes: A phase transition model and scalability dynamics. *Journal of Behavioral Finance*, 12(3):169–182, 2011.

[119] W. Yan, R. Woodard, and D. Sornette. Diagnosis and prediction of market rebounds in financial markets. *ArXiv e-prints*, March 2010.

[120] Tongkui Yu. Scaling in different dynamic regimes of a multi-agent stock market model. volume 1, pages 143–146. IEEE, 2010.

[121] Tongkui Yu and Honggang Li. Dynamic regimes of a multi-agent stock market model. MPRA Paper 14339, University Library of Munich, Germany, November 2008.

[122] W.-X. Zhou and D. Sornette. Evidence of a worldwide stock market log-periodic anti-bubble since mid-2000. *Physica A: Statistical Mechanics and its Applications*, 330:543–583, December 2003.

[123] W.-X. Zhou and D. Sornette. Renormalization group analysis of the 2000-2002 anti-bubble in the US S&P500 index: explanation of the hierarchy of five crashes and prediction. *Physica A: Statistical Mechanics and its Applications*, 330:584–604, December 2003.

[124] W.-X. Zhou and D. Sornette. Antibubble and prediction of China's stock market and real-estate. *Physica A: Statistical Mechanics and its Applications*, 337:243–268, June 2004.

[125] W.-X. Zhou and D. Sornette. Testing the stability of the 2000 US stock market "antibubble". *Physica A: Statistical Mechanics and its Applications*, 348:428–452, March 2005.

[126] W.-X. Zhou and D. Sornette. Fundamental factors versus herding in the 2000-2005 US stock market and prediction. *Physica A: Statistical Mechanics and its Applications*, 360:459–482, February 2006.

[127] W.-X. Zhou and D. Sornette. Is there a real-estate bubble in the US? *Physica A: Statistical Mechanics and its Applications*, 361:297–308, February 2006.

[128] W.-X. Zhou and D. Sornette. A case study of speculative financial bubbles in the South African stock market 2003-2006. *ArXiv Physics e-prints*, January 2007.

Index

BFGS update, 99
Boltzmann constant, 47
Boltzmann function, 46
Brownian motion, 20
bubble, 100

Cantor set, 24, 26
Cauchy's Residue Theorem, 88
central limit theorem, 22, 42
characteristic function, 38, 39
chartist, 6
Cont-Bouchaud percolation model, 12
control parameter, 43
convolution, 37
critical phenomena, 32, 78
critical point, 32, 43, 44
cumulant, 36, 38, 39

decent direction, 98
decimation, 35–37
diamond lattice, 45
discrete scale invariance, 43
DJIA, 15
DJTA, 15
Dow theory, 3, 15, 108
dyadic expansion, 23

economic recession, 1
Elliott wave principle/theory, 3, 17
expected value, 38
exponential distribution, 52, 57

Fourier
    Fourier convolution, 38
    Fourier transform, 38
fractal dimension, 24, 25
fractal set, 24
fractals, 24
free energy, 43
FTSE 100, 103

fundamental analysis, 14
fundamentalist, 6

Hausdorff-Besicovitch dimension, 24
hierarchical model, 30, 51, 78
Hurst exponent, 8

independently identically distributed (*iid*), 22
Ising Model, 80, 81

Laplace transform, 87
least square estimation, 92
line search, 98, 100
log-periodic power law, 51, 91

market depth, 13
market prediction model, 14
Markov process, 52
Markov property, 52
Martingale hypothesis, 81
Mellin transform, 86
memoryless property, 52
microscopic mechanism model, 6
moment, 38, 39

neural networks, 14
Newton's method, 97
    for optima, 98

partition function, 46
phase transition, 32, 78
pole, 88
power law, 45
primary market, 1

quadratic interpolation method, 98
quasi-Newton method, 98

random walk, 20, 23, 28
reaction-diffusion model, 6
regime

anti-bubble regime, 101
bearish anti-bubble regime, 102, 103
bubble regime, 101
bullish anti-bubble regime, 102, 103
inverted anti-bubble regime, 102
renormalization group, 23, 35
flow map, 43–45
formalism, 43
method, 45
process, 35
rescaling, 35, 41
residue, 88
risk-driven model, 80

scale invariance, 26, 43
secondary market, 1
self-similarity, 26
spin network system, 45
stable distribution, 36
stochastic multi-agent model, 8
stochastic search, 93

Taboo/Tabu search, 93
Taylor series expansion, 39
technical analysis, 14
time series method, 14
topological dimension, 24, 25

utility function, 52, 53

Weierstrass function, 86